Doctoral Thesis

博士論文

Mechanistic analysis of enhanced RNAi activity by 5'-end modification of the siRNA guide strand

(siRNA ガイド鎖の 5'末端修飾による RNA 干渉活性向上メカニズムの解析)

ブレチン　ヴィンセント

Brechin Vincent

Doctoral Thesis

博士論文

Mechanistic analysis of enhanced RNAi activity by 5'-end modification of the siRNA guide strand

(siRNA ガイド鎖の 5'末端修飾による RNA 干渉活性向上メカニズムの解析)

ブレチン　ヴィンセント

Brechin Vincent

The University of Tokyo

Department of Computational Biology and Medical Sciences

Graduate School of Frontier Sciences

2020

Table of contents

I. List of abbreviations

Ago2: Protein Argonaute 2
APS: Ammonium Persulfate
ASO: AntiSense Oligonucleotide
$Ca(OAc)_2$: Calcium acetate
cDNA: Complementary DNA
cis-NAT: Cis Natural Antisense Transcripts
d(1/?): Dilution
dsiRNA: double-stranded *break* (DSB)-induced small RNAs
DNA: Deoxyribonucleic acid
DNase: Deoxyribonuclease
DNEM: Dulbecco's Modified Eagle's Medium
DTT: Dithiothreitol
EDTA: Ethylene Diamine Tetraacetic Acid
EGTA: Ethylene Glycol-bis(β-aminoethyl ether)-N,N,N′,N′-Tetraacetic Acid
EtOH: Ethanol
FA dye: *Formaldehyde*
FBS: Fetal Bovine Serum
GCG: Glycogen
HEPES-KOH: 4-(2-hydroxyethyl)-1-piperazine ethane sulfonic acid – potassium hydroxide
hATTR: Hereditary amyloidosis transthyretin
IVT: In Vitro Transcription
KOAc: Potassium acetate
LNP: Lipid Nanoparticules
$Mg(OAc)_2$: Magnesium acetate
Min.: Minute(s)
MQW: Milli Q Water (ultrapure water)
mRNA: Messenger RNA
miRNA: microRNA
NaOAc: Sodium Acetate
ncRNA: Non-Coding RNA
O/E : OverExpression
O/N: Overnight
PBS: Phosphate Buffer Solution
PCR: Polymerase Chain Reaction
PIC: Protease Inhibitor Cocktail
piRNA: PIWI Interacting RNA
rasiRNA: repeat-associated small interfering RNAs
RISC: RNA-Induced Silencing Complex
RNA: Ribonucleic acid
RNAi: RNA interference
RNasin plus: Ribonuclease inhibitor plus
rRNA: ribosomal RNA
RT: Room Temperature (~ 25˚C)
SAM: S-adenosyl-methionine
SDS-PAGE: Sodium Dodecyl Sulfate PolyAcrylamide Gel Electrophoresis

siRNA: Small interfering RNA
sncRNA: small non-coding RNA
snoRNA: small nucleolar RNAs
T4 PNK: T4 Polynucleotide kinase
TAE buffer: Tris base/Acetic acid/EDTA buffer
TBE buffer: Tris/Borate/EDTA buffer
TBS-T: Tris-buffered saline-Tween 20
TEMED: Tetramethylethylenediamine
TGS: TRIS-Glycine-SDS
trans-NAT: Trans Natural Antisense Transcripts
TRIS: tris(hydroxymethyl)aminomethane
tRNA: Transfer RNA
UTR: untranslated region
UV: UltraViolet
V: Volt
VEGF: Vascular Endothelial Growth Factor
(v/v): volume/volume
(v/w): volume/weight

II. Introduction

1. Overview of the RNA interference mediated gene silencing

1.1 Discovery of RNA interference mediated gene silencing

RNA interference (RNAi) is a general mechanism for regulating gene expression based on the specific sequence degradation of transcribed RNAs. The first evidence of this phenomenon, although it was not identified as such until several years later, was in the 1990s by R. Jorgensen's team during his research on Petunia's staining mechanisms (Napoli et al., 1990). Wishing to observe a change in the flower's coloring, they introduced a second copy of the pigmentation gene into the genome of plant and unexpectedly obtained an extinction of the coloration (Napoli et al., 1990). These experiments called co-suppression revealed a widespread mechanism in plants involved in the protection of the genome against transposable elements and RNA viruses (Vaucheret and Fagard, 2001). Acting on RNAs already transcribed, this mechanism has been baptized "Post Transcriptional Gene Silencing" or PTGS. In the 1990s, numerous molecular analysis carried out on C. elegans (Guo and Kemphues, 1995) and N. crassa (Cogoni et al., 1996), harboring inactive transgenes showed that transcription both on the resident gene and on the transgene are still active, however transcripts are rapidly degraded in the cytoplasm. On February 19th, 1998, an article considered today as foundation of the RNAi field clearly established the suppressive role of small non-coding RNA molecules (Fire et al., 1998) and was rewarded eight years later the Nobel Prize in Physiology and Medicine. This discovery marked the world of experimental genetics, cell biology and more recently, medicine. A. Fire et al. found that the introduction of double-stranded RNA (dsRNA) into C. elegans cells can specifically reduce the expression of proteins by binding them to their mRNAs for several generations. This phenomenon of gene extinction called RNAi allowed to analyze and understand the function of many proteins (Fire et al., 1998). In the following years, many teams managed to highlight the RNAi phenomenon in other species such as Drosophila (Kennerdell and Carthew, 1998), Xenopus (Oelgeschlager et al., 2000), mouse (Svoboda et al., 2000), trypanosome (Ngô et al., 1998), planar, zebrafish (Zamore et al., 2000) and protists (Ruiz et al., 1998).

As such, RNAi designates the specific regulations for gene expression directed by a small RNA molecule that serves as guide. These regulations can induce the transcription stop of the targeted gene which is the nuclear pathway of the RNAi

(Castel and Martienssen, 2013) or act on the mRNA level either by a mechanism of degradation or an inhibition of the translation. These are the pathways of post-transcriptional gene silencing: the small interfering RNA (siRNA) pathway, the microRNA (miRNA) pathway (Naqvi et al., 2009) and the PIWI interacting RNA (piRNA) pathway (Siomi et al., 2011).

1.2 Different types of RNA silencing pathway: How do they work?

1.2.1 RNA silencing biogenesis summarized

Small RNAs are non-coding dsRNAs of 20-25 nucleotides (nts) (Tomari and Zamore, 2005). They arise from processing long precursor RNAs in the nucleus (only for miRNA) and / or in the cytoplasm. These RNAs act in single-stranded form by matching the target RNA sequence and preventing the expression of the gene in question either by cleaving this RNA or by inhibiting its translation into protein. This association with the target RNA is made through a protein complex associated with small RNA and involved both in its maturation and in its function (Wilson et al., 2015).

1.2.2 Three distinct pathways

Firstly, the use of RNAi in mammals were considered difficult due to the existence of interferon response. Indeed, in mammals the introduction of dsRNA induces cellular responses including the production of interferons that block protein synthesis independently to the sequence of antisense RNA. However, soon after the initial description of the interference, the presence of small RNAs of ~ 20 nucleotides were demonstrated in plants where co-suppression was observed (Hamilton and Baulcombe, 1999). The description of a specific sequence nuclease induced by dsRNA in Drosophila (Hammond et al, 2000) suggested small interfering RNAs can act as a guide to recognize target RNAs. This prompted Thomas Tuschl's team to use the small RNAs produced from the cleavage of long-stranded dsRNAs to induce RNA interference in mammals (Elbashir et al, 2001). Since then, better understanding of RNA interference mechanism has been made and this has become a powerful tool in molecular biology to "Knock Down" or silence genes to study their function.

Soon after the siRNA discovery, it was observed they were not the only small RNA capable of "interference". In 2001, several teams identified another type of small

RNA deriving from a single-stranded precursor RNA. This contain a strongly paired region in secondary stem-loop structure which rise to “microRNAs”. (Lagos-Quintana et al, 2001). This type of regulatory RNA was observed as early as in 1993 in C. elegans with the characterization of the lin-4 gene product (Lee et al, 1993), Until then it had been assumed it was a specificity of C. elegans. Then in 2006, piRNA was discovered in Drosophila with function to protect the germ line against transposable elements (Aravin et al, 2006, Girard et al, 2006) establishing the idea that there are several classes of interference (Aravin et al, 2001).

These 3 types of small regulatory RNAs differ in their biogenesis and their mode of action. I will further develop in detail siRNA and miRNA pathway as below.

1.2.3 siRNA pathway

As explained above, gene silencing by siRNAs was the first to be described (Hamilton and Baulcombe, 1999). siRNA pathway is involved in antiviral response by the presence of dsRNA cell-induced in the cytoplasm. Now siRNA is used as a molecular tool for silencing gene expression in functional studies and also in therapeutics.

1.2.3.1 History of siRNA and Argonaute

Same as the other small regulatory RNAs, the mechanism and function of siRNAs is the interaction of a protein complex and a guide to "target" mRNA. The first discovery made in this direction was the observation of a specific nuclease activity induced by the introduction of dsRNA in Drosophila (Hammond et al, 2000) which was named RISC for "RNA-Induced Silencing Complex". Small RNA around 20 nucleotides had been described to interact with RISC allowing them to guide it towards the target mRNA. The catalytic action of this nuclease from the Argonaute family protein is the heart of the siRNA mechanism. The Argonaute protein was first demonstrated in A. thaliana in a study of a leaf-shape mutation (Bohmert et al, 1998). It was shown that Argonaute 1 (Ago1) protein was necessary for the co-suppression mechanism in A. thaliana. The gene encoding this protein was related to the C. elegans Rde1 ("RNAi deficient") gene.

Hannon's group extended these studies to Drosophila by implementing the Argonaute 2 protein (Ago2) in post-transcriptional silencing. Since then, Argonaute protein family has been proven to be found in all eukaryotes, with the exception of a few yeasts, including S. cerevisiae. The phylogenetic study of the Argonaute proteins family (Parker and Barford, 2006) shows diversity of Argonaute proteins in C. elegans and plants, reflecting the biological importance of this type of regulation. In mammals, we can count 7 to 8 Argonaute proteins that can be grouped into two subfamilies: Argonaute proteins 1,2,3,4 (Ago1, 2, 3 and 4) and Piwi proteins (Piwi-Like 1, 2 and 3 in mice). The Piwi protein subfamily is absent in plants, fungi *and* S. pombe and therefore more restricted in its distribution than Argonaute subfamily proteins. They are generally involved in piRNA pathway which is essential for the regulation of transposable elements in germ line cells.

1.2.3.2 Detailed biogenesis of siRNA

RISC is organized around Argonaute protein and RNA guide. In mammals only Ago2 has an endonucleolytic activity that allows the cleavage of the target RNA. This activity is carried out by the PIWI domain of the protein as shown in the structure of P. furiosus Argonaute protein (Song et al, 2004). This study revealed a homology of Piwi domain with the catalytic domain of RNase H vertebrate retroviruses capable to hydrolyze the RNA strand in a double-stranded DNA: RNA. In the case of Ago2 protein, the hydrolysis of the targeted RNA is due to the perfect complementarity with the small "guide" RNA (or almost perfect, one or two mismatches outside the cleavage site can be tolerated).

In siRNA-mediated gene silencing, dsRNA is often exogenous (RNA virus) or the consequence of an experimenter as was in the case of the experiments carried out by Fire and Mello (dsRNA of several hundred nucleotides). It was therefore necessary to describe the appearance of small RNAs of 20 nucleotides after the introduction of these long sequences. This step in the biogenesis of small RNAs is carried out by an enzyme of the family of RNase III essential for the development, Dicer (Berstein et al, 2004). From a dsRNA template Dicer generates small RNAs of 20 nucleotides.

All such discoveries contributed in drawing a general diagram of the siRNA mechanism **(Figure 1).** Long dsRNAs introduced into the cell (artificially or from RNA

virus) are supported by Dicer, which will hydrolyze them into small RNAs of around 20 nucleotides. The last ones are then incorporated into RISC by associating them with Ago2 protein. In RISC, only the "guide" strand is retained. The "passenger" strand derived from the double strand is cleaved and dissociated from Ago2 (Matranga et al, 2005). The choice of the guide strand is determined by several criteria including the stability of the pairing of small RNA ends (Noland et al, 2013). Once RISC is functional (after expulsion of the passenger) it can interacts with the target mRNA. It is the perfect complementarity between the sequence of the target mRNA and the small "guide" RNA that will allow the endonucleolytic cleavage by the Argonaute protein. The cleavage will allow the degradation of the two generated RNA fragments by the action of the 3'-5' and 5'-3' exonucleases which leads to a complete disappearance of the target RNA. Numerous studies have shown that RNAi pathway is not only specific to the somatic lineage (germline also have siRNAs) but is also involved in genome integrity by protecting against parasite DNAs such as transposons and viruses (Ghildiyal and Zamore, 2009).

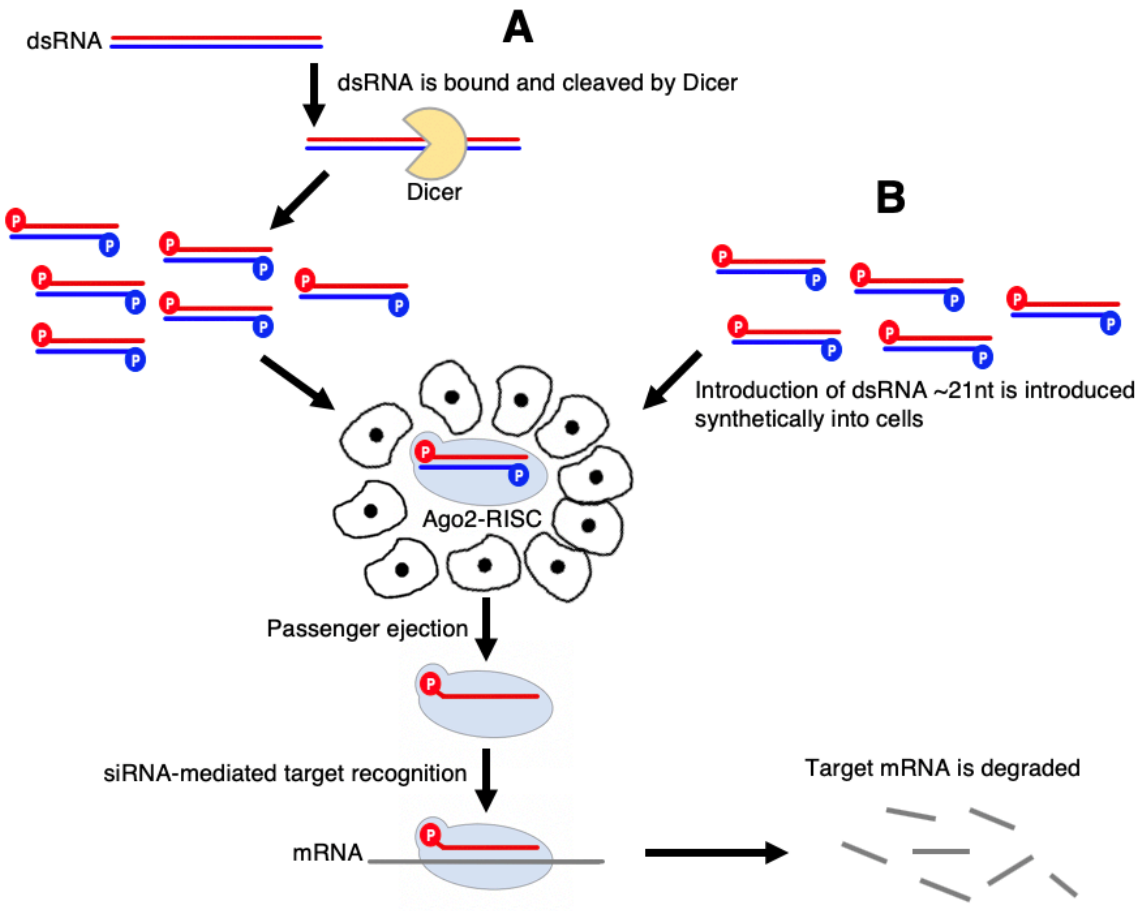

Figure 1. Pathway of the siRNA processing.

Initiation of the RNA interference by the siRNA pathway: The siRNAs, generated either by dicer cleavage of dsRNA into 21-nucleotide siRNAs (**A**) or by synthetic construction (**B**), are introduced into the cells, where they integrate into Ago2 protein forming the RNA-induced silencing complex (RISC). After expulsion of the passenger strand, the guide strand of siRNA drives RISC to the mRNA containing its complementary sequence, which triggers the cleavage of the target and the gene silencing. (Tuzmen et al, 2010 modified)

1.2.3.3 Origin of the siRNA: specific case of the endo-siRNAs

In siRNA mediated gene silencing, dsRNA is often exogenous (Exo-siRNAs) and derives from viral replication intermediates or experimental introduction of long or small dsRNAs. However, there are also dsRNAs with endogenous origin which can also trigger the siRNA mechanism via endo-siRNAs. In mammals, due to the absence of RNA-dependent RNA polymerase, dsRNA formation is possible in three genomic contexts **(Figure 2):**

(1) Convergent transcription on a locus (cis-NAT)

(2) Interaction between two complementary sequences transcribed by different loci such as transposable element sequences or pseudogenes (trans-NAT)

(3) Formation of a loop-rod RNA structure, distinct from the miRNA precursors, which can derive from the inverted repetition of a sequence.

In each of these cases, the dsRNA precursor enters in the "classical" or canonical siRNA mechanism by the action of the Dicer protein and allows the regulation of the target genes (Tam et al, 2008, Watanabe et al, 2006). The role of endo-siRNA is not restricted to antiviral action. A study in mouse oocytes has shown that the absence of Dicer and Ago2 proteins results in the de-repression of transposable elements (Watanabe et al, 2008). Endo-siRNAs have a redundant role in the piRNAs to protect germ line against transposable elements.

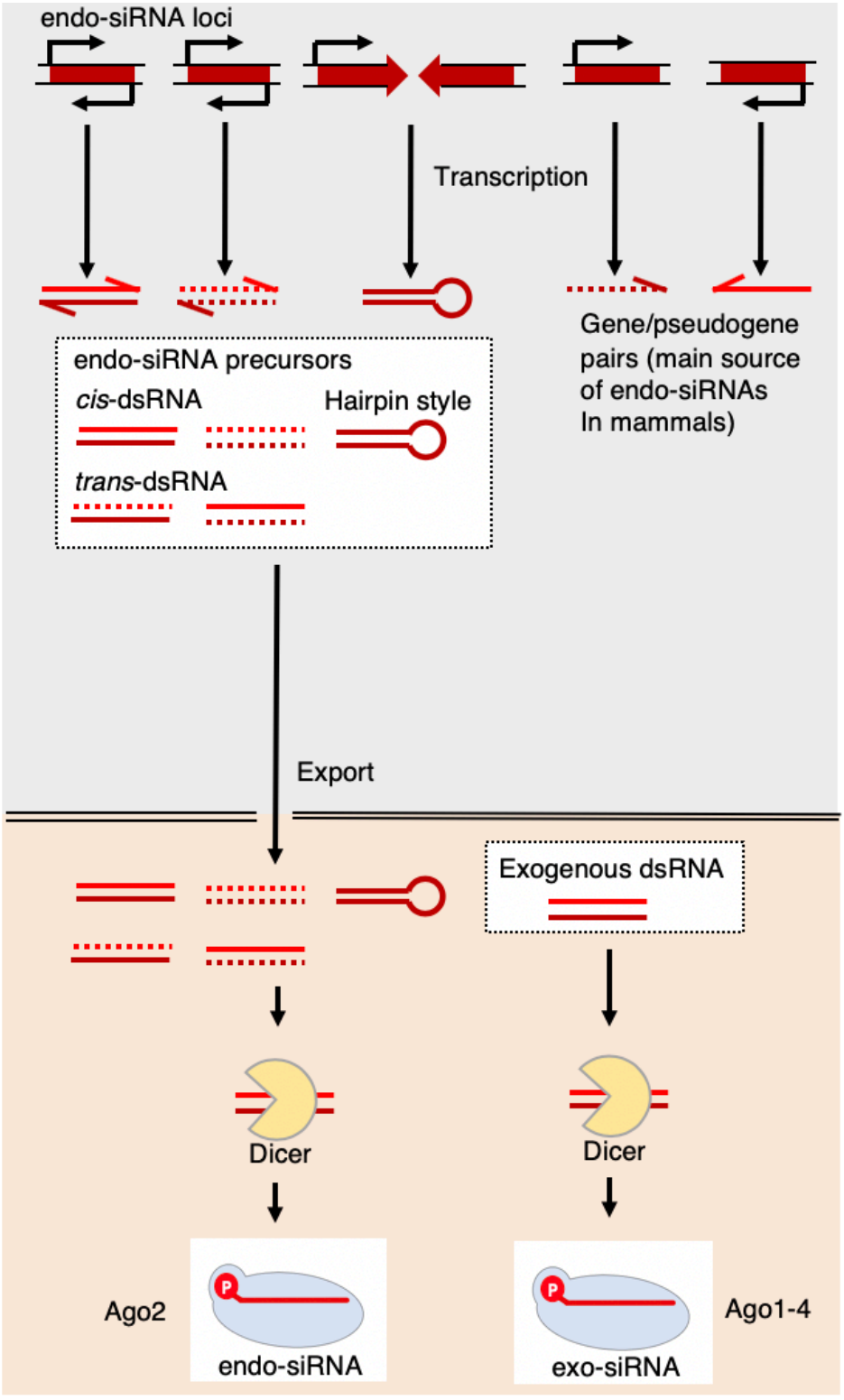

Figure 2. Potential origins of the endo-siRNA.
Endo-siRNA can be derived from convergent transcripts covering all or some parts of a gene. They can also be produced from transcripts forming loop rods as is the case for microRNA precursors. Finally, they can be derived from a reverse transcription occurring on a pseudogene then forming a sense / antisense pair. In all these cases, the precursor is supported by Dicer, which cuts it into a 21-base pair fragment and then incorporates it into the RISC complex. (Siomi et al, 2011 modified)

1.2.4 miRNA pathway

The regulation of microRNAs (miRNAs) differs from siRNA by the mechanism implemented, but also by the biogenesis of the small RNA. Indeed, unlike the siRNA mechanism which is triggered by the introduction of dsRNA and mainly from exogenous origin, the miRNA silencing involves a single-stranded endogenous sequence.

1.2.4.1 History of miRNA pathway

Historically, the first description of a miRNA was made by Ambros group showing that the lin-4 gene involved in the control of larval development in C. elegans does not encode any protein, but allows the accumulation of a small RNA (Lee et al, 1993). Genetics demonstrated that lin-4 negatively regulated the expression of several other genes via the 3' untranslated region of their mRNA. Knowledge of the lin-4 sequence made it possible to identify the presence of several partially complementary sequences in the 3 'untranslated region of target genes such as lin-14 (Lee et al, Wightman et al, 1993). In these studies the expression of the small RNA lin-4 has an impact on the amount of LIN-14 proteins without modifying the amount of mRNA. This finding suggests small RNA to be transcribed by the lin-4 gene and binds the 3'UTR region of the messenger RNA of the lin-14 gene blocking its translation.

Lin-4 RNA became the prototype of miRNAs (Lagos-Quintana et al, 2001). This is also the case of the gene let-7, another gene involved in the development of C. elegans which also allows the expression of a small RNA of 22 nucleotides (for the most abundant form) and has the same mode of action as miRNA lin-4 (Reinhart et al, 2000). Let-7 gene homologues have been identified in humans, Drosophila and other animals (Pasquinelli et al, 2000). This very abundant class of small RNA is involved in the regulation of many cellular pathways (differentiation, proliferation, apoptosis ...) in many organisms.

1.2.4.2 Detailed biogenesis of miRNA compared to siRNA

There are nearly 2000 genes encoding miRNAs in humans producing approximately 2500 mature microRNAs (miRBase database). These "miRNA" genes do not directly encode small RNAs but encode their precursors called pri-miRNAs (Lee et al, 2002). This primary transcript is in most cases a “transcript product” of the RNA Polymerase II and is capped and polyadenylated (Saini et al, 2007). Pri-miRNA sequences are also found in conventional gene sequences. Here, the sequence of the mRNA of the gene has the role of precursor. This case of miRNA "intronic" (misleading name because the sequence of the precursor miRNA is sometimes in the last exon) represents in average 50% of the miRNAs (Saini et al, 2007). In the case of "intron" miRNAs, the level of expression is often correlated with the messenger RNA host, indicating that the messenger RNA plays the role of pri-miRNA. Nevertheless, there are some cases where intern promoters of intron allows the transcription of pri-miRNA independent of the messenger RNA (Monteys et al, 2010). Regardless of its origin, pri-miRNA is a highly structured transcript that may contain one or more stem-loop structures ~ 70 nucleotides. Each of these stem-loops is going to be at the origin of a miRNA. miRNAs are often organized in clusters and thus pri-miRNAs are able to generate different miRNAs (Altuvia et al, 2005).

The first step of miRNA biogenesis is the cleavage of the pri-miRNA stem-loops at their base by a "micro-processor". This “micro-processor” complex is composed of Drosha (a dsRNA specific endonuclease of the RNase III family - other member of the mammalian family with Dicer) and DGCR8 (or Pasha in Drosophila) protein essential for the stabilization of Drosha on its substrate (Denli et al, 2004, Gregory et al, 2004). This complex allows the cleavage at 11-nucleotide of the stem-loop base to rise the pre-miRNA intermediate precursor (Han et al, 2004). Activity of the micro-processor complex occurs in the nucleus and the pre-miRNAs thus produced are supported by a transport pathway to the cytoplasm associated with exportin 5 (Lund et al, 2004, Yi et al, 2003). Exportin 5 is a protein of the importin β family that allows transport to the cytoplasm via the use of RanGTP as energy. It recognizes pre-miRNAs through the Drosha cleavage signature that generates a protruding 3'OH end of two nucleotides (Okada et al, 2009).

Once in the cytoplasm, Dicer will cleave pre-miRNAs and produce miRNA duplexes ~ 20 nucleotides. In mammals there is only one protein Dicer but in Drosophila there are two paralogs that are specialized: Dicer 1 is specific to the cut of pre-miRNAs and Dicer 2 is specific to dsRNA and silencing siRNA. In mammals, there is no indication that miRNA duplexes are preferentially integrated with a particular Argonaute protein. Nevertheless in the proposed model, only Ago2 has the ability to eliminate the "passenger" strand by hydrolysis. Other Argonaute proteins depend on destabilization of the duplex due to a mismatch. In contrast to the mechanisms involved in siRNA, miRNA has no indication of endonucleolytic hydrolysis of the target mRNA by Ago2 (except for the cleavage of HOXB8 mRNA) (Yecta et al, 2004) but rather degradation by the normal degradation pathway after de-adenylation and decay of RNA (Wu et al, 2006) **(Figure 3).** The translation inhibition does not allow to induce a de-adenylation of the transcript. It is therefore necessary for the miRISC complex to recruit other partner proteins. Destabilization of mRNA by miRNA occurs via a recruitment of the CCR4 / NOT complex in miRISC (in Drosophila, Behm-Ansmant, 2006, in mammals, Chen et al, 2009). CCR4 / NOT is a protein complex that plays a decisive role in the processive de-adenylation of mRNAs and therefore acts as "active" degradation. This de-adenylation of the message by the miRISC complex is accompanied by the recruitment of the DCP1 / DCP2 complex. This complex allows the removal of the 5' cap of the messenger RNA. The combination of these two complexes will then render the miRNA-targeted transcript sensitive to cellular exonucleases and allow its degradation (Chen et al, 2009).

The recruitment of these protein complexes passes through the GW182 family proteins (TNRC6 A, B and C in humans). This family of proteins is able to interact with Argonaute proteins via a repeated motif rich in Glycine-Tryptophan (GW) to which they owe their names (Till et al, 2007). The GW182 or TNRC6 protein act as a platform for the recruitment of all the factors necessary for deadenylation and decay. Artificial tethering of GW182 in Drosophila (Behm-Ansmant et al., 2006) and in mammals (Li et al., 2008) have shown the importance of this protein because this anchorage allows the induction of a silencing similar to a miRNA but independently of Argonaute proteins and miRNA (Lazzaretti et al, 2009). This indicates that GW182 is sufficient to provide the silencing function. GW182 proteins are present in the cytoplasm both in soluble

form but also in aggregates of proteins with nucleic acids called P-bodies (Processing Bodies, according to nomenclature initially introduced in yeast (Sheth et al, 2003)). These structures contain the enzymes of the RNA degradation machinery such as Xrn1 (the 5 'exonuclease present in the cytoplasm) or DCP1 (the mRNA decheting enzyme) (Eystathioy et al, 2003). The presence of Argonaute proteins have also been demonstrated in P-bodies, suggesting a role for these structures in small RNA regulation (Liu et al 2005, Sen and Bau 2005). However, the presence of mammalian cells and flies of detectable P-bodies do not seem necessary to trigger silencing by siRNAs and miRNAs (Serman et al, 2007), suggesting rather a role in storage, recycling or assembly components of the silencing machinery (Leung and Sharp, 2013).

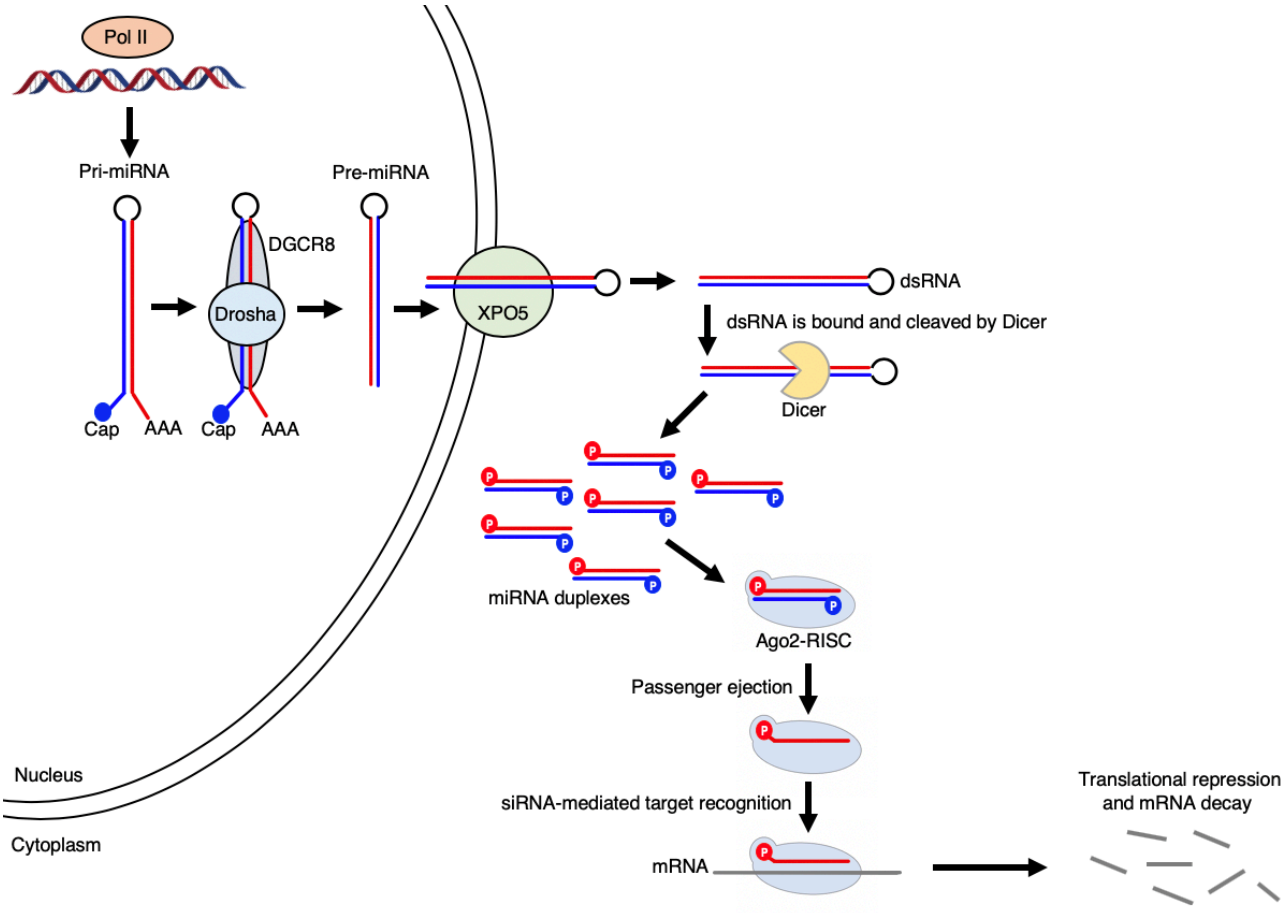

Figure 3. Canonical pathway of the microRNA.
miRNA genes are generally transcribed by a RNA polymerase II which produces a capped and polyadenylated transcript, the pri-miRNA. This pri-miRNA holding a stem-loop structures will be cleaved at its base by the RNase III Drosha associated with DiGeorge syndrome critical region 8 (DGCR8) to produce 60–70-nucleotide precursor miRNAs (pre-miRNAs). After exportation from the nucleus to the cytoplasm by exportin 5 (XPO5), the pre-miRNA is cut by Dicer a ribonuclease III to give a miRNA double strand of about 22 nucleotides. One strand of the mature miRNA (the guide strand in red) is loaded into the miRNA-induced silencing complex (miRISC) with Ago2 and allows to drive this effector complex on the target mRNAs by sequence complementary binding and mediates gene suppression by targeted mRNA degradation and translational. (Lin et al. 2015 modified)

2. RISC machinery, heart of the RNA silencing

After describing two RNA silencing pathways in detail, I would like to focus on the heart of the RNA silencing composed with the RISC machinery in the next chapter.

2.1 Composition of the RISC machinery: Ago2 core of the RISC assembly

Proteins of the Argonaute family detailed before in this dissertation are often in large numbers in eukaryotic genomes. There are 26 in C. elegans, 10 in A. thaliana, 5 in D. melanogaster and 1 in S. pombe and 8 in humans.

Even though Ago 1–4 are capable of loading miRNAs, the activity of endonucleases belongs exclusively to Ago2. Although it has been shown that Ago 3 also has a slicer activity, this activity depends on the guide RNA and that limits this slicer-activity (Park et al 2017). This diversity of Argonaute proteins reflects the complexity of RNA silencing in each organism. Despite the diversity of small RNA pathways in eukaryotes, all small RNAs are loaded into RISC. The structure and proteins involved in this complex vary by pathway and species, but it contains at least one Argonaute-like protein (Kuhn & Joshua-Tor 2013). dsRNA will drive Argonautes towards its target (a long single-stranded RNA) which will induce its degradation or block its translation, deadenylation or decay. Argonautes are therefore essential proteins for the function of RNA silencing**.**

2.2 Architecture of Ago2

2.2.1 Different domains of Ago2

Argonaute proteins are characterized by four main domains: PAZ domain, MID domain (in the middle), the PIWI domain and the N domain. The PAZ domain has the function of fixing the 3' end of the RNA, the MID domain is anchored to the 5’ phosphate of the guide strand and the PIWI domain has a structure close to RNase H and carries the function of cleaving targeted RNA, called slicing **(Figure 4)**. 4 catalytic amino acids forming the DEDX motif (X being D or H) are conserved in most PIWI domains (Kuhn & Joshua-Tor 2013) (Schirle et al, 2012), (Nakanishi et al, 2012)**.**

In C. elegans, there is a third family of Argonaute proteins as far apart from PIWI as Ago and specific to nematodes: WAGO (Argonaute worms) (Meister 2013).

WAGOs are a family of 12 proteins involved in the management of secondary siRNAs (Yigit et al 2006, Gu et al 2009).

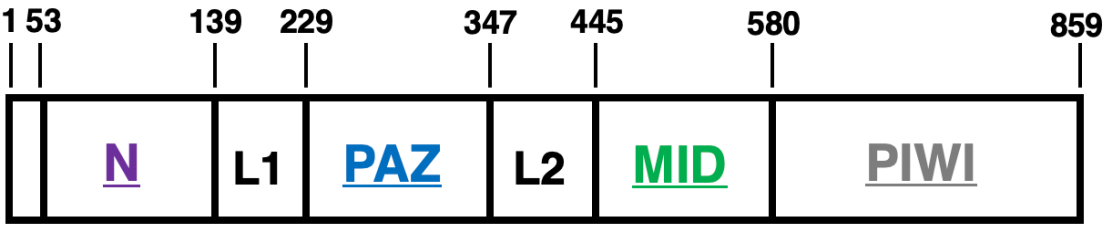

Figure 4. **Schema of Ago2 primary sequence.** (Schirle et al, 2012 modified)

2.2.2 Structure of Ago2

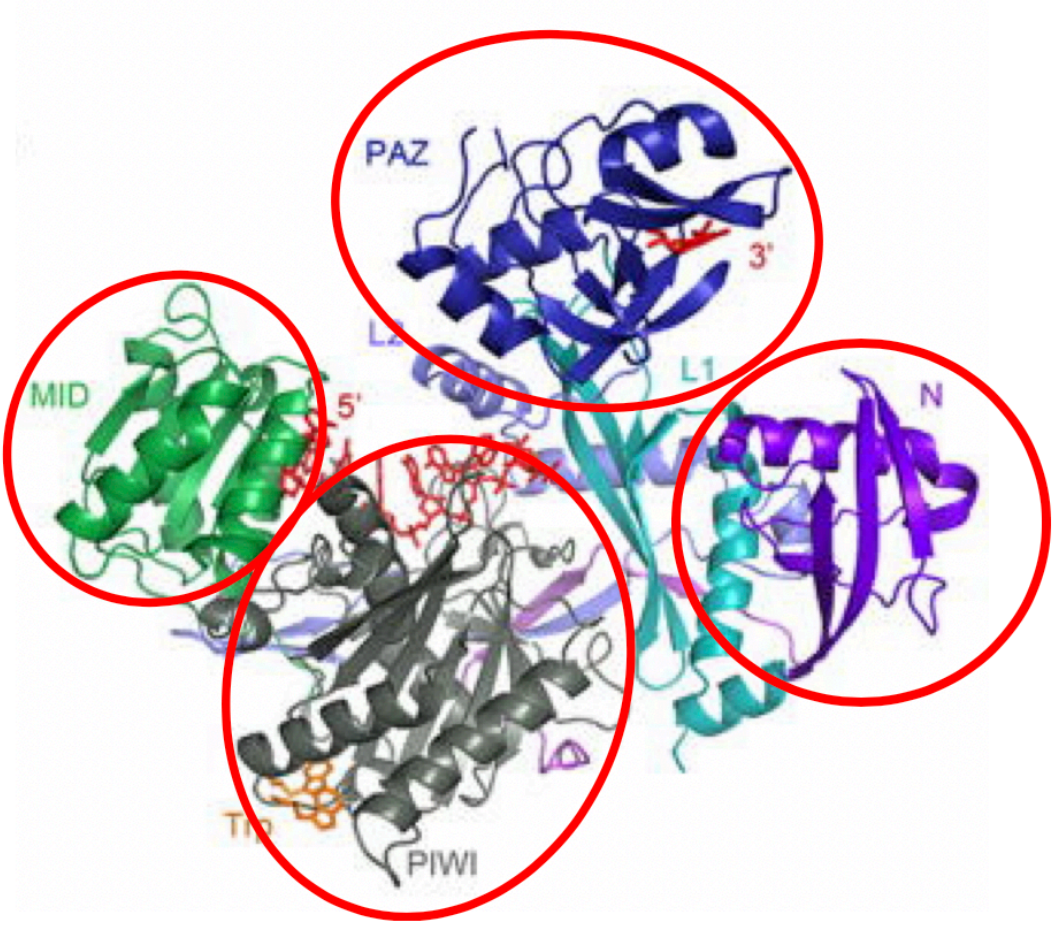

Figure 5. **Ago2 crystal structure showing the four domains.**
In red circles: PAZ (Dark blue), N (purple), PIWI (grey), MID (green). RNA guide (in red) is also shown and traced for nucleotides 1–8 and 21. (Schirle et al, 2012 modified)

2.3 The RISC assembly

RISC assembly is divided in two major steps before the silencing of the target: loading and maturation.

2.3.1 Loading RNA duplex into Ago Protein

Dicer produces a dsRNA of 21 to 28 nts. These siRNA duplexes produced are later loaded into Ago with the help of Hsc70/Hsp90 chaperone machinery (Tsuboyama et al, 2017). In plants, HSP70/90s are necessary in vitro for the functioning of RISC complexes. A dimer of HSP90 can bind Ago1 (step 1) to induce a conformational change and allow dsRNA binding (step 2). Once Ago1 is loaded, the hydrolysis of ATP induces the release of HSP90 (step 3) and the return to the initial configuration of Ago1. This can trigger the cleavage of the passenger strand (step 4) (Iki et al, 2010). A similar mechanism has been described in D. melanogaster (Iwasaki et al, 2010). Finally, in human cell lines, HSP90 chaperone proteins are also critical to the stability of the RISC complex prior to siRNA loading. After treating with geldanamycin, an HSP90 inhibitor, the abundance of miRNAs is maintained but the loading of siRNAs into Ago2 is strongly affected (Johnston et al, 2010). Then, the strand loaded into Ago will be the guide strand and the other strand maintained by the pairing of bases will be the passenger strand. The passenger strand will be ejected later leaving the guide strand loaded in Ago alone. In flies, mismatches in the miRNA precursors will induce their loading on specialized miRNAs Argonautes while the mismatch-free duplexes will be loaded into the siRNA pathway argonautes. This is the case, for example, in D. melanogaster where Ago1 loads miRNAs.

2.3.2 Maturation selection and elimination of the passenger strand

The main selective criteria for the guide strand (whether miRNAs or siRNAs) is thermodynamic. Strand of the duplex with less stable 5' end is preferentially loaded in Ago proteins. Depending on where in the strand, a simple additional hydrogen bond is sufficient to make the guide strand and decide which siRNA strands directs RNAi (Schwarz et al., 2003). In addition, loading in Ago requires the guide strand phosphorylation (Nykanen et al, 2001). In the siRNA pathways, the separation of the two strands of the duplex is dependent on the endonucleolytic cleavage of the

passenger strand. The Piwi domain is able to cut the phosphodiester bond of the passenger strand of siRNAs duplexes which greatly reduces thermodynamic stability of the duplex and facilitates its separation (Kwak & Tomari 2012). In contrast in the miRNA synthesis pathways, the mismatches between the two strands prevent cleavage and the passenger strand is separated from the guide strand without being cleaved. In both cases, the N-terminal domain of Ago is particularly important in the separation of the two strands (Kwak & Tomari 2012) **(Figure 6).** In D. melanogaster, mammals and plants Ago2 is able to cleave the passenger strand into 9 and 12 nts fragments which are then removed from the RISC.

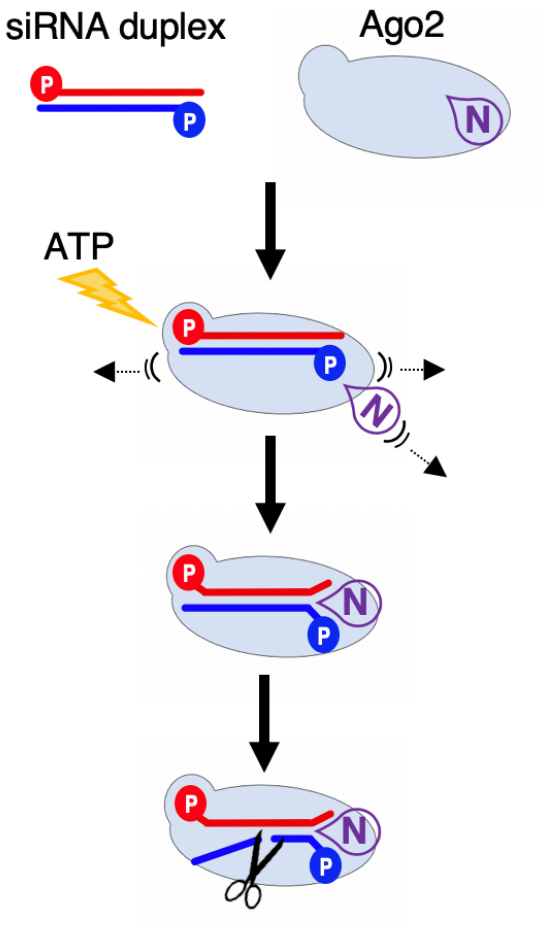

Figure 6. Model for assembling RISC in humans.
After loading of the siRNAs duplex into Ago, the N domain of the protein initiates duplex opening. The opening requires cleavage of the passenger strand. (Kwak & Tomari 2012 modified)

3. siRNA and therapeutics: Where are we now?

3.1 Application of siRNA in therapeutics

3.1.1 siRNA as biological tool

The number of genes in the 23 pairs of human chromosomes is estimated at 20,000 to 30,000 (Novina and Sharp, 2004). Now, the genome is sequenced and decryption of these genes function is an immense task to accomplish (Harborth et al, 2003). To this end, a number of technologies have been developed: the analysis of genes can be carried out by studying their expression at the cellular level under given conditions (proteomics, cDNA chips, etc.) or by studying the repercussion of the extinction of a given gene. This mode of studying the functionality of a gene is based on several techniques, including the "Knock Out" (KO) which consists of extinguishing the expression of a gene by homologous recombination. Another frequently used technique is to specifically direct mutations at a gene, making it possible to understand its role.

By using the RNAi mechanism, we can thus study the function of the genes of any organism in a simpler and faster way than with the techniques employed till now. This was for example easily done in C. elegans by feeding it directly to bacteria expressing dsRNA (Timmons et al, 1998, Timmons et al, 2001) and injecting nucleic acids into the cavity of their body or by soaking them in a solution of these same RNAs (Tabara et al, 1998). Thus, 19000 genes of this worm have already been studied thanks to a set of 12000 dsRNA to try to apprehend the problems of obesity and aging (Novina and Sharp, 2004). In Drosophila, it has been studied cholesterol metabolism, heart formation, embryonic development and other basic cellular processes using this technique (Kuttenkeuler et al, 2004).

3.1.2 siRNA as tool for validating therapeutic targets

Although genomic approaches allow a gene to be associated with a disease phenotype (Wianny et al, 2000), these data alone cannot define the role of protein encoded by this gene in the pathological process. The development of KO mice is a good way to study the relationship between a biological gene and a disease, since KO phenotypes show a good correlation with drug efficacy (Zambrowicz et al, 2003).

However, the cost and time involved in the development of such models indicate the need to develop methods to validate in vitro targets before starting in vivo studies (Rondinome et al, 2006). Given the success of RNAi in studying gene function in lower eukaryotes such as C. elegans or D. melanogaster, it is not surprising that this approach has been adopted to analyze the function of genes, and particularly the validation of targets in mammalian systems (Rondinome et al, 2006). Indeed, the pharmaceutical industry is flooded with new genes whose functions are poorly understood and constitutes thousands of potential targets (Usman 2004). The use of the RNAi mechanism is very attractive in this context since it is fast, reproducible, efficient and simple to implement on cellular systems. In addition, this technique can be adapted to any target, knowing that a priori, only the mRNA sequence information is needed to design the dsRNAs. These are now easily accessible, thanks to advances in oligonucleotide chemistry (Usman 2004).

3.1.3 siRNA: applications in therapeutics

The growing interest of researchers for this powerful tool did not stop there. It plans to use RNA interference for a therapeutic purpose (Wall et al., 2003). RNA interference mechanism will develop treatments trying to avoid side effects. It has been shown that a single mismatch between the siRNA and messenger RNA sequences abolishes extinction (Amarziguioui et al, 2003). In addition, these treatments have an ease of synthesis and low dosage in comparison to therapeutic tools based on proteins or antibodies (Leung et al, 2005).

3.1.3.1 Viral diseases

Since RNAi appears to be an ancient anti-viral defense mechanism in insects, the inhibition of virus replication has been considered a good starting point for the evaluation of the therapeutic potential of this strategy. Viral RNAi replication has been demonstrated in vitro for a wide variety of viruses including RNA viruses such as HIV, rotavirus, respiratory syncytial virus, influenza virus, poliovirus, as well as viruses. DNA such as papillomavirus or herpes virus (Herpes Simplex Virus, HSV) (Golzio et al, 2004). The RNAi mechanism has also been shown to be effective in inhibiting hepatitis B and C viruses (Radhakrishnan et al, 2004). Although most of these studies

have been conducted in vitro, promising results have been obtained to inhibit viral multiplication in mice, particularly with respect to hepatitis B virus (Giladi et al, 2003), influenza virus (Tompkins et al, 2004) or other respiratory viruses (Bitko et al, 2005).

3.1.3.2 HIV

Among the viral diseases, there is a particular one which represents a great challenge for the researchers, it is the infection with HIV. Although many antiviral molecules have already been developed, it is commonly observed that the resistance of the strains to the prescribed drugs is increased (Little et al, 2002) which is why it is necessary to persevere in the search for new treatments. The phenomenon of RNA interference since its discovery brings a lot of hope. siRNAs can interfere with different stages of the intracellular cycle of virus replication (Kitabwalla et al, 2002). However, this strategy also has its limits given the behavior of the virus. Indeed, it is enough for a difference of one base pair between the target sequence and the siRNA to drastically reduce the effect, whereas the reverse transcriptase has a high error rate, estimated at 1/1000 per replication cycle. On another hand, there is a great diversity of sequences between infected individuals, so the design of efficient siRNAs is complicated. A more realistic approach seems to target the receptors or co-receptors that the virus uses for HIV infection (Kitabwalla et al, 2002).

3.1.3.3 Cancers

Cancer cells express proteins that differ qualitatively and quantitatively from those of normal cells, and in some cases the tumor cell may even express a protein that does not exist naturally in the cell. We therefore see the interest of the specific inhibition of target proteins in anti-cancer therapy. On another hand, the absence of specific miRNA has been demonstrated in carcinoma cells, implying that cancerous development can be stopped by introducing these missing miRNAs (Agrawal et al, 2003). Growth and survival of tumor cells have been inhibited using RNAi to target several key oncogenes or tumor-promoting genes, including angiogenic and growth factors, or their receptor (vascular endothelial growth factor, epidermal growth factor receptor), human telomerases, viral oncogenes or translocated oncogenes (Friedrich

et al, 2004). This tumor growth inhibition potential has also been demonstrated in vivo (Duxbury et al, 2004).

3.1.3.4 Other diseases

The high sequence specificity of the RNAi mechanism reveals a very promising approach to inhibit the expression of genes responsible for neurodegenerative diseases, such as Alzheimer's disease, Huntington's disease or spinocerebellar ataxia, for which there are no treatment yet (Shankar et al 2005). Another major application of RNAi extinction is the treatment of age-related macular degeneration (AMD). Indeed, the eye is one of the most accessible and supportive tissues for local administration of siRNA (Usman 2004). The molecular target (the vascular endothelial growth factor (VEGF)) in the treatment of this disease is clinically validated for a long time. (De Fougerolles et al, 2007). However, all these new treatments developed above were just promising until the case of the hATTR proved siRNA as a new therapeutic.

3.1.4 Application of siRNA: Clinical aspect

Since its discovery in 1998 and the identification of the various elements involved, the field of siRNA has been booming. Given the relative youth of siRNA, there are already a remarkable number of in vivo studies published to describe the pre-clinical development of therapeutic siRNAs, or siRNA-based methods to validate therapeutic targets for small molecules (Behlke et 2006, Kim et al 2007). Large pharmaceutical companies and the academic world have hastened to exploit the prowess of siRNA to accelerate the discovery and validation of new drug molecules while biotechnology companies have preferred to place their hopes in the development of innovative therapeutics. This boom in siRNA has led to the creation of new “start-ups” in the field (Alnylam in 2002) and also changes in the orientation of certain companies previously specialized in ribozyme research or anti-sense strategy (Sirna Therapeutics in 2003). Subsequently, some large pharmaceutical companies joined biotechnology companies establishing collaborations for the development of new therapeutics (Novartis, Merck, etc.). More than 30 pharmaceutical or biotechnology companies declared to have an interest or programs in ongoing development of siRNA therapies.

(Behlke et 2006). The evolution in the development of new therapies has been rapid since siRNA technology has progressed. In barely 6 years, it has advanced from in vitro cell culture trials to the stage of human clinical trials. First clinical trial started at the end of 2004 to patients suffering from AMD. This rapid progression is unprecedented in medicine and proves the fabulous potential of RNAi in therapy. However, given the difficulties in developing effective transfection methods, the first trials mainly concerned pathologies for which administration of siRNA is possible and easy. Thus, there are treatments for ocular pathologies: the eye being accessible to local injections and respiratory pathologies: the lungs can be reached by the upper airways. Likewise, liver disease is subject of therapeutic trials, since it is an organ naturally involved in the biodistribution of siRNAs.

The siRNA technique therefore opens up unprecedented perspectives in the field of specific inhibition of gene expression which can be used to develop new therapeutics for humans. However, there remains major obstacle to the widespread use of siRNA: having an effective technique for delivering siRNAs. Indeed, for therapeutic applications challenges are stability, biodistribution, targeting, cell penetration of siRNA or induction of possible side effects. This implies having recourse to suitable systems and the research efforts of scientists have already made it possible in order to develop therapeutics based on siRNA which are currently under clinical evaluation. For the most advanced, concerning the treatment of age-related macular degeneration, clinical trials are already in phase III. However, many questions remain regarding the use of siRNA for the treatment of human disease. Chronic diseases like hepatitis C or HIV require long-term treatment, and there is still not enough time to review the potential effects of repeated or prolonged use of siRNA on normal cell metabolism. It is quite conceivable that such toxic effects will not be revealed for months or even few years. Although it seems very promising, big pharma and startups struggles to make siRNA technology efficient and safe requiring numerous studies (and clinical trials) in order to ensure its effectiveness not only in defined applications but also its overall harmlessness to the body.

3.1.4.1 siRNA, U turn toward a revolution in therapeutic: Case of the hATTR

Hereditary amyloidosis is a particularly rare and aggressive disease affecting about 50000 patients in the world. It is due to the accumulation in the nerves and organs of a mutated protein that causes loss of sensitivity and mobility, pain, digestive heart and sexual disorders. The disease begins in adulthood and causes death 4 to 10 years later. Until now, the best treatment available only allowed to curb 25% of the disease. For the remaining 75%, the treatments were purely symptomatic: a cane, orthopedic shoes or painkillers. The first drug announced in August 2018 by Alnylam (the American biotech who developed it); a new therapeutic class based on a natural mechanism silencing a harmful or disordered gene; has been approved by the American and European market. They named it Onpattro (patisiran from the name of its molecule). This medicine is prescribed to treat hereditary transthyretin amyloidosis (hATTR) in adults, a rare potentially life-threatening and potentially life-threatening genetic disorder affecting approximately 50,000 people in the world **(Figure 7).** The green light from the European Commission came less than three weeks after an initial authorization to market Onpattro in the United States for the same indication. Onpattro is based on the principle of siRNA mechanism discovered in the late 1990s. This mechanism already developed previously in my thesis makes it possible to prevent the mRNA from transmitting the order of a defective gene to produce abnormal proteins.

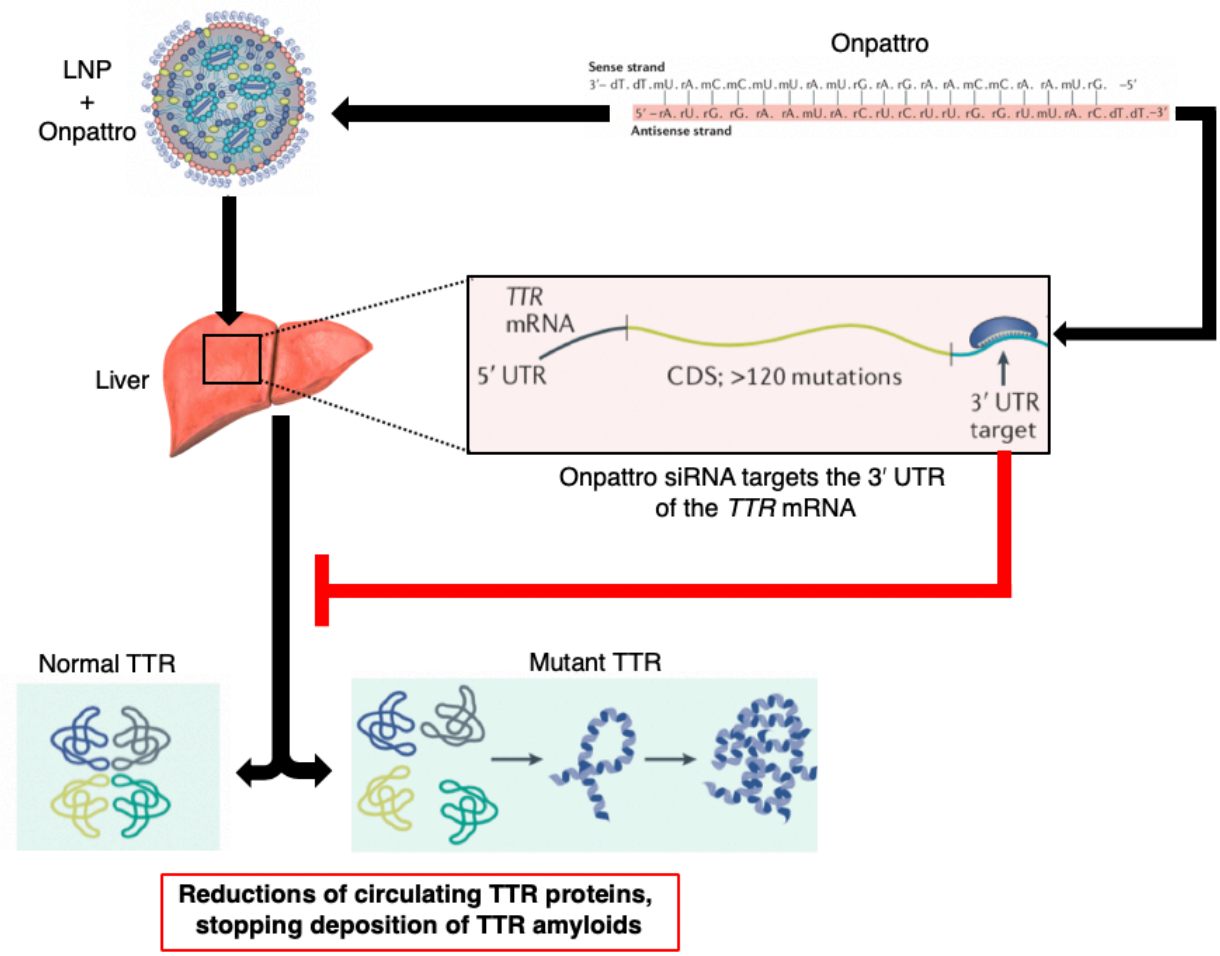

Figure 7. mechanism of patisiran in therapeutic.
Onpattro (Patisiran) is a small interfering RNA (siRNA) packaged in Lipid Nanoparticules (LNP). Patisiran's siRNA targets the 3′ untranslated region (UTR) of the *TTR* mRNA, inhibiting both production of the mutant and the normal TTR. RNA interference (RNAi) silencing results in reductions of circulating TTR proteins, stopping deposition of TTR amyloids and slowing the disease progression. (Setten et al, 2019 modified)

3.2 Improvement of siRNA therapeutic: the use of chemical modifications

After the success of Patisiran, Alnylam and other biotech companies around the world are digging the trail of this new therapeutic weapon for many other indications such as cancers, hepatitis B, cardiovascular, ophthalmological, renal or even neurodegenerative diseases like Alzheimer's. However, the cost of treatment, which required more than 15 years of development, has been set at $ 450,000 per patient per year in the United States, making it one of the most expensive treatments in the world.

On this purpose, siRNA drugs still have room for improvement, particularly in their efficacy and stability to reduce the dosage and the cost. The key for such amelioration is chemical modifications of siRNAs. A good example of chemical modification is Patisiran where both small RNA strands are heavily but not totally modified with 2′-*O*-methylation in order to improve the stability and the silencing activity (Adams et al, 2018). Nevertheless, there are different patterns of strategy for chemical modifications and I will briefly detail them below.

3.3 Different types of chemical modification

Below are described the most common chemical modification used to improve siRNA:

3.3.1 Phosphate backbone modifications

The phosphates forming the backbone of the nucleic acids can undergo chemical modifications, in particular on the P=O double bond (Guo et al, 2010).

Phosphorothioate: The use of sulfur to substitute the P=O bond with the P=S bond. Cytotoxicity was observed when P=O were largely or completely replaced by P=S in siRNA (Stessl et al, 2009).

Boranophosphate: It is also possible to use boron and form P=B bonds instead of P=O bonds. This makes possible to significantly increase the resistance of siRNA to nucleases without altering its quenching power even when the bore is placed on the terminal phosphate or phosphates of the sense strand (Hall et al, 2004).

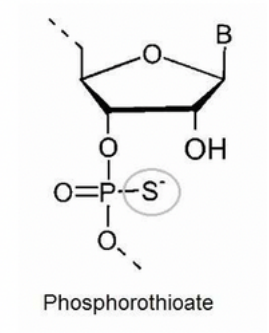

Figure 8. Phosphate backbone modifications, example with the Phosphorothioate (B=Base)

3.3.2 Ribose modifications

Numerous ribose modifications have been described in particular on the 2' carbon (Adams et al, 2018, Egli et al ,2019), normally carrying a hydroxyl group. It can be the following substitutions: 2'-O-methyl, 2'-halogen such as fluorine or 2'-amine. Hydroxyl group at 2 'can also be removed (2'-deoxy). Finally, the nucleic acid can be "blocked" by a 2'-O-CH 2 -4 'bridge or "unblocked" by breaking the 3'-2' bond

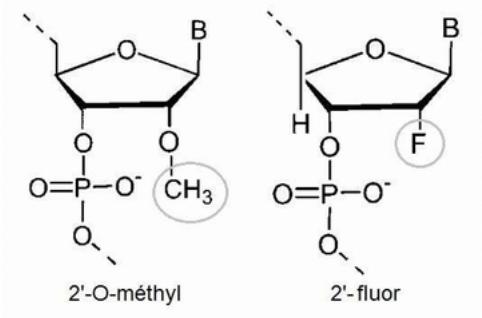

Figure 9. Ribose modifications, example with the 2'-O-methyl and the 2'-Fluorine (B=Base).

3.3.3 Termini 5’ and 3’ modifications

siRNA endpoint modifications positioned at the 5’ or 3’ of the guide or the passenger strand involve the binding of ligands such as folate, cholesterol, biotin (vitamin B8), streptavidin fluorescent molecule or the modification of the phosphate. Various studies report that the 5 'and 3' terminal modifications of the sense or passenger strand are well tolerated and retain the functionality of siRNA (Bumcrot et al, 2006). For example, conjugation of cholesterol or folate at the 3 'end of the sense strand allows for selective

distribution to the liver and jejunum or cancer cells respectively (Lorenz et al., 2004, Guo S et al., 2006, Elkayam et al, 2016). These molecules are considered addressing molecules. Another chemical modification for siRNA less common is mentioned below for information:

3.3.4 Nucleobase modifications

Different groups can be added to the nucleotide bases of siRNA nucleotides to form 2,4-difluorotoluyl, 5-bromo-uridine, 5-iodo-uridine, 4-thiouridine, N-3-methyl-uridine, 2,6-diaminoguanine (Parrish JZ and Xue, 2003). In C. elegans, siRNAs synthesized with uridines containing a C4 sulfur or C5 bromine retained their quenching power while C5-3-aminoally uridines deactivated them completely (Parrish JZ and Xue, 2003). For other groups, it appears that the modified nitrogenous bases are more tolerated in the sense or terminal strand than on the antisense strand in the central region (Parrish JZ and Xue, 2003).

4. 5'-end modification of the siRNA guide strand: story of 6-(3-(2-carboxyethyl)phenyl)purine (6-mCEPh-purine)

In a previous study describing the crystal structure of the MID domain of human Ago2, Frank et al. found that AMP and UMP bind up to 30-fold higher affinity than CMP or GMP in the 5'-end nucleotide binding pocket of Ago2 **(Figure 10)**. Based on this finding, we hypothesized that chemically modifying the 5' end base of the guide strand can be an effective strategy to increase the affinity of the siRNA duplex in Ago2's pocket and lead to an enhancement of siRNA knockdown potency **(Figure 11)**.

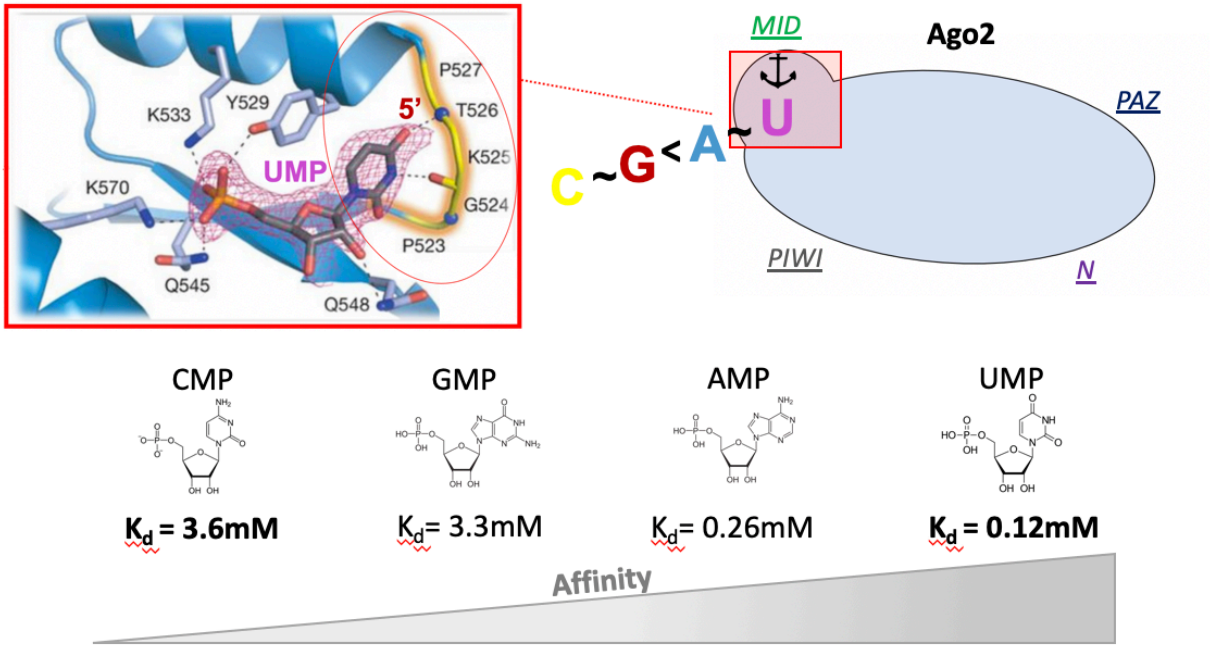

Figure 10. AMP and UMP bind with up to 30-fold higher affinity than either CMP or GMP in the 5'-end nucleotide binding pocket of Ago2.
Using different monophosphate nucleotides and using Nuclear Magnetic Resonance (NMR) spectroscopy, it was showed UMP & AMP bind with up to 30-fold higher affinity than either CMP or GMP. (Frank et al, 2010 modified)

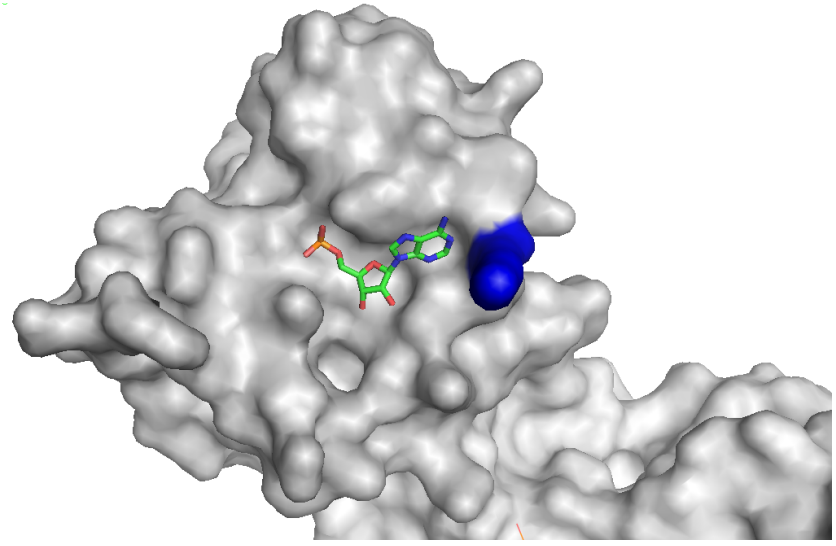

Figure 11. Pocket of Ago2 in the MID domain with AMP.
Modification of the 5' end base of the guide strand could be an effective strategy to increase the affinity of the siRNA duplex in Ago2's pocket.

For this purpose, collaborators at Kyowa Kirin have performed an in-silico screening of modifications at the 5'-end base of the guide strand. This analysis suggested a potential usability of the empty space around the 6th position of the adenine nucleobase **(Figure 12)** which seemed to be suitable to be targeted for additional interaction. Based on these notions, "6-mCEPh-purine", an adenine-derived nucleotide analogue bearing a hydrophobic moiety and an acidic functional group at the position 6 was designed to fill in the empty space **(Figure 12)**. Strikingly, our collaborators have found that the "6-mCEPh-purine" compound can enhance the RNAi activity by ~3 fold in cultured human cells as well as in vivo mouse models.

As developed above, it is critical to understand the precise effect of chemical modifications on the assembly and function of RISC to ameliorate siRNA therapeutics. For this purpose, my research presented below aims at deciphering which mechanistic step in the RNAi pathway 6-mCEPh-purine chemical modification enhances the siRNA potency to complete the cell-based and in vivo studies by Kyowa Kirin.

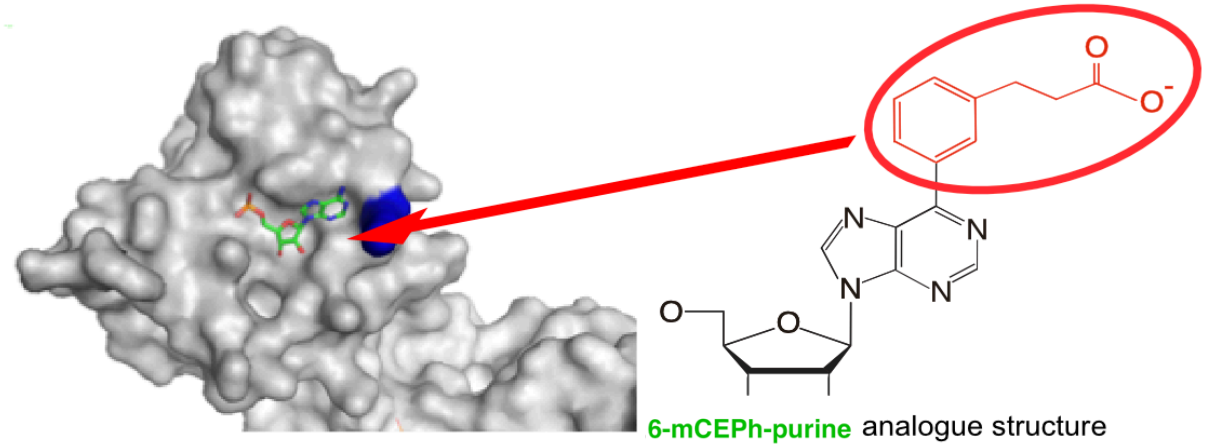

Figure 12. Design of new nucleo-based chemical modifications.
Using Structure Based Drug Design, our collaborator Kyowa Kirin synthesized AMP derivatives at the position 6th to fill the empty place in the MID domain pocket expecting to achieve new interactions. Amongst ~ 200 different derivatives, the analogue called 6-mCEPh-purine which hold the chemical modifications shown in red was selected.

III. Results

1. Material preparation

In order to study the mechanism of this modification properly, it was important to prepare all the necessary materials. These materials include three main parts with the cell lysate from HEK293T cells where Ago2 is overexpressed **(Figure 13A)**. The target RNA cap-radiolabeled at the 5' end for the cleavage assay **(Figure 13B)** and the five siRNA duplexes which bore different nucleotides (A, U, BrdA, 6-mCEPh-purine or G) at the 5′ end of the guide strand **(Figure 13C).** When the guide strand was radiolabeled at the 5' end, the radioactivity level was sometimes slightly different amongst the different nucleotides but always adjusted and normalized by the addition of MQW. The different mobility of the nucleotides on the gel is due to the different chemical structure amongst them **(Figure 13C).**

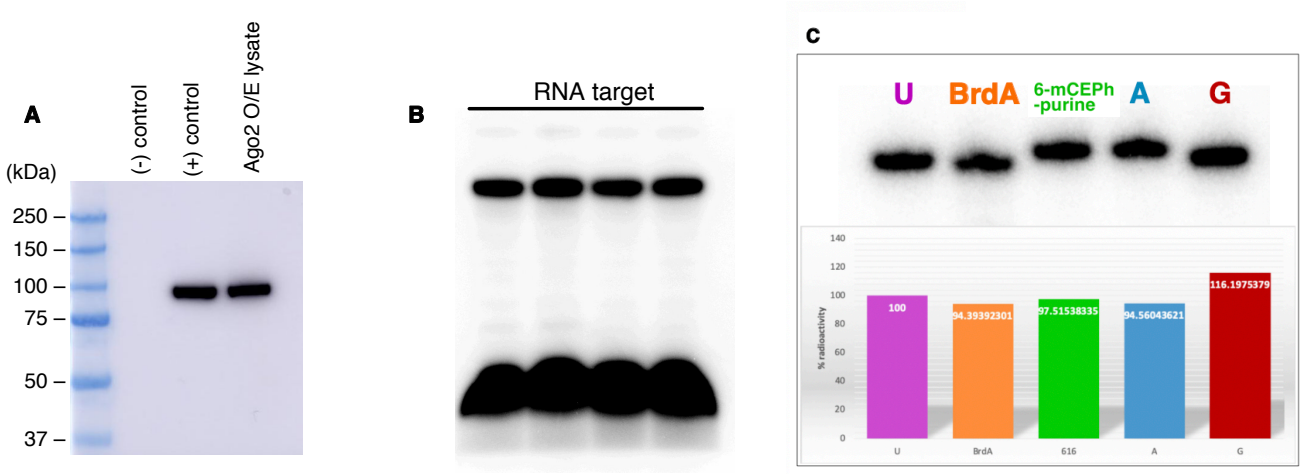

Figure 13. Material preparation.
(A) Western Blot showing Ago2 O/E lysate in HEK293T cells compared to a positive and a negative control. (B) UREA gel showing the preparation of the target RNA used for the cleavage assay (the four lanes represent different samples of the same target). (C) Example of radioactive signal normalized amongst the different duplexes radiolabeled used (here are represented the duplexes radiolabeled at the guide strand).

2. Study of 6-mCEPh-purine modification

2.1 The target cleavage activity is enhanced by the 6-mCEPh-purine modification

As a primary point to understand how 6-mCEPh-purine modification affect the enhancement of the RNAi *in vitro*, I first wanted to perform a cleavage assay which is an easy well-known experiment. However, it was primordial first to set up the condition of this experiment to obtain the most accurate result possible. Dilution of the lysate was a key point **(Figure 14).** A 5′ cap-radiolabeled target RNA bearing a complementary sequence to the guide strand **(Figure 14B)** was prepared and added to the mixture. To assemble RISC, I incubated the siRNA duplex with a 5′ adenine (A) as guide 5′-end nucleobases **(Figure 14A)** in the lysate of Ago2 over-expressed in HEK293T cells. I then added the target RNA and examined the time courses of the target cleavage reaction at different dilutions. The dilution of the lysate 1/5 showed the best resolution **(Figure 14C).** Then the target cleavage assay using a series of siRNA duplexes bearing A, U, 6-mCEPh-purine, BrdA or G at the 5′ end of the guide strand (**Figure 15A**) was done. However, the base-pairing and the thermodynamic stability of the different siRNA duplexes is undeniably changed when the 5' end of the nucleobase is modified. The consequence to have different siRNA duplexes with different 5' end will affect which strand of the duplex is picked as guide strand in the incorporation of Ago2. In order to adjust and balance this effect, I decided to introduce a universal base called 5-nitroindole to the position 19 of the passenger strand. This universal base is recognized to link in front of the 5′ end of the guide strand (Loakes et al, 1994, Kawamata et al, 2011). Additionally, to directly monitor the cleavage, the target RNA which carries a sequence complementary to the guide strand of the duplex was 5′ cap-radiolabeled **(Figure 15B)**. To make RISC assembly (**Figure 15B**), I incubated four different siRNA duplexes holding A, U, 6-mCEPh-purine and G at the 5' end of the guide in the lysate from HEK293T cells where I overexpressed Ago2. Next, I added the radiolabeled target RNA and monitored the reaction at different defined time courses. As expected, 6-mCEPh-purine exhibited a stronger signal for the target cleavage activity compared to the other nucleotides **(Figure 15C and 15D)**. This outcome confirmed the previous results showing the efficiency of 6-mCEPh-purine modification found in cells and *in vivo* by our partner Kyowa Kyrin.

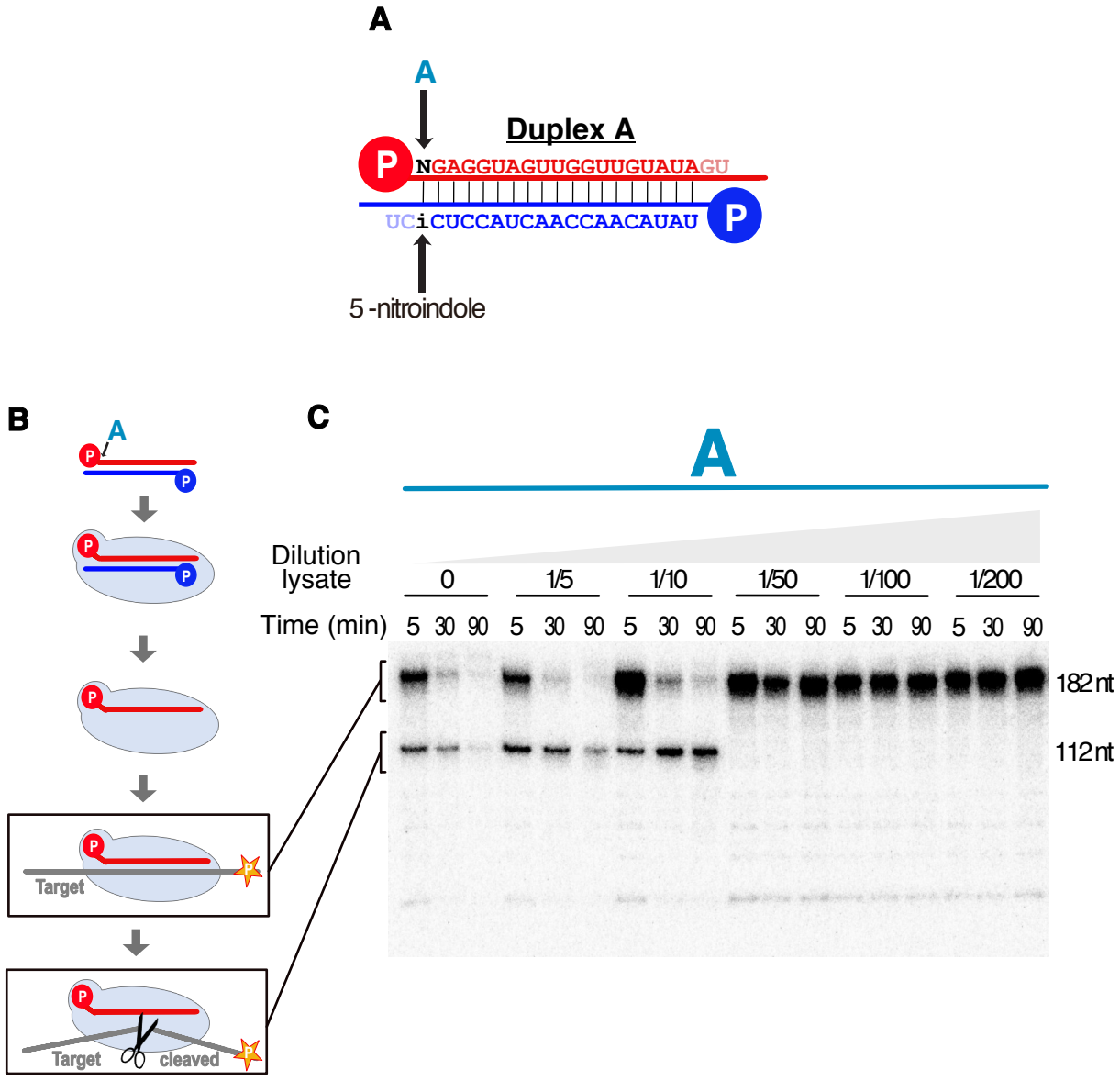

Figure 14. Effect of the lysate dilution during the cleavage assay.
Best resolution for a cleavage assay using the appropriate dilution (1/5) is shown here. (A) Duplex A (no radiolabeled) was used in this set of experiments. It bore a nucleotides A at the 5′ end of the guide strand and 5-nitroindole at position 19 of the passenger strand. Both the guide and passenger strands had a 5′ monophosphate. (B) Scheme of RISC assembly and target cleavage. The target RNA was 5′ cap-radiolabeled. (C) A representative result of the target cleavage assay after different dilutions. The upper and lower bands correspond to the full-length and cleaved target, respectively.

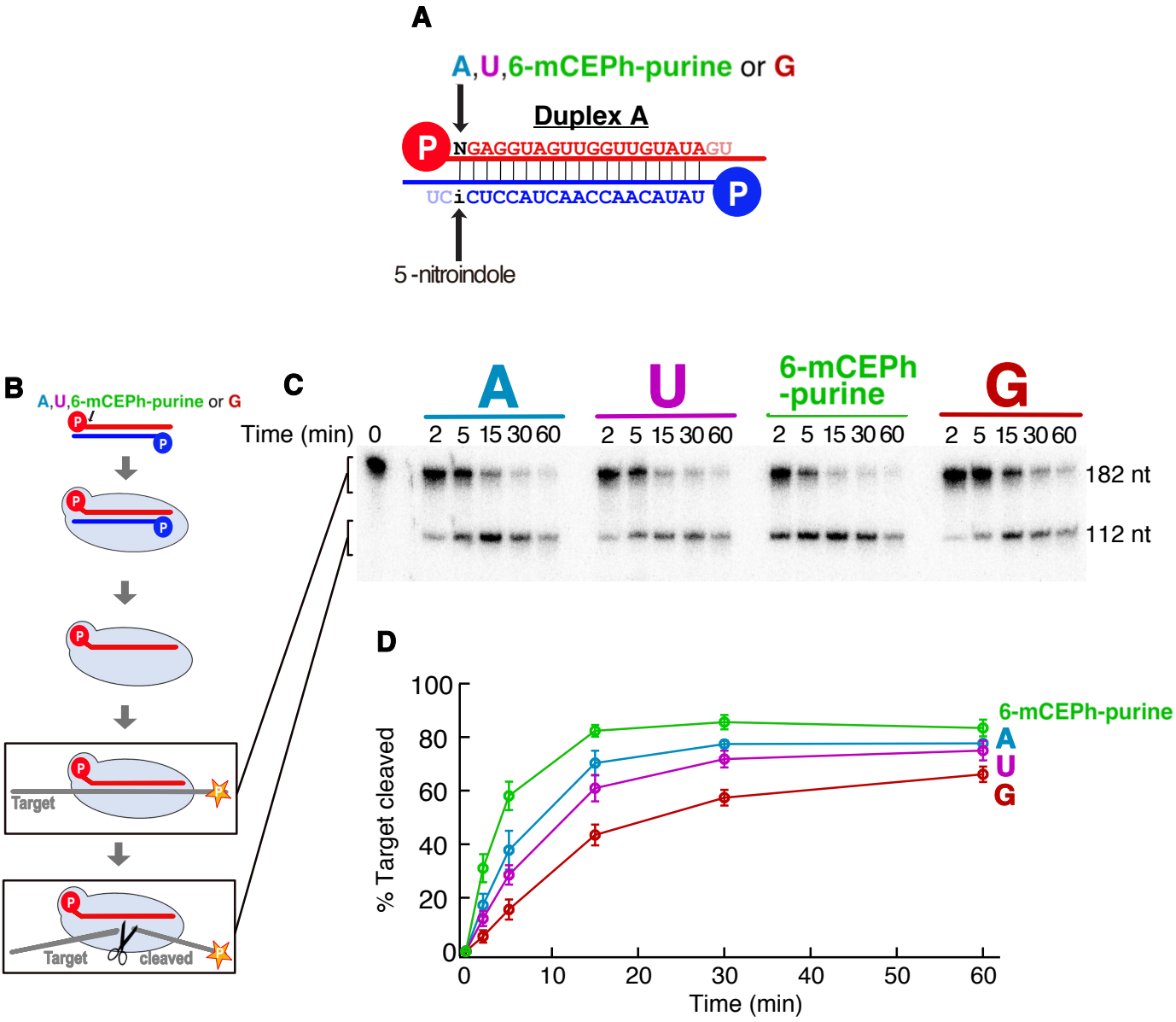

Figure 15. The 6-mCEPh-purine modification improves the target cleavage activity. (A) Four siRNA duplexes used in this set of experiments. They bore different nucleotides (A, U, 6-mCEPh-purine or G) at the 5′ end of the guide strand and 5-nitroindole at position 19 of the passenger strand. Both the guide and passenger strands had a 5′ monophosphate. (B) Scheme of RISC assembly and target cleavage. The target RNA was 5′ cap-radiolabeled. (C) A representative result of the target cleavage assay. The upper and lower bands correspond to the full-length and cleaved target, respectively. The decreasing amount of the target cleaved (112nt) is due to it degradation in the lysate with the time (D) Quantification of the target cleavage assay. The graphs show the average ± SD from three independent experiments.

2.2 Influence of the temperature on RISC formation

To directly examine the effect of the 6-mCEPh-purine modification on RISC assembly, I radiolabeled the 5′ end of the four siRNA duplexes **(Figure 16A)** and monitored the formation of pre-Ago2-RISC and mature Ago2-RISC in Ago2-overexpressing HEK293T cell lysate using previously established assay that utilizes native agarose gel electrophoresis. It has been demonstrated in these previous studies (Kwak et al. 2012, Kawamata et al, 2011, Yoda et al, 2010) that HEK293T cell lysate forms Ago-containing complexes on native agarose gels. When the Ago2 protein is overexpressed, visible amounts of pre-RISC and mature RISC can be detected on these agarose gels. Here, I used this system to quantify the different quantities of mature RISC and pre-RISC between the nucleotides used (A, U, G or 6-mCEPh-purine).

However, according to the previous result of the target cleavage assay, it was important to attest which temperature will be the best for the following assay. Amongst three different temperature chosen **(Figure 16B, 16C, 16D)**, enhancement effect of 6-mCEPh-purine on mature RISC formation was consistently observed in all conditions although the kinetics were different. Then for technical reason, to handle the different samples at different time courses, I decided to set up the future experiments at 25˚c as described in Yoda et al, 2010.

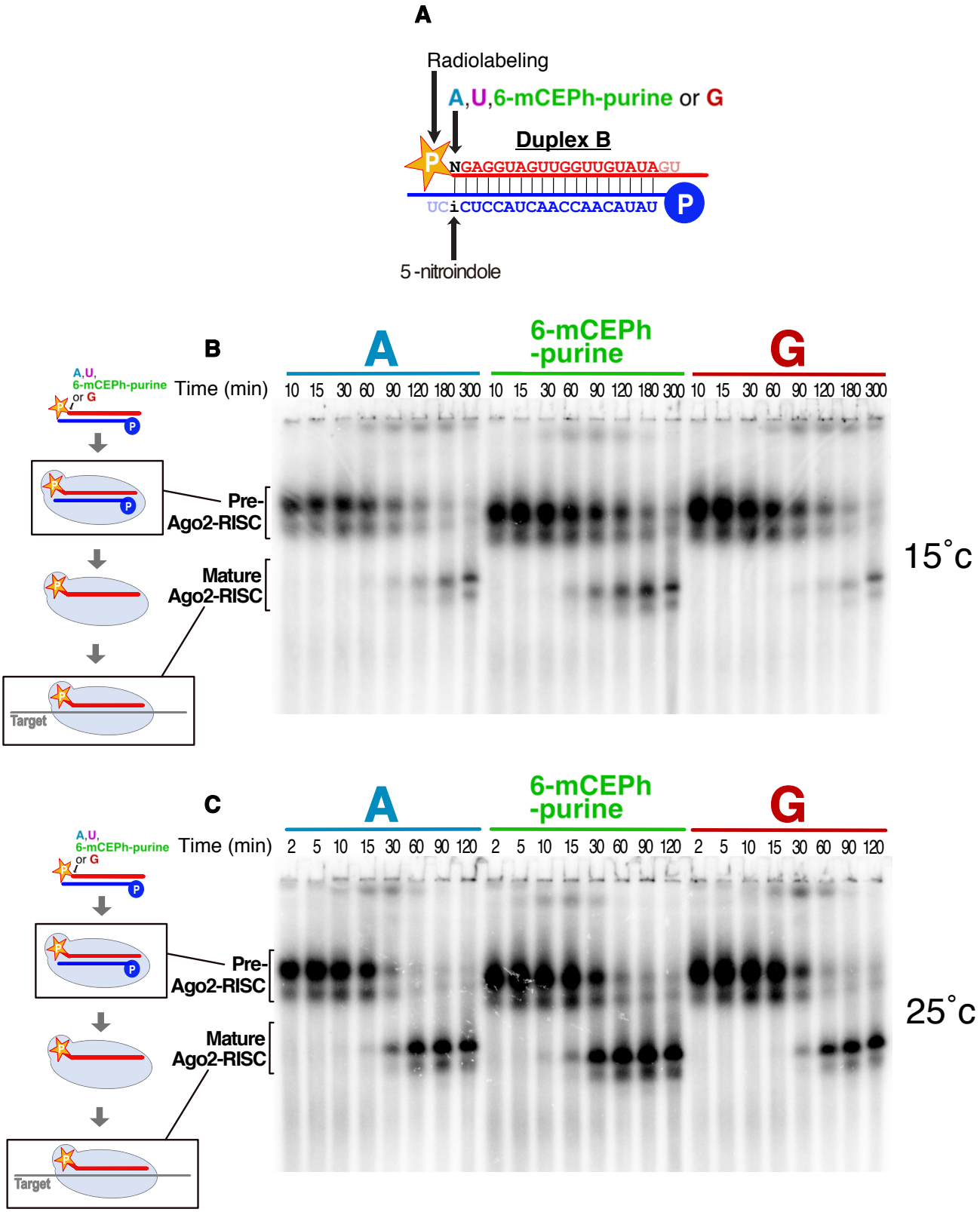
A
Radiolabeling
A,U,6-mCEPh-purine or G
Duplex B
NGAGGUAGUUGGUUGUAUAGU
UCiCUCCAUCAACCAACAUAU
5 -nitroindole
B
A,U,
6-mCEPh-purine
or G
Time (min)
A
6-mCEPh
-purine
G
10 15 30 60 90 120 180 300 10 15 30 60 90 120 180 300 10 15 30 60 90 120 180 300
Pre-
Ago2-RISC
Mature
Ago2-RISC
Target
15˚c
C
A,U,
6-mCEPh-purine
or G
Time (min)
A
6-mCEPh
-purine
G
2 5 10 15 30 60 90 120 2 5 10 15 30 60 90 120 2 5 10 15 30 60 90 120
Pre-
Ago2-RISC
Mature
Ago2-RISC
Target
25˚c

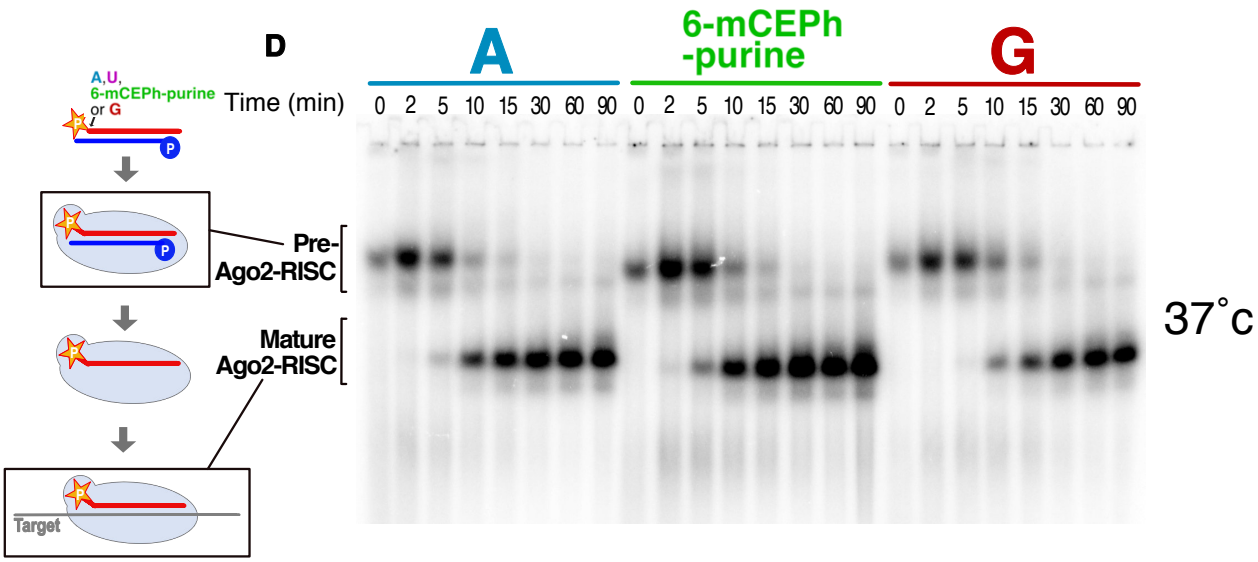

Figure 16. Influence of the temperature on RISC assembly (formation of pre-Ago2-RISC and mature Ago2-RISC) in presence of target.
(A) Three siRNA duplexes used in this set of experiments. They bore different nucleotides (A, 6-mCEPh-purine or G) at the 5′ end of the guide strand and 5-nitroindole at position 19 of the passenger strand. The guide strand was radiolabeled at the 5′ monophosphate, whereas the passenger strand had a non-radiolabeled 5′ monophosphate. (B) A representative result of the native agarose gel assay at 15˚c. (C) A representative result of the native agarose gel assay at 25˚c. (D) A representative result of the native agarose gel assay at 37˚c.

2.3 Mature RISC formation is improved by 6-mCEPh-purine modification

In order to dig more into the mechanistic and to inspect the 6-mCEPh-purine modification effect on the RISC assembly, I radiolabeled the 5′ end of the four siRNA duplexes at the 5’ end of the guide **(Figure 17A)** and observed the formation of pre-Ago2-RISC and mature Ago2-RISC in the same lysate using HEK293T cell where Ago2 was overexpressed.

To successfully accomplish this task, I used a powerful biochemical tool using native agarose gel electrophoresis assay which was well detailed in some previous study of Tomari laboratory (Kwak et al. 2012, Kawamata et al, 2011, Yoda et al, 2010). In this experiment, I used an uncleavable 30-nt 2′-*O*-methyl target which was matching complementary to the guide strand. This target non-radiolabeled was added in the reaction mix to specifically catch mature Ago2-RISC as a sharp signal in contrast to the target cleavage assay **(Figure 17B**, also see below**)**. As presented in **Figure 17C and D**, the pre-Ago2-RISC quantity seemed to be widely similar amongst the four different duplexes. Oppositely, the result presented 6-mCEPh-purine **in Figure 17C** and **Figure 17E**, showed 6-mCEPh-purine modification noticeably arranged to increase the formation of mature Ago2-RISC **(Figure 17C and 17E)**.

This first results from the native agarose gel assay demonstrated a strong consistence with the previous finding of the enhancement of target cleavage activity **(Figure 15D)**.

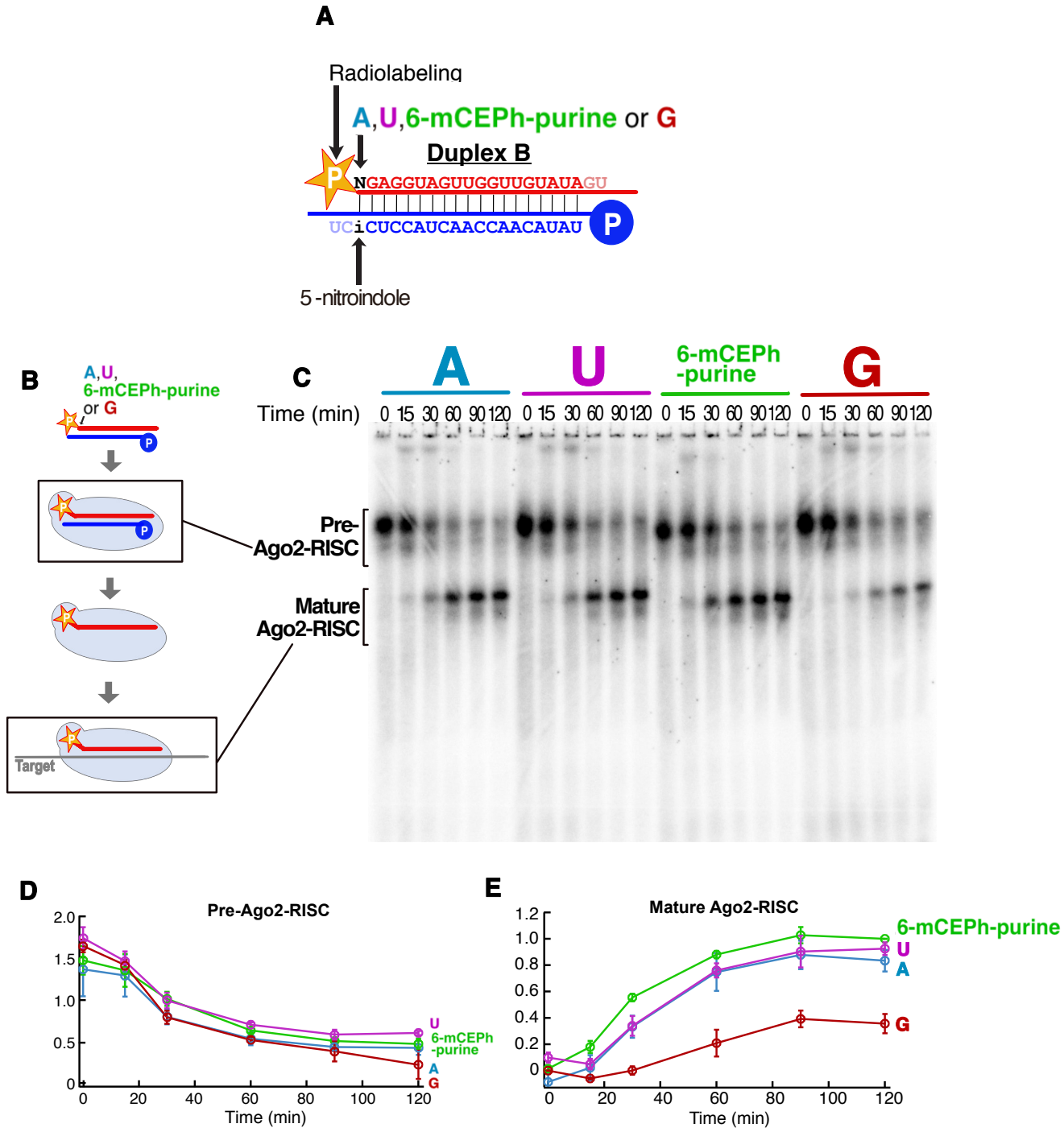

Figure 17. The 6-mCEPh-purine modification improves mature RISC formation.
(A) Four siRNA duplexes used in this set of experiments. Each of them bore different nucleotides (A, U, 6-mCEPh-purine or G) at the 5′ end of the guide strand and 5-nitroindole at position 19 of the passenger strand. The guide strand was radiolabeled at the 5′ monophosphate, whereas the passenger strand had a non-radiolabeled 5′ monophosphate. (B) Scheme of RISC assembly. A non-radiolabeled, uncleavable target oligonucleotide complementary to the guide strand was added to trap mature Ago2-RISC. (C) A representative result of the native agarose gel assay. (D and E) Quantification of pre-Ago2-RISC (D) and mature Ago2-RISC (E) formation. The quantified signals were normalized to the mature RISC value of 6-mCEPh-purine at 120 min. The graphs show the average ± SD from three independent experiments.

2.4 6-mCEPh-purine modification slightly enhanced the guide strand selection

Next, I wanted to know how 6-mCEPh-purine modification can increase the amount of mature RISC formation without probable modulation in the amount of pre-RISC formed.

In my previous experiment where the guide strand was radiolabeled, it was difficult to differentiate which strand was loaded on the pre-RISC step. Indeed, the passenger and guide strands cannot really be separated in the pre-RISC signal on the native agarose gel. As such, there is a possibility that 6-mCEPh-purine may help the asymmetric selection of the guide strand by fixing the orientation of the duplex loading.

To further look into this possible hypothesis, I decided this time to radiolabel the passenger strand and not the guide strand in the four siRNA duplexes **(Figure 18A)**. I then incubated these four duplexes in the HEK293T cell lysate, which overexpress Ago2, and added them in to mix with a 2′-*O*-methyl oligonucleotide target complementary to the passenger strand (In the previous experiment, the target was complementary to the guide strand). The formation of pre-Ago2-RISC and mature Ago2-RISC on native agarose gel was monitored as indicated in the schema **(Figure 18B)**. The amount of mature RISC in this experiment where the passenger was radiolabeled **(Figure 18C)** were overall lower than those observed when the guide was radiolabeled **(Figure 17C)**. Most likely due to the relatively weak thermodynamic stability between 5-nitroindole and the four different nucleotides (Loakes et al, 1994). This result suggested that the four duplexes have an asymmetry in the guide-strand selection. Nonetheless, 6-mCEPh-purine modification moderately but notably reduced the formation of passenger-derived mature RISC, compared to A, U and G **(Figure 18C and 18E)**, showing that 6-mCEPh-purine can further enhance the guide strand selection after the duplex loading. However, the difference observed did not totally explain the enhancement of the guide-derived mature RISC formation by the 6-mCEPh-purine modification noticed in **Figure 17C**. Additionally, and for information, the pre-Ago2-RISC quantity seems to be widely similar among the four different duplexes (**Figure 18C and 18D**).

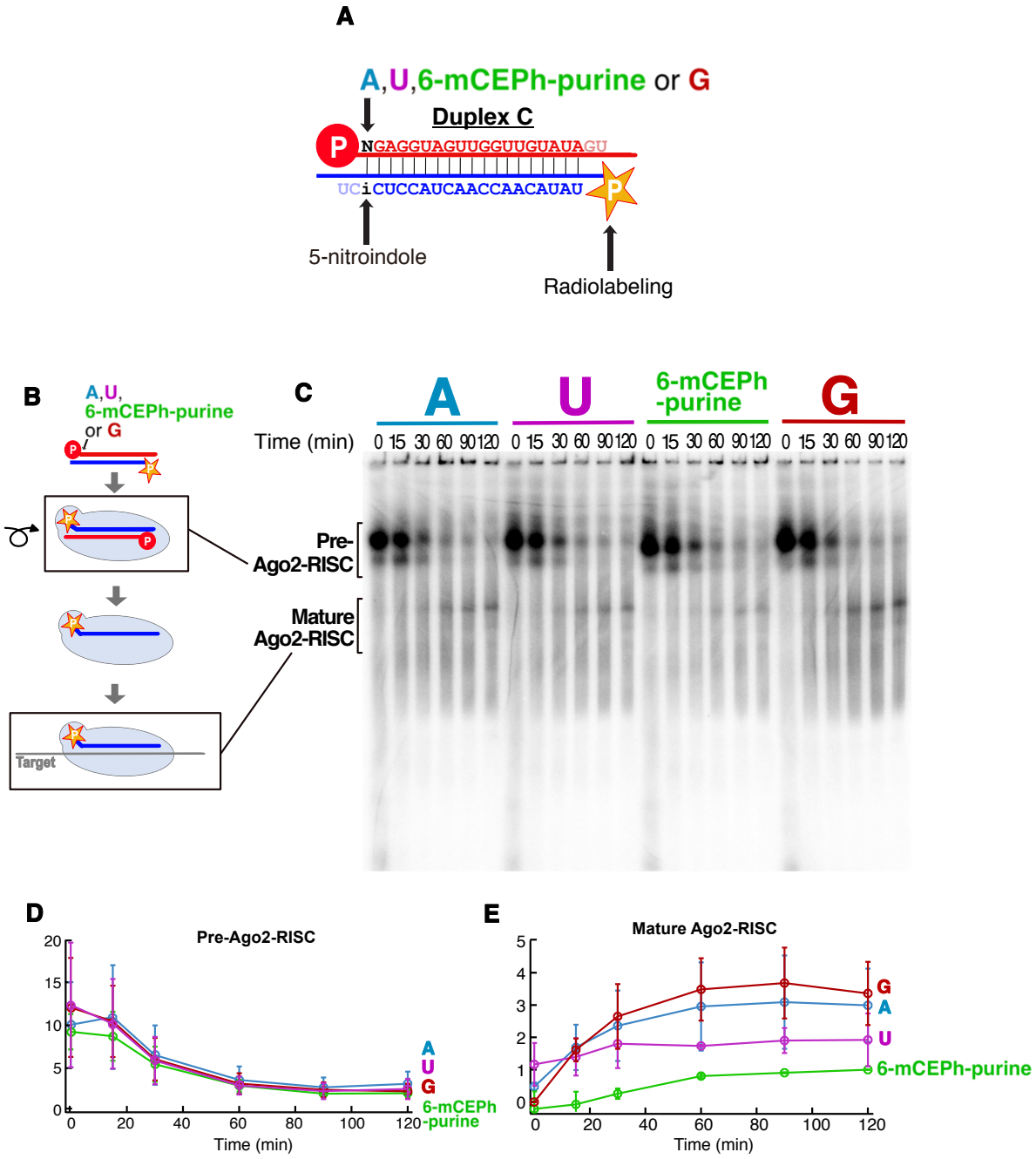

Figure 18. The guide strand selection is slightly enhanced by the 6-mCEPh-purine modification.

(A) Four siRNA duplexes used in this set of experiments. Each of them bore different nucleotides (A, U, 6-mCEPh-purine or G) at the 5′ end of the guide strand and 5-nitroindole at position 19 of the passenger strand. The passenger strand was radiolabeled at the 5′ monophosphate, whereas the guide strand had a non-radiolabeled 5′ monophosphate. (B) Scheme of RISC assembly. A non-radiolabeled, uncleavable target oligonucleotide complementary to the passenger strand was added. (C) A representative result of the native agarose gel assay. (D and E) Quantification of pre-Ago2-RISC (D) and mature Ago2-RISC (E) formation. The quantified signals were normalized to the mature Ago2-RISC value of 6-mCEPh-purine at 120 min. The graphs show the average ± SD from three independent experiments.

2.5 6-mCEPh-purine enhances mature RISC formation independently of the guide strand selection

The previous experiment with the passenger radiolabeled may explain the improvement of mature RISC formation but there is another possibility for this enhancement. Indeed 6-mCEPh-purine modification may improve the guide strand anchoring into Ago2 protein after the ejection of the passenger strand.

To check this new hypothesis where 6-mCEPh-purine modification may improve the guide strand anchoring into Ago2 protein after the ejection of the passenger strand, I decided to change the 5′ monophosphate of the passenger strand to an amino linker **(Figure 19A)**. The function of this amino linker is to block the loading of the passenger strand into the pocket of Ago2 protein (Chiu et al, 2002, Czauderna et al, 2003). Appropriately, the guide strand bearing 5′ 6-mCEPh-purine, A, U or G are always chosen as the guide because the orientation of the duplex loading is strictly determined **(Figure 19B)**. Again, in this set of experiment, with 6-mCEPh-purine modification I noticed a remarkable improvement of the mature RISC formation compared to the other nucleotides **(Figure 19C and 19E)**. However, the pre-RISC formation stayed equal among the four duplexes **(Figure 19C and 19D)**. This new result indicates 6-mCEPh-purine modification can improve mature RISC formation in a total independence to the guide strand selection.

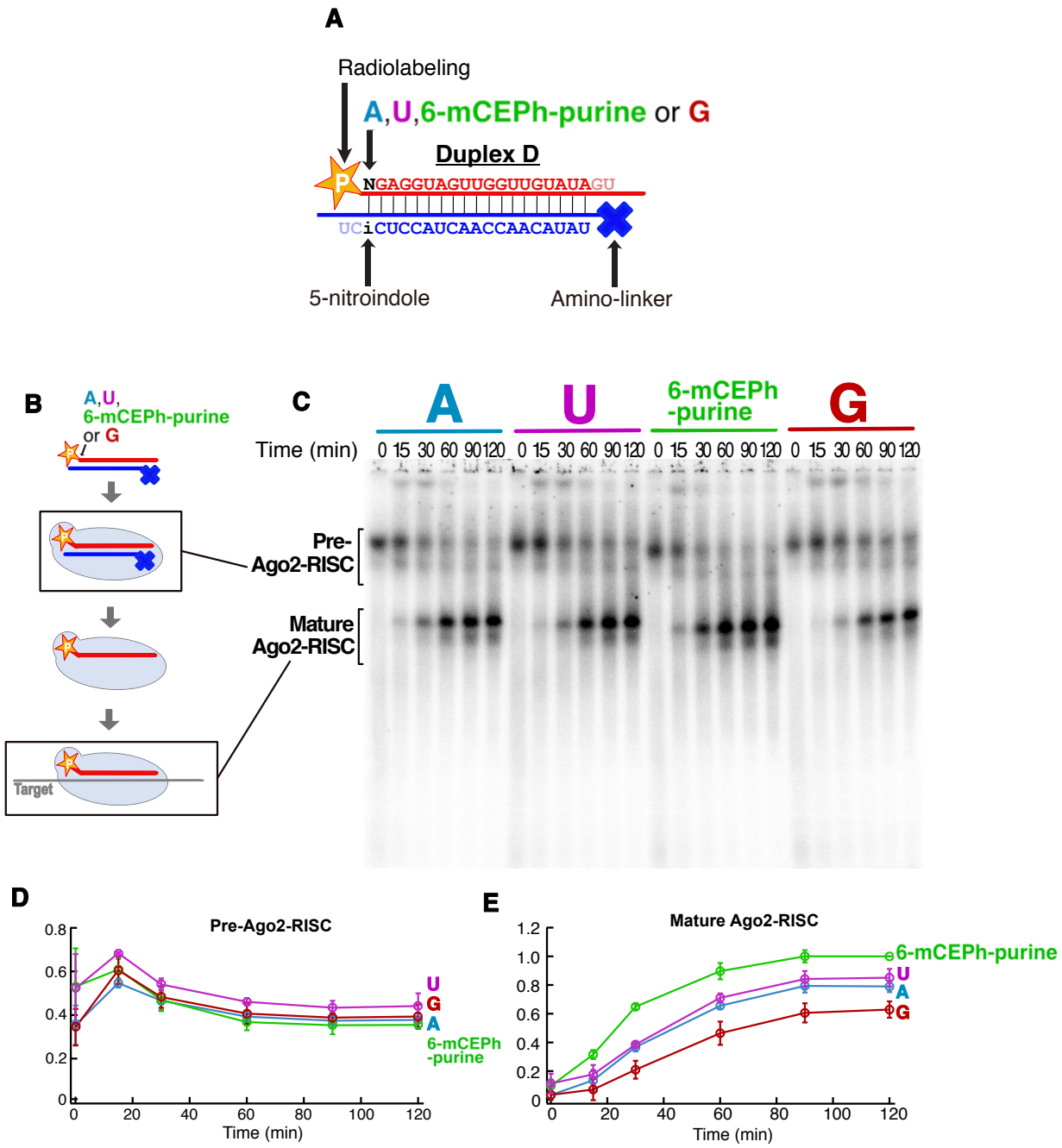

Figure 19. 6-mCEPh-purine enhances mature RISC formation independently of the guide strand selection.

(A) Four siRNA duplexes used in this set of experiments. Each of them bore different nucleotides (A, U, 6-mCEPh-purine or G) at the 5′ end of the guide strand and 5-nitroindole at position 19 of the passenger strand. The guide strand was radiolabeled at the 5′ monophosphate, whereas the passenger strand held a 5′ amino linker that fixes the loading orientation by blocking this strand from being anchored in the 5′ nucleotide-binding pocket of Ago2. (B) Scheme of RISC assembly. A non-radiolabeled, uncleavable target oligonucleotide was added. (C) A representative result of the native agarose gel assay. (D and E) Quantification of pre-Ago2-RISC (D) and mature Ago2-RISC (E) formation. The quantified signals were normalized to the mature Ago2-RISC value of 6-mCEPh-purine at 120 min. The graphs show the average ± SD from three independent experiments.

2.6 The duplex loading step is not affected by the different 5′-end nucleotides

In all the previous experiment using native agarose gel, the pre-RISC signal was always identical among the different duplexes. Nevertheless, RISC assembly is a continuous process and the formation of pre-RISC is only transient. With this feature, it is still unsure if the 6-mCEPh-purine modification has any effect on the efficiency of duplex loading. To come to a specific conclusion, I decided to introduce a 2′-*O*-methyl at the position 9 of the passenger strand. This modification to this position is well known to stop the slicing and the ejection of the passenger strand (Myoshi et al, 2005, Leuschner et al, 2006) **(Figure 20A and 20B)** allowing me to directly observe the duplex loading efficiency. The data found demonstrated that pre-Ago2-RISC formation was equal among the four different siRNA duplexes bearing 5′ 6-mCEPh-purine, A, U or G **(Figure 20C and 20D)**. Together with the previous data, this new result suggested 6-mCEPh-purine modification does not interact to the efficiency of siRNA duplex loading into Ago2 to form pre-RISC, but enhanced the mature RISC stability after the ejection of the passenger strand.

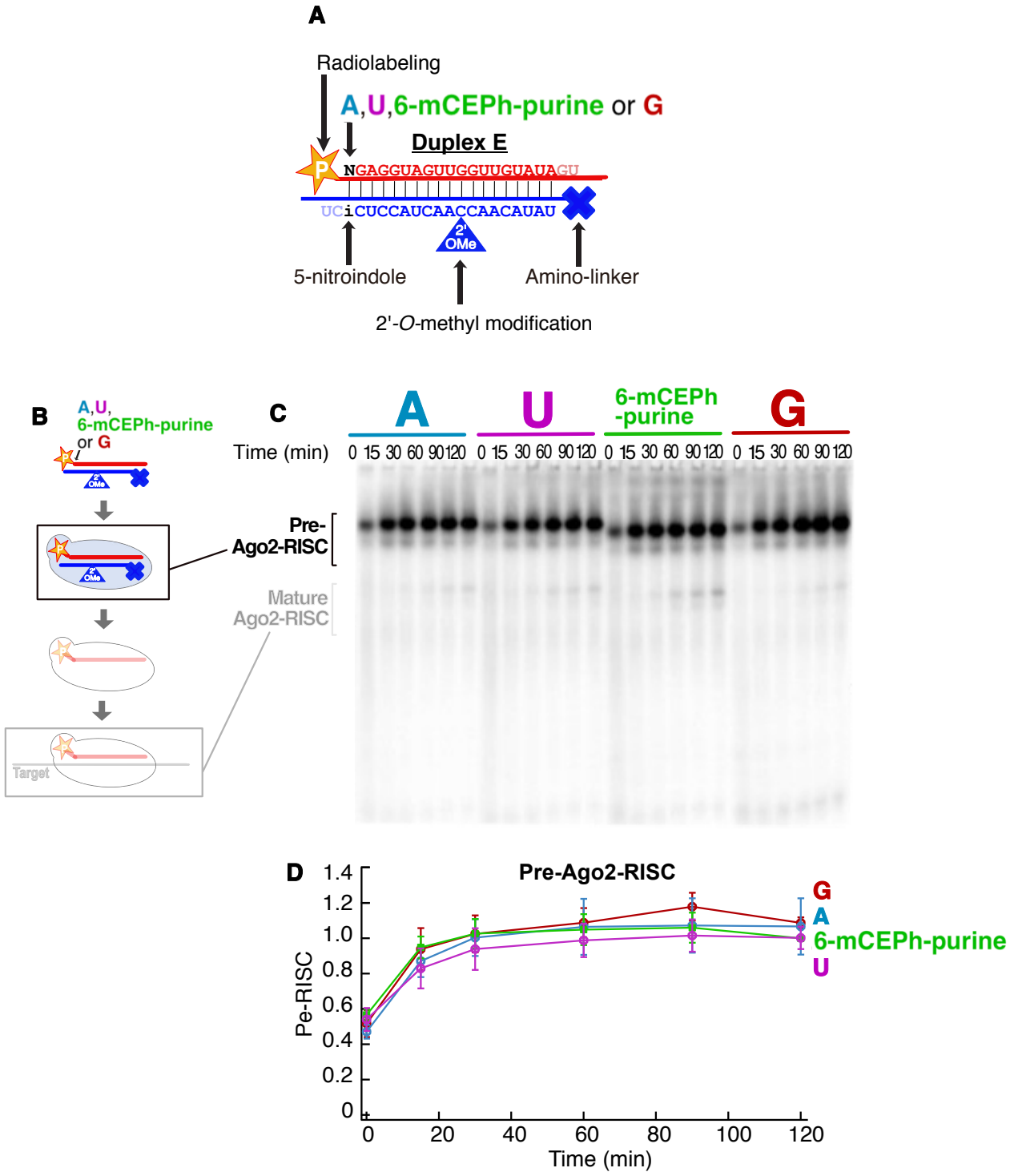

Figure 20. Efficiency of duplex loading is not affected by different 5′-end nucleobases. (A) Four siRNA duplexes used in this set of experiments. Each of them bore different nucleotides (A, U, 6-mCEPh-purine or G) at the 5′ end of the guide strand and 5-nitroindole at position 19 of the passenger strand. The guide strand was radiolabeled at the 5′ monophosphate, whereas the passenger strand held a 5′ amino linker that fixes the loading orientation and a 2′-*O*-methyl modification that blocks passenger ejection. (B) Scheme of RISC assembly. A non-radiolabeled, uncleavable target oligonucleotide was added. (C) A representative result of the native agarose gel assay. (D) Quantification of pre-Ago2-RISC formation. The quantified signals were normalized to the pre-Ago2-RISC value of 6-mCEPh-purine at 120 min. The graphs show the average ± SD from three independent experiments.

2.7 Enhanced formation of mature RISC by 6-mCEPh-purine is not influence by the Target.

In some previous studies, it has been reported that interactions between mature RISC and its targets can assist destabilization of the guide strand from human Ago2-RISC (De et al, 2013, Park et, 2017). In this set of experiment, I wanted to evaluate the effect of 6-mCEPh-purine modification on RISC assembly in the absence of a target and see if this target may have any influence.

To detect the mature RISC formation as a sharp and consistent signal on the native agarose gel and to avoid any binding to heterogenous mRNAs present in the lysate, I continually included a complementary non-radiolabeled 30-nt 2′-*O*-methyl oligonucleotide in all sets of experiments using the native agarose gel. In the absence of the target, mature Ago2-RISC was detected as a smeared signal on the gel (**Figure 21A and 21B**).

To avoid this smear without adding the target, I treated HEK293T lysate overexpressing Ago2 with a micrococcal nuclease (MNase) to digest and remove the endogenous mRNAs (Svitkin et al, 2004).

After quenching the MNase activity with EGTA, I then executed a native agarose gel assay with and without adding a 2′-*O*-methyl target oligonucleotide **(Figure 22A, 22B, 22D)**. In this condition, I was able to monitor mature Ago2-RISC as a sharp signal from pre-Ago2-RISC without the target RNAs (**Figure 22C**) and with target as previously (**Figure 22E**). Again, when I compared the four different duplexes (**Figure 23A, 23B**), I observed an identical formation of pre-Ago2-RISC among the duplexes bearing A, U, 6-mCEPh-purine or G **(Figure 23C, 23D)** and a significant enhancement of the formation of mature Ago2-RISC with 6-mCEPh-purine **(Figure 23C, 23E)**. I therefore determined that the observed improvement by 6-mCEPh-purine of the mature RISC formation was totally independent of the presence of the target.

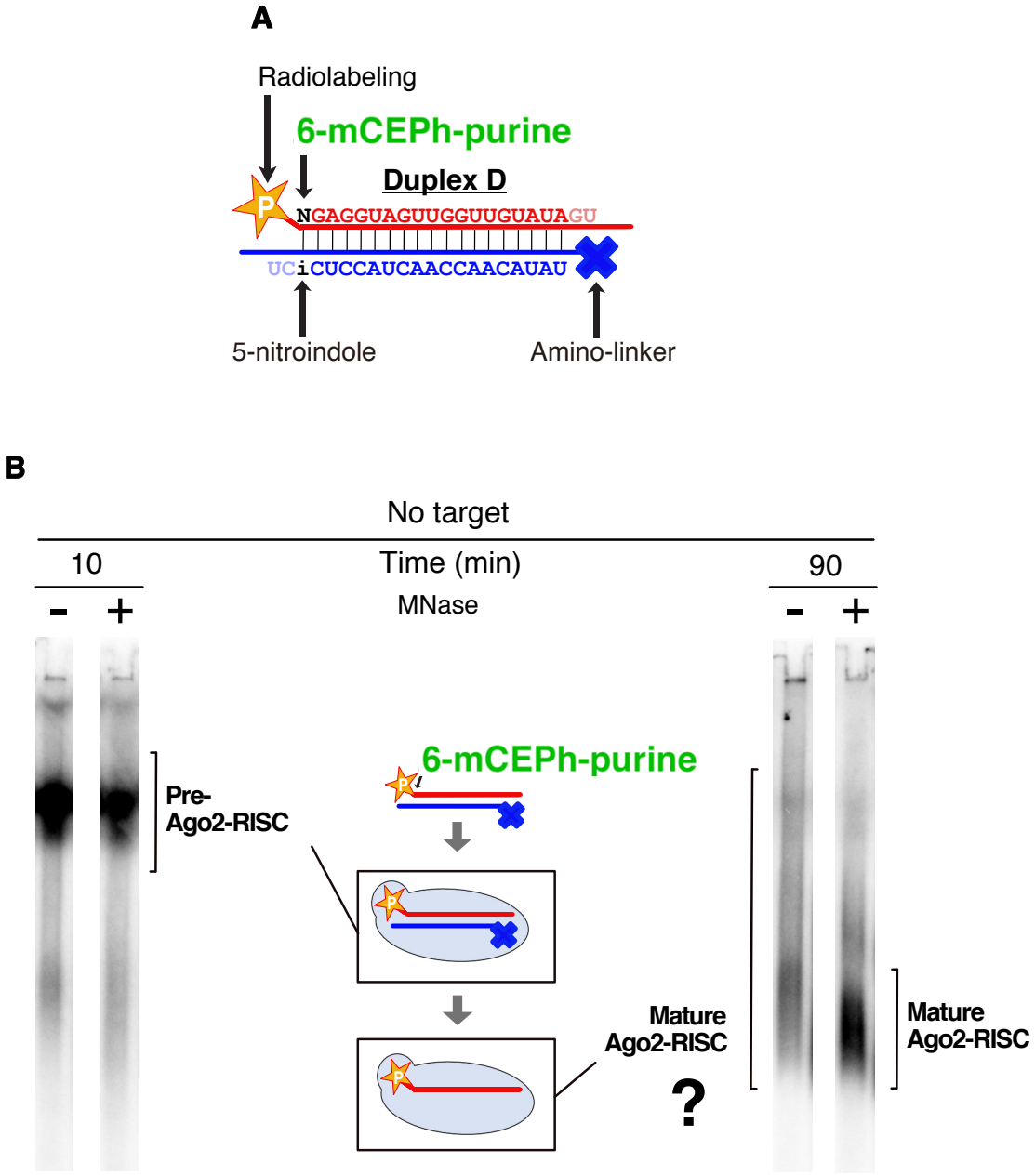

Figure 21. Effect of the MNase treatment to detect mature Ago2-RISC.
Digestion of endogenous mRNAs by the MNase treatment allowed the detection of mature Ago2-RISC as a discrete signal on the native agarose gel in the absence of targets. (A) siRNA duplex used in this set of experiments. Only the duplex which bore 6-mCEPh-purine at the 5′ end of the guide strand and 5-nitroindole at position 19 of the passenger strand was used in this set. The guide strand was radiolabeled at the 5′ monophosphate, whereas the passenger strand held a 5′ amino linker that fixes the loading orientation by blocking this strand from being anchored in the 5′ nucleotide-binding pocket of Ago2.

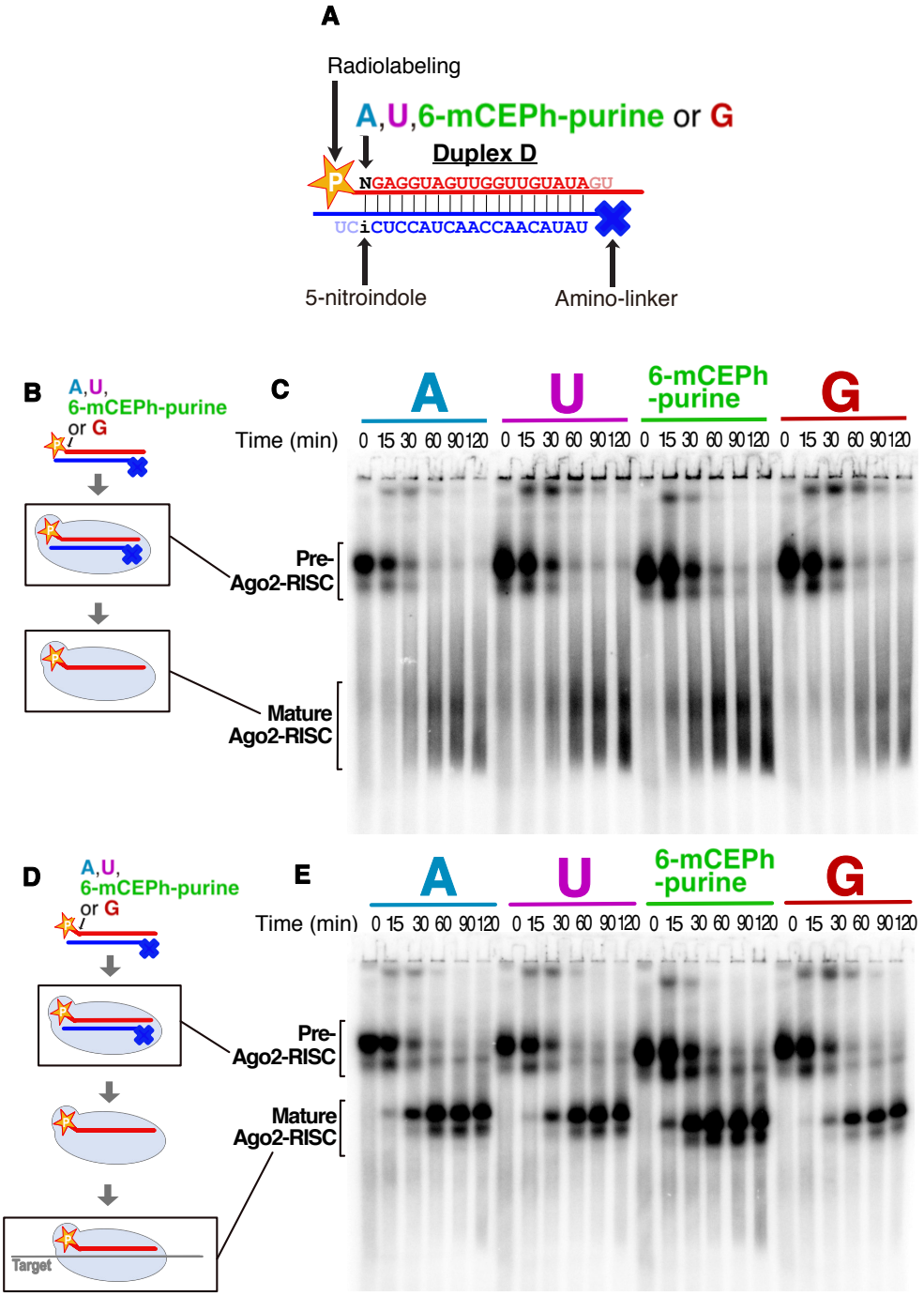

Figure 22. Effect of the micrococcal treatment with and without target.
(A) Four siRNA duplexes used in this set of experiments. Each of them bore different nucleotides (A, U, 6-mCEPh-purine or G) at the 5′ end of the guide strand and 5-nitroindole at position 19 of the passenger strand. The guide strand was radiolabeled at the 5′ monophosphate, whereas the passenger strand held a 5′ amino linker that fixes the loading orientation. (B) Scheme of RISC assembly. The lysate was treated with MNase for the depletion of endogenous mRNAs, and no target was added. (C) A representative result of the native agarose gel assay. (D) Scheme of RISC assembly. The lysate was treated with MNase for the depletion of endogenous mRNAs, and target was added. (E) A representative result of the native agarose gel assay.

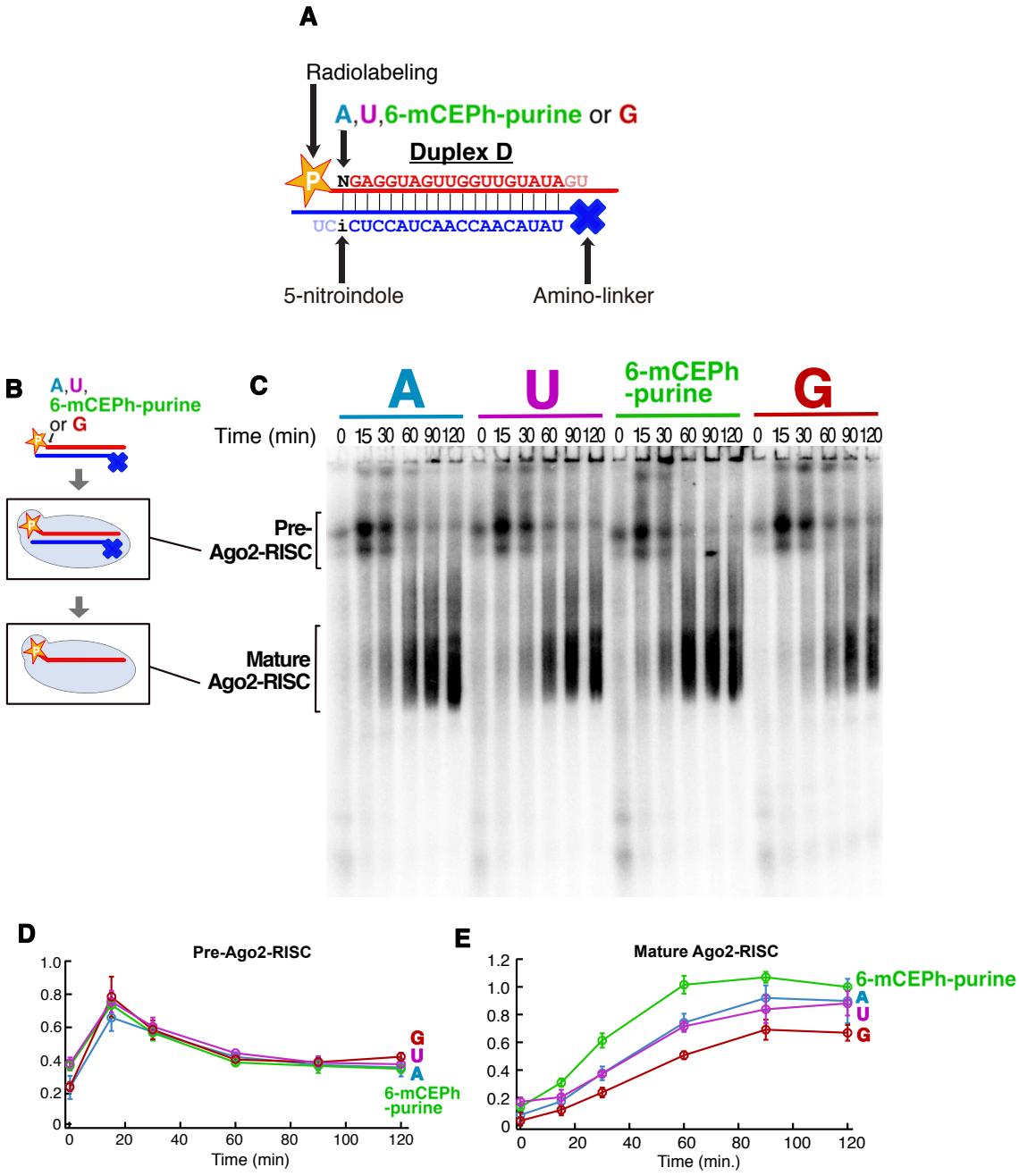

Figure 23. The target does not influence enhanced mature RISC formation by 6-mCEPh-purine.

(A) Four siRNA duplexes used in this set of experiments. Each of them bore different nucleotides (A, U, 6-mCEPh-purine or G) at the 5′ end of the guide strand and 5-nitroindole at position 19 of the passenger strand. The guide strand was radiolabeled at the 5′ monophosphate, whereas the passenger strand held a 5′ amino linker that fixes the loading orientation. (B) Scheme of RISC assembly. The lysate was treated with MNase for the depletion of endogenous mRNAs, and no target was added. (C) A representative result of the native agarose gel assay. (D and E) Quantification of pre-Ago2-RISC (D) and mature Ago2-RISC (E) formation. The quantified signals were normalized to the mature Ago2-RISC value of 6-mCEPh-purine at 120 min. The graphs show the average ± SD from three independent experiments.

3. Complementary study with another modification: BrdA

After the promising results of 6-mCEPh-purine modification, I next decided to check another modification called BrdA provided by our partner Kyowa Kirin which is also an AMP analogue that holds Bromine at 8th position of adenine.
The binding mode of 8-Bromo AMP is the same as AMP, except Bromine gains new hydrophobic interaction with Tyr529. The effect of this 5'end substitution was evaluated by our partner Kyowa Kirin using an individual luciferase targeting siRNA. By calculating the IC50 values, BrdA substitution showed several-fold higher activity than others.

To directly examine the effect of BrdA modification on RISC assembly, I operated on the same way presented in **Figure 17**, radiolabeling the 5′ end of the four siRNA duplexes **(Figure 24A, 25A, 26A)** and monitoring the formation of pre-Ago2-RISC and mature Ago2-RISC in Ago2-overexpressing HEK293T cell lysate using a native agarose gel electrophoresis. In this assay, a non-radiolabeled, uncleavable 30-nt 2′-*O*-methyl target oligonucleotide complementary to the guide strand was included in the reaction mix to trap mature Ago2-RISC **(Figure 24B).** In another similar assay, target was not included **(Figure 25B)**. As shown in **Figure 23C, 23D, 24C and 24D**, the amounts of pre-Ago2-RISC were comparable among the four different duplexes. In contrast, the 6-mCEPh-purine modification still promoted the formation of mature Ago2-RISC **(Figure 24C, 24D, 25C, 25D)**. However, BrdA modification showed an unexplainable lower band that does not allow any quantification of this modification **(Figure 24C and 25D)**. To check if this band was specific to Ago2 or not, I decided to compare the presence of BrdA with another nucleotide (here A) in presence of overexpressed Ago2 lysate or naïve lysate (which not overexpress Ago2) **(Figure 26A and B).** The results **Figure 26C** demonstrated this lower band of BrdA was not specific to Ago2. It was impossible in this condition to compare BrdA modification with the other nucleotides.

This data showed that BrdA-modified siRNAs can be non-specifically trapped by something else, which cannot be detected by conventional reporter assays.
According to this result, the molecular platform which allowed to detect the efficiency of 6-mCEPh-purine modification may also detect potential “side effects” of chemical modifications in vitro.
In future study, it will be interesting to analyze the unexplainable lower band present on the gel by mass spectroscopy in order to determine which factors trapped BrdA modification.

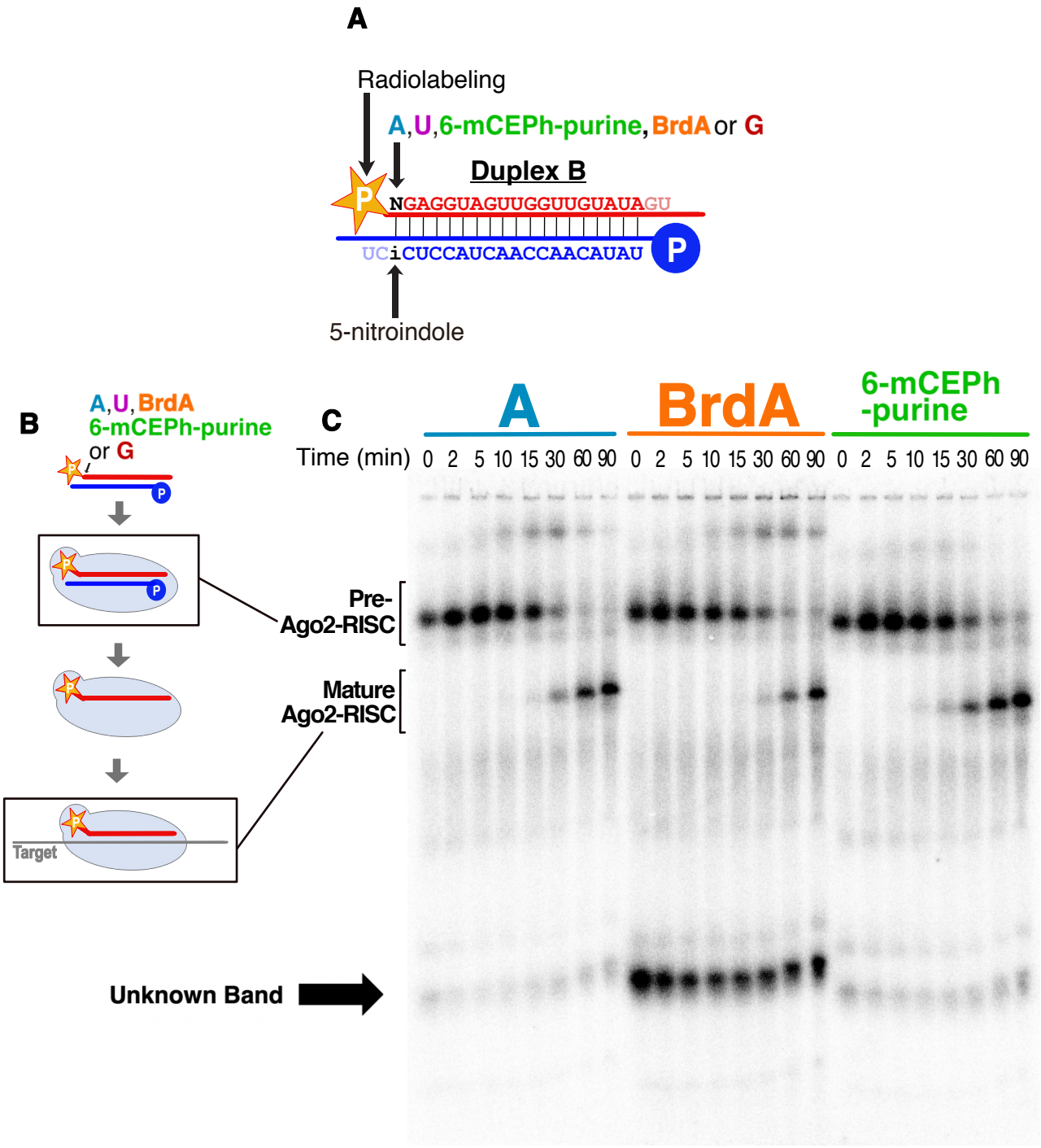
A
Radiolabeling
A,U,6-mCEPh-purine, BrdA or G
Duplex B
NGAGGUAGUUGGUUGUAUAGU
UCiCUCCAUCAACCAACAUAU
P
5-nitroindole
B
A,U, BrdA
6-mCEPh-purine
or G
Target
C
A
BrdA
6-mCEPh
-purine
Time (min) 0 2 5 10 15 30 60 90 0 2 5 10 15 30 60 90 0 2 5 10 15 30 60 90
Pre-
Ago2-RISC
Mature
Ago2-RISC
Unknown Band

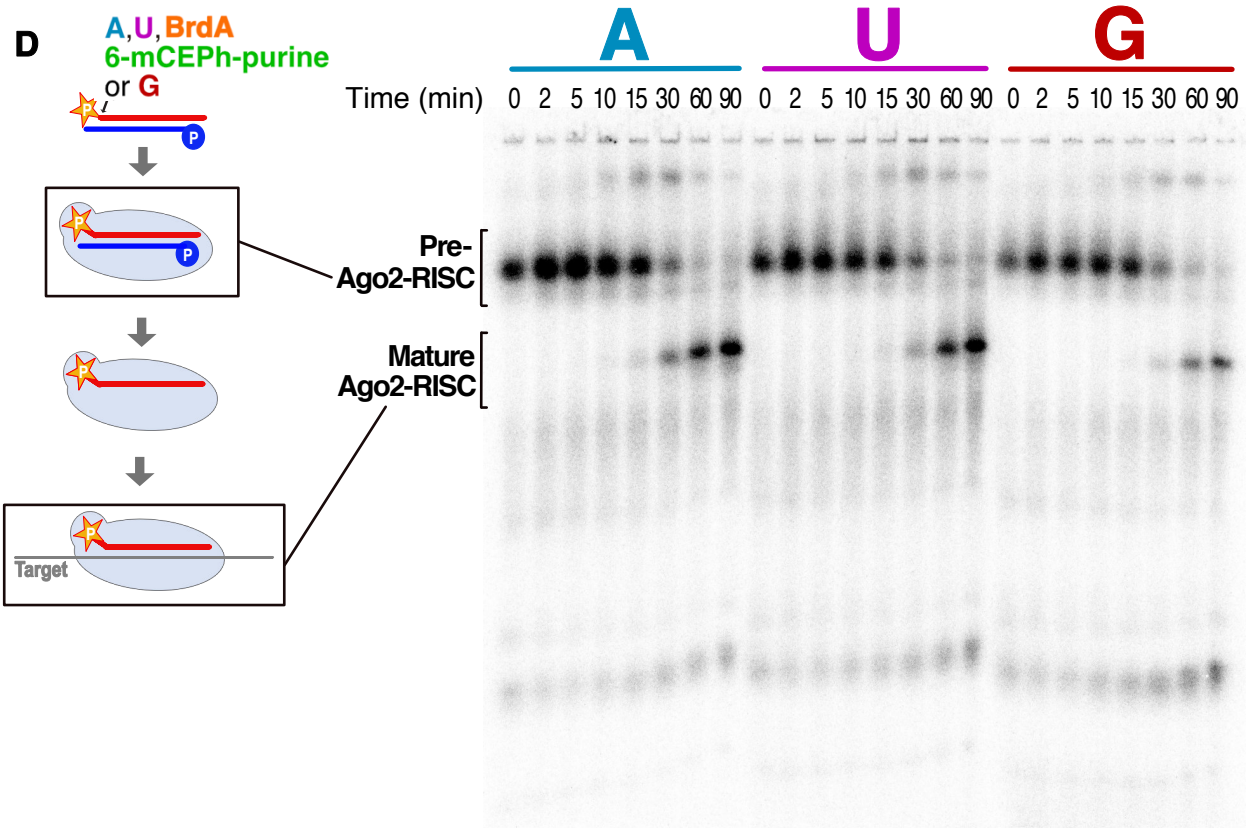

Figure 24. BrdA modification shows a strange lower band (target added).
(A) Five siRNA duplexes used in this set of experiments. Each of them bore different nucleotides (A, U, 6-mCEPh-purine, BrdA or G) at the 5′ end of the guide strand and 5-nitroindole at position 19 of the passenger strand. The guide strand was radiolabeled at the 5′ monophosphate, whereas the passenger strand had a non-radiolabeled 5′ monophosphate. (B) Scheme of RISC assembly. A non-radiolabeled, uncleavable target oligonucleotide complementary to the guide strand was added to trap mature Ago2-RISC. (C) A representative result of the native agarose gel assay. (D) Scheme of RISC assembly. A non-radiolabeled, uncleavable target oligonucleotide complementary to the guide strand was added to trap mature Ago2-RISC. (E) A representative result of the native agarose gel assay.

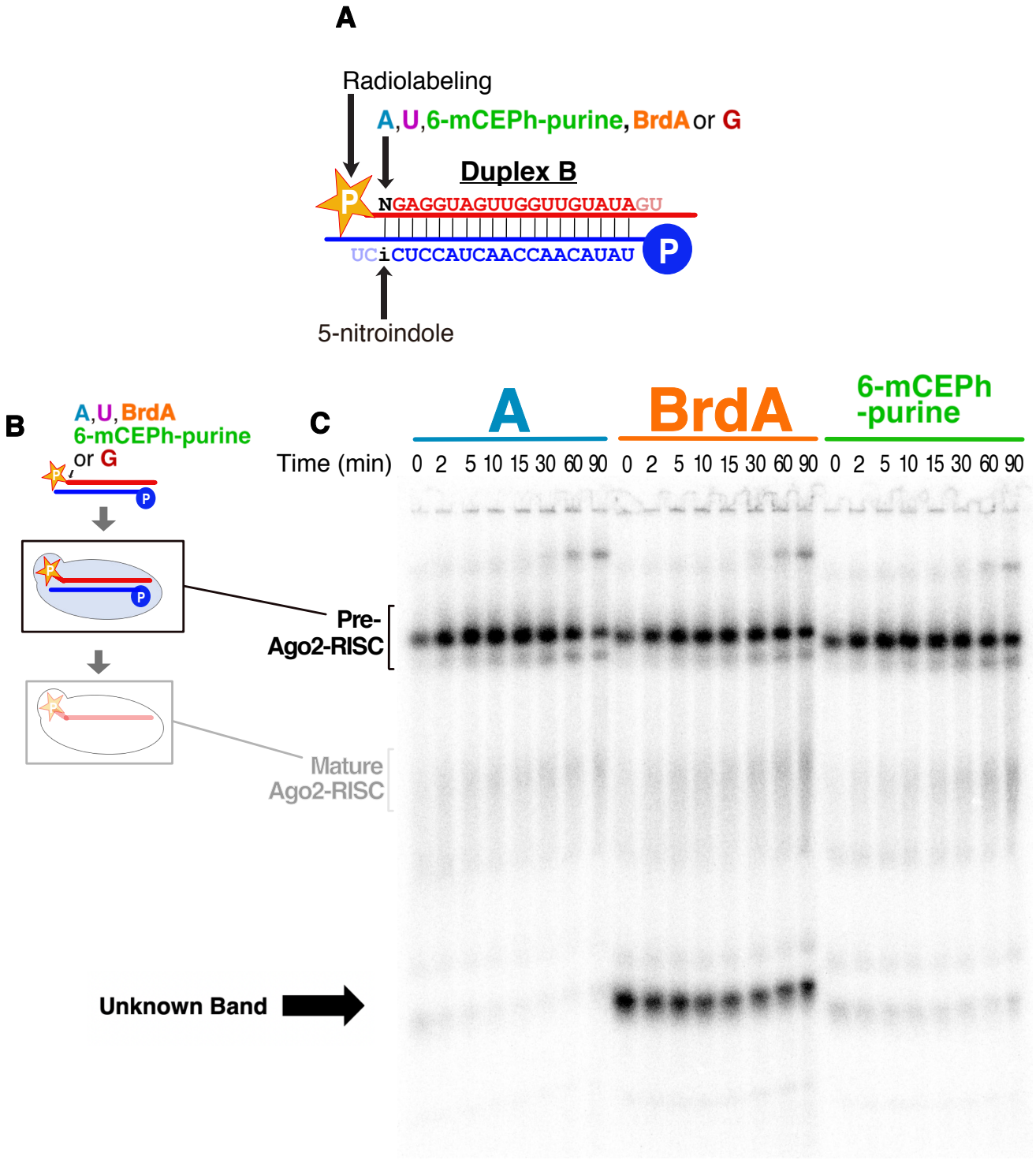
A
Radiolabeling
A,U,6-mCEPh-purine, BrdA or G
Duplex B
NGAGGUAGUUGGUUGUAUAGU
UCiCUCCAUCAACCAACAUAU
5-nitroindole
B
A,U, BrdA
6-mCEPh-purine
or G
Pre-
Ago2-RISC
Mature
Ago2-RISC
C
A
BrdA
6-mCEPh
-purine
Time (min) 0 2 5 10 15 30 60 90 0 2 5 10 15 30 60 90 0 2 5 10 15 30 60 90
Unknown Band

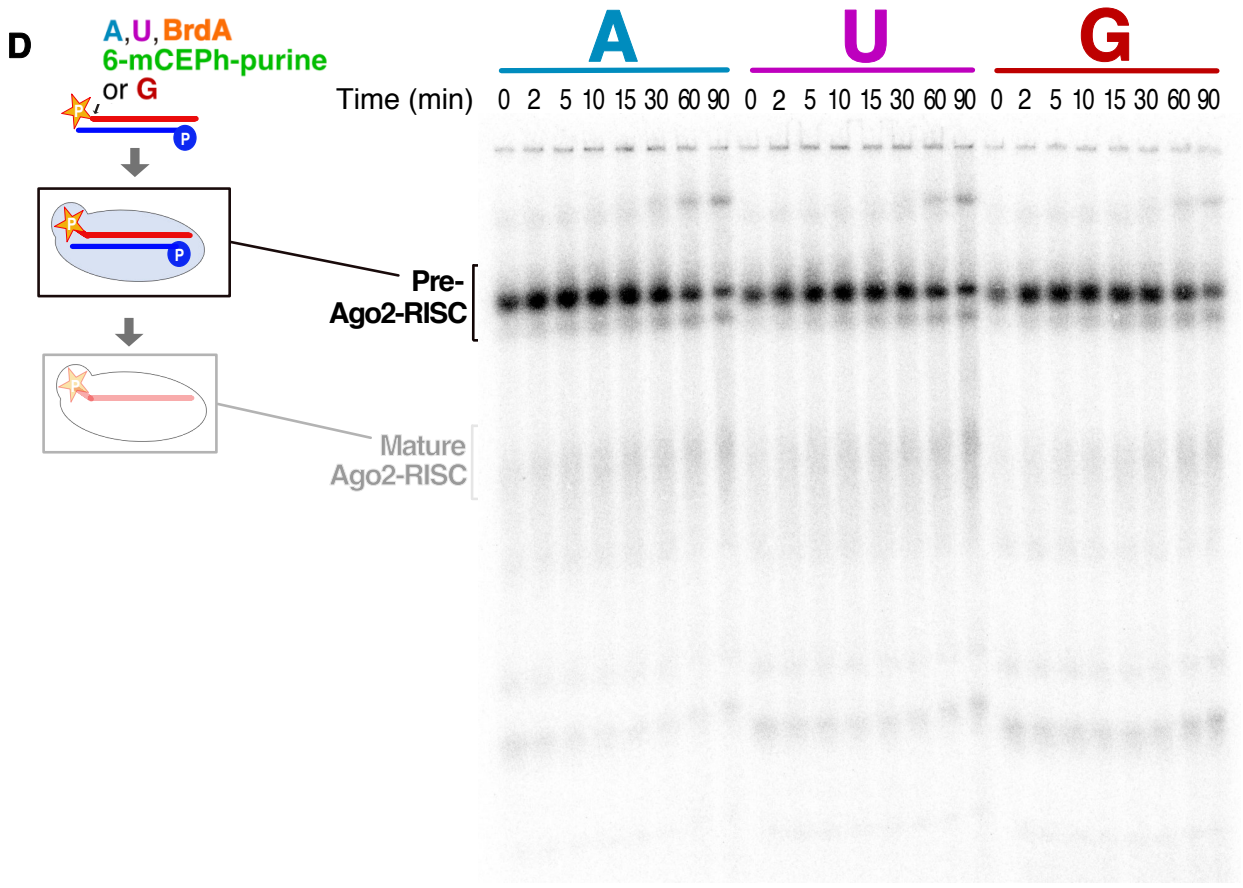

Figure 25. BrdA modification shows a strange lower band (no target added).
(A) Five siRNA duplexes used in this set of experiments. Each of them bore different nucleotides (A, U, 6-mCEPh-purine, BrdA or G) at the 5′ end of the guide strand and 5-nitroindole at position 19 of the passenger strand. The guide strand was radiolabeled at the 5′ monophosphate, whereas the passenger strand had a non-radiolabeled 5′ monophosphate. (B) Scheme of RISC assembly. No target oligonucleotide complementary to the guide strand was added. (C) A representative result of the native agarose gel assay. (D) Scheme of RISC assembly. A non-radiolabeled, uncleavable target oligonucleotide complementary to the guide strand was added to trap mature Ago2-RISC. (E) A representative result of the native agarose gel assay.

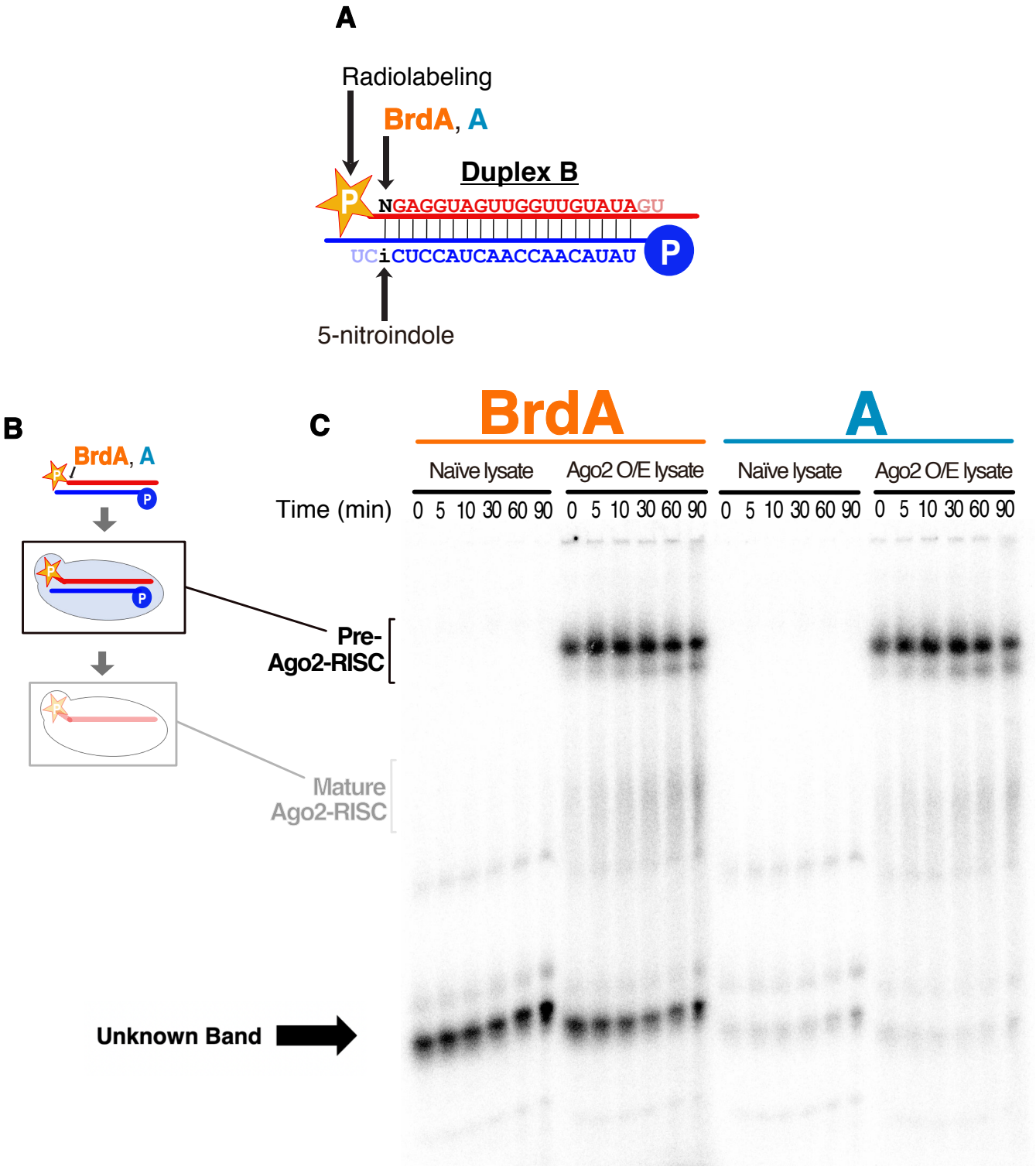

Figure 26. BrdA is not specific to Ago2.
(A) Two siRNA duplexes used in this set of experiments. Each of them bore different nucleotides (A or BrdA) at the 5′ end of the guide strand and 5-nitroindole at position 19 of the passenger strand. The guide strand was radiolabeled at the 5′ monophosphate, whereas the passenger strand had a non-radiolabeled 5′ monophosphate. (B) Scheme of RISC assembly. No target oligonucleotide complementary to the guide strand was added. (C) A representative result of the native agarose gel assay.

IV. Discussion

General Conclusion

siRNA chemical modifications on the RNAi activity has already been developed in many studies (Egli et al, 2019, Setten et al, 2019, Khvorova et al, 2017). Nevertheless, most of these researches only evaluated the final result of the target silencing using luciferase reporter assays in cultured cells without describing anything about the mechanism.

In my study, by using a specific approach of biochemical techniques including a target cleavage assay and a native agarose gel electrophoresis assay, I succeeded to analyze the precise mechanism of a chemical modification present at the 5′-end of the guide strand. Indeed, each step during Ago2-RISC assembly was monitored to address the primordial question on how this kind of modification is working.

6-mCEPh-purine modification: the mechanism revealed

Summary on the following schema **(Figure 27)**; I found that the 6-mCEPh-purine modification improved the formation of mature RISC in two distinct ways:

- (1) 6-mCEPh-purine improves the guide strand selection by fixing the loading orientation of siRNA duplexes **(Figure 18).**
- (2) 6-mCEPh-purine increases the stability of mature RISC after passenger strand ejection **(Figure 19).**

It also clarified that there is no difference for the amount of pre-Ago2-RISC formed **(Figure 20)**. Altogether these results demonstrated 6-mCEPh-purine do not have any effect on the efficiency of duplex loading while the orientation of the duplex in pre-Ago2-RISC can change **(Figure 18).** In many studies, it has been showed that the loading of siRNA duplexes into Ago depends on an important initial step where the guide 5′ monophosphate is anchored in the 5′ nucleotide-binding pocket (Schirle et al, 2012, Elkayam et al, 2012, Nakanishi et al, 2012, Iwasaki et al, 2015). It is reasonable to think that the guide 5′ nucleobase, close to the 5′ monophosphate is also anchored in the pocket of Ago2 at the step of duplex loading. However, the improvement in the formation of pre-Ago2-RISC by 6-mCEPh-purine was imperceptible and was visible only at mature Ago2-RISC formation step. We can easily imagine two different possible explanations for this observation:

Firstly, the “double-stranded state” of siRNA duplexes in pre-Ago2-RISC may have an additional anchor spot for Ago2 masking the effect of the 5′ nucleobase anchoring. If it is the case as it was previously shown in Drosophila Ago1, where preferred nucleobases (A and U) provided more prominent effect in mature Ago1-RISC than in pre-Ago1-RISC (Kawamata et al, 2011), this anchor spot is certainly lost after the passenger ejection, making the 5′ nucleobase anchoring more important at this time.

Secondly and alternatively, due to some structural constraints, the 5′ nucleobase may not totally be anchored in the pocket of the MID domain immediately after the duplex loading. Certainly, the total stabilization and perfect anchoring of this 5’ nuclobase occurs only after the ejection of the passenger strand. In both cases, 6-mCEPh-purine modification at the 5′ nucleobase of the guide strand demonstrated the formation of more mature Ago2-RISC **(Figure 19)** which fully explains the better RNAi efficiency observed *in vitro* **(Figure 15)**, in cells and *in vivo* according to our partner Kyowa Kirin.

6-mCEPh-purine compared to other modifications for siRNA enhancement

6-mCEPh-purine is a chemical modification at the 5’ end of the guide strand. My analysis in this study allowed to understand the mechanism of this modified siRNAs in vitro at each step during Ago2-RISC assembly which will play an important part in developing RNAi drugs more efficiently. However, as developed in the chapter 3.3 Different types of chemical modification of my introduction there are different ways to approach chemical modification for the development of siRNA therapeutic. For example, the last breakthrough with Patisiran indicated for the treatment of hereditary transthyretin amyloidosis (hATTR) in adults exhibited different chemical modifications including the increasement of the 2′-O-methyl content. Below, I will discuss the different well-known modifications which can be simultaneously applied to siRNA to maximize the efficiency and compare it with 6-mCEPh-purine 5' nucleobase modification strategy.

First, the ribose modifications including 2′-O-methyl or 2’F which are attractive and popular modifications significantly increase the resistance of siRNAs to serum

nucleases, decrease immune stimulation and improve the binding affinity. (Cummins et al, 1995, Monia et al, 1996, Choung et al, 2006, Robbins et al, 2007).

The 2'-O-methyl modification present in Patisiran is one of the most interesting chemical modifications. Its effects are variable according to its occurrence and its position within the siRNA. 2'-O-methylation of a strand decreases the probability of its selection as a guide strand: applied to the previously identified passenger strand, it reduces its probability of loading into the RISC and consequently increases the effectiveness of the guide (Chen PY et al, 2008). This modification also avoids a Toll-like receptor mediated immune response (Robbins et al., 2007). 2'-O-methyl modification of the terminal ribose of the sense strand is often used in commercially available siRNAs.

Unlike most other 2 'modifications that can only be obtained on already formed siRNAs, the 2'-F modification does not disrupt RNA polymerases: it is possible to synthesize RNAs using ribose pyrimidines 2'-F (2'-F-pyrimidine). Long dsRNAs in pyrimidines have been replaced by 2'-F-pyrimidines to retain the ability to be primed in siRNA by Dicer. In an in vivo mouse study, 2'-F-pyrimidine siRNAs showed extinguishing power and prolonged plasma half-life compared to unmodified siRNAs (Layzer et al., 2004). This, however, did not translate into increased therapeutic potency in the animal, partly due to other adverse pharmacological parameters.

Another common modification of siRNA is the introduction of supplemental phosphorothioates, which is a modification of the phosphodiester linkages of siRNA (Nair et al, 2017). This modification also shows tremendous results. Indeed, a Sulfur with the P=S bond (phosphorothioate) which substitute the P=O bond can be used to increase the stability of the DNA oligonucleotides. This modification also provides an additional resistance and a great stability of siRNAs against nucleases (Jahns et al, 2015). However, with ribose modifications including 2′-OMe or F the enhancement of the stability and the improvement of the affinity have already perfectly been achieved without causing any toxic effects and reduced cell growth (Harborth et al, 2003) as was in the case where the use of phosphorothioates modification was high.

Other modifications with the deoxyribose have also proven to be effective. These siRNA hybrids have better stability and allows reduction of collateral extinctions. This last property is due to the relative instability of the guide-mRNA DNA-strand

couple compared to an equivalent guide-mRNA-RNA pair. Since the guide DNA supports less mismatch, it does not have the ability to extinguish mismatched mRNAs (Ui-Tei et al., 2008). This modification also facilitates the loading of the duplex into the RISC (Manoharan, 2004). This property is currently exploited today and commercial siRNAs often contain 3 'outgoing ends consisting of deoxyribonucleotides. However, these substitutions cannot be made anywhere in the double-strand: the presence of deoxyribonucleotides in the first two-thirds (3'-5 ') of the guide strand or at the 3' end of the passenger strand completely abolishes the power of extinction (Ui-Tei et al., 2008).

6-mCEPh-purine is a 5′ nucleobase modification. This chemical modification of the siRNA is less commonly used in siRNA design (Peacock et al., 2011) but demonstrated tremendous results as it was developed in the study lead by our partner Kyowa Kirin and my mechanistic investigation. Indeed, close to the 5’ phosphate, 6-mCEPh-purine with this 5′ nucleobase modification helps to acquire more stability of the 5’ end of the guide into Ago2. After reviewing the most common modifications, a question remained: How to situate 6-mCEPh-purine with these other modifications but also with the 5' phosphate modification as 5'-(E)-vinylphosphonate (5'-E-VP) which adopt similar strategy to enhance siRNA efficiency (Lima et al, 2012, Prakash et al, 2016, Prakash et al, 2017, Haraszti et al, 2017)?

Essential RNA silencing requires the recognition of the 5′- phosphate of a siRNA guide strand by the Argonaute protein in RISC (Martinez et al, 2002). However, the 5′- phosphate is rapidly removed by metabolic enzymes such as phosphatase for siRNAs introduced on an exogenous way. Efficient strategy to improve efficacy was to build phosphatase-resistant compounds. This chemical stabilization of the 5′-phosphate have been accomplished with the 5'-E-VP. While 5′-E-VP is known to lead to a better efficiency of guide incorporation in Ago2 improving the stability, the strategy to stabilize the guide strand in the MID domain pocket of Ago2 does not merely depend on the 5’ phosphate as it was demonstrated in my study. For that its rational to rethink the design of siRNA by chemical modification to obtain a better efficiency of RNA silencing. Additionally, all the chemical modifications cited previously have pros and cons and further progress may be obtained with the association of all these to

maximize efficiency. Fine combination and good balance of these multiple available possibilities will help siRNA therapeutic as a future new era of medicine.

Importance of my study

As the recent first drug using siRNA as therapeutics validated on the market has shown, siRNA has an enormous potential to cure many diseases in a natural way. However, there is still room for improvement in their efficiency while reducing their dosage and costs (Egli et al, 2019, Setten et al, 2019, Khvorova et al, 2017). My study developed in this thesis will provide a robust molecular platform to understand in vitro the mechanism of any chemically modified siRNAs at each step during Ago2-RISC assembly which will play a part to develop more efficiently RNAi drugs. Moreover, this molecular platform developed in my thesis may be used as a powerful tool though with some limitations.

Limitation of my study and perspective

A key approach to improving siRNA efficacy is chemical modifications. Through an in-silico screening of modifications at the 5′-end nucleobase of the guide strand, an adenine-derived compound called “6-mCEPh-purine” was identified to improve the RNAi activity in cultured human cells and in vivo mouse models. Using a series of biochemical approaches to evaluate the effect of the 6-mCEPh-purine modification quantitatively at each step in the assembly of the RNAi effector complex called RISC, I provided a molecular platform to further study the mechanism of chemically modified siRNA. Indeed, this system can be used to detect the effect of any chemical modifications with their combinations in order to improve the future drug development using RNA silencing as engine. However, there may be limitation to this molecular platform.

As it was shown in this thesis with BrdA where I did not succeed in monitoring the effect of this modification as an unknown band appeared preventing any quantification in the assembly of RISC. Some chemical modification may interact with different other proteins and not directly with Ago2 avoiding any measurement.

It is necessary to compare and complete in vitro finding using this molecular platform with in cell and in vivo study. Sometimes it can appear differently between in

vivo and in vitro study. If there is any discrepancy between in vitro, in cell, and in vivo data, that may propose a great opportunity to open new doors to science by asking why and where the discrepancy comes from.

The development of siRNA therapeutic is just starting to emerge and a good balance with the use of chemical modification is needed. Attesting the efficiency of siRNA is crucial to the further development of new medicine. The molecular platform developed in my thesis can be a powerful tool in accomplishing that.

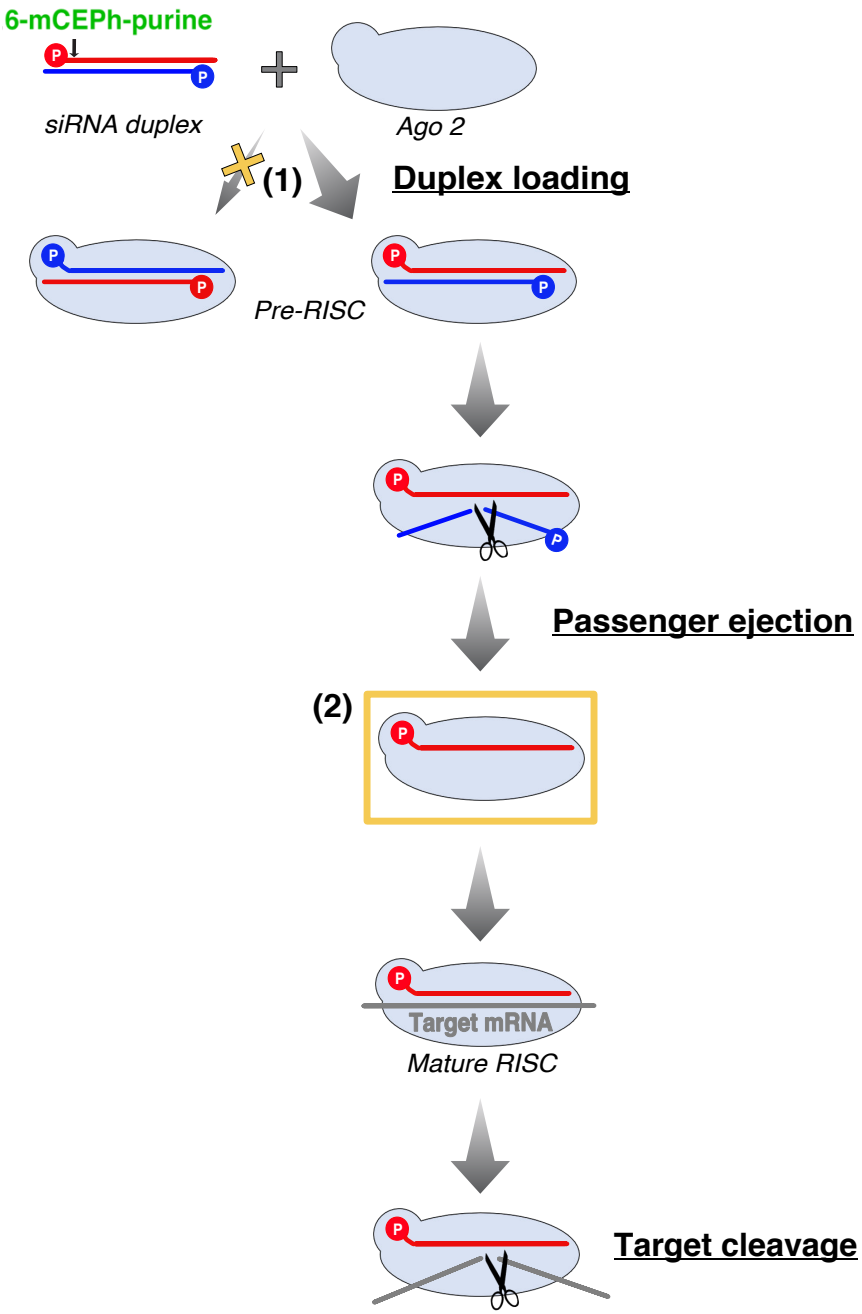

1) 6-mCEPh-purine helps the guide strand selection.
2) 6-mCEPh-purine increases the stability of mature RISC after passenger strand ejection.

Figure 27. A model for the molecular mechanism by which 6-mCEPh-purine enhances the RNAi activity.
6-mCEPh-purine modification improves the formation of mature RISC in two different ways: (1) 6-mCEPh-purine helps the guide strand selection. (2) 6-mCEPh-purine increases the stability of mature RISC after passenger strand ejection.

V. Materials and methods

1. HEK293T Cells culture

HEK293T cells were cultured in Dulbecco's Modified Eagle's Medium (DMEM) (Sigma) supplemented with 10% (v/v) Fetal Bovine Serum (FBS) (Sigma) at 37 °C in 5% CO_2.

2. HEK293T cells maintenance (detailed)

1. Dulbecco's Modified Eagle's Medium (DMEM) supplemented with 10% (v/v) Fetal Bovine Serum (FBS) (Sigma) and 0.05% Trypsin-EDTA solution was pre-warm in a 37°C waterbath.
2. The old culture medium from 10 cm petri dishes containing HEK293T cells confluent ~ 80% was removed and discarded
3. Cells was washed one time with 1 mL of 1x PBS (pH ~ 7.4) (Phosphate Buffer Saline solution) previously prepared.
4. PBS was aspirated.
5. ~ 1 mL 0.05% Trypsin-EDTA solution was added in each 10 cm dish and moved slowly.
6. Each dish was placed in the 37˚C incubator during 2-3 minutes.
7. ~ 3 mL of new medium was directly added (Trypsin-EDTA solution effect was inhibited adding the medium).
8. The detached cells was observed using a microscope (If cells are still aggregating, they may be detached "manually" by gentle pipetting to facilitate the dispersal).
9. 1 mL of the medium containing the cells from step 7was added in a dish filled with 9 mL of fresh medium.
10. The cells was homogenized in the dish and checked with a microscope.
11. New cultures was incubated at 37°C, 5% CO_2.

3. Overexpression of Flag-tagged hAgo2 protein in HEK 293T cells

HEK293T cells ~ 80% confluent were transfected with a plasmid DNA (pIRESneo-Flag-HA-Ago2 **(Meister et al., 2004) (Naruse et al., 2018) (Figure 28)** utilized to express Flag-tagged Ago2) by using Lipofectamine 3000 transfection reagent (Thermo Fisher).

On the day before the transfection, exponentially growing cells were plated into 10-cm dishes at a density of 1.2×10^6 cells per ml in antibiotic-free medium. The following day (24 h later), the cells were transfected with 10 μg per 10-cm dish plasmid DNA and harvested 48 h after.

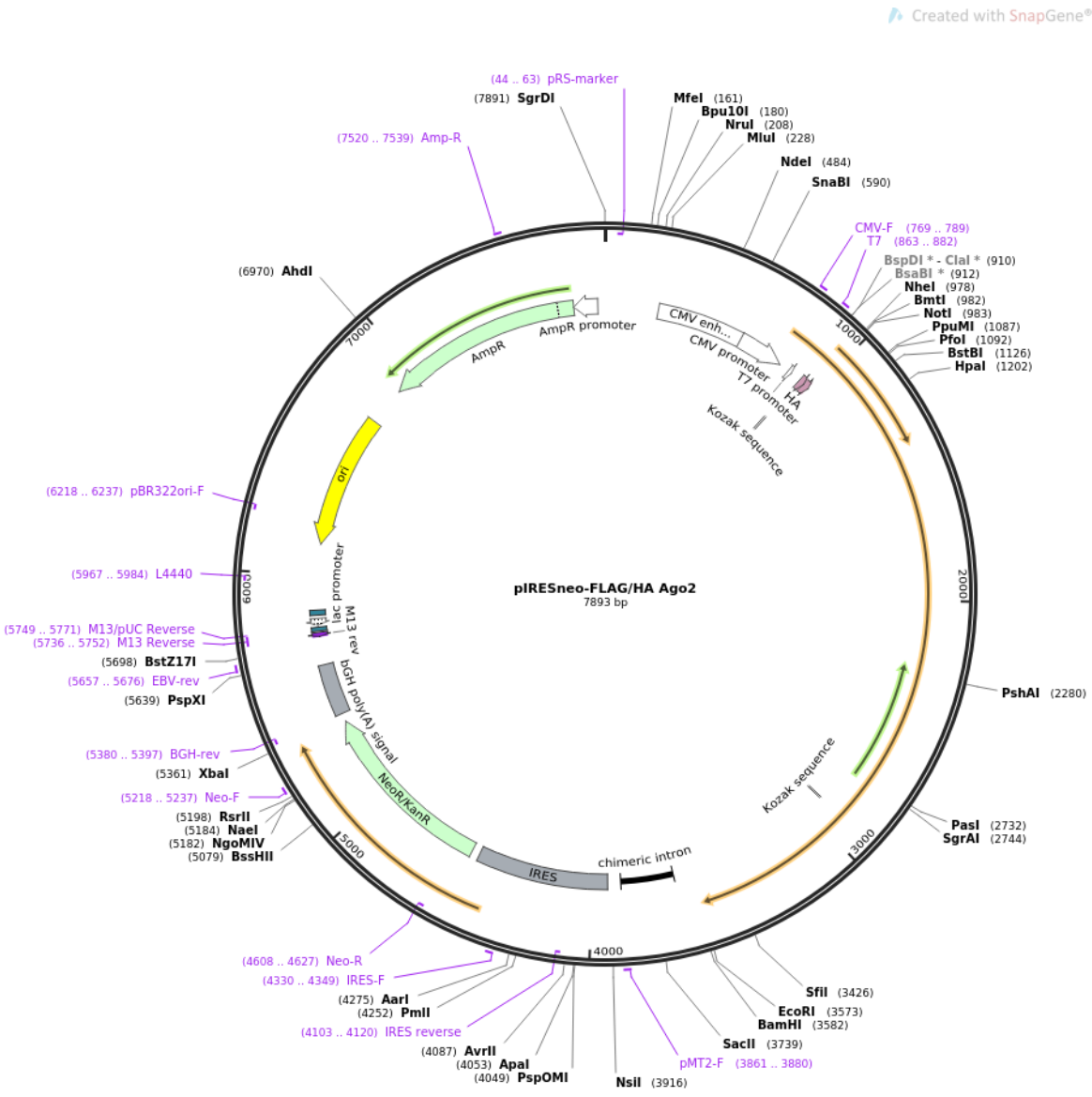

Figure 28. Overview of pIRESneo-FLAG/HA Ago2 plasmid.
(https://www.addgene.org/10822/)

4. Cell lysate preparation

HEK293T cells grown on 10-cm dishes were washed three times with cold PBS, (pH ~ 7.4) and collected by centrifugation at 1,000 x *g* for 3 min. at 4°C.

The cell pellet was resuspended in two packed-cell volume of lysis buffer (30 mM HEPES-KOH (pH 7.4), 100 mM potassium acetate 2 mM magnesium acetate) containing 5 mM DTT and 1× EDTA-free Complete Protease Inhibitor tablets (Roche) and subjected to Dounce homogenization.

Subsequently, the Lysate (cytoplasmic fraction) was clarified by centrifugation at 17,000 x *g* for 30 min at 4 °C. The supernatant was flash frozen in liquid nitrogen and immediately stored at - 80 °C single-use aliquots.

5. Western Blot and antibodies

To attest the expression level of Flag-tagged hAgo2 protein in HEK293T cells, separation was processed by SDS-PAGE 8% **(Table 1 and 2)** in TGS buffer and western blotting was performed on PVDF membranes. (TGS buffer was picked to run the SDS-PAGE 8 % gels in denaturing conditions and to help maintain the pH and the temperature of the environment).

PVDF membranes was blocked in a solution of 5% milk powder (diluted in TBS-T solution) and rinsed in TBST-T before antibody detection.

The primary antibodies included polyclonal rabbit anti-FLAG (1:1,000 ; Sigma-Aldrich), monoclonal mouse anti- hAgo2 (1:2000; Abcam, Cambridge, UK).

The secondary antibodies for chemiluminescent detection were horseradish peroxidase-conjugated goat anti-rabbit (or anti-mouse) IgG antibodies (Jackson ImmunoResearch, West Grove, PA, USA).

Chemiluminescence was induced by Luminata Immobilon Forte Western HRP Substrate (Millipore), and the images were acquired by Amersham imager 600 (GE Healthcare Life Sciences).

Protein size (kDa)	Gel percentage (%)
4-40	20
12-45	15
10-70	12.5
15-100	10
25-200	8

Flag-HA-Ago2
~100kDa

Table 1. Choice of the SDS gel percentage according the protein size.

Protogel (30%)	3.33 mL
4x wide range buffer	3.13 mL
MQW	5.97 mL
APS (20%)	62.5 μL
TEMED	7.5 μL
TOTAL	**12.5 mL**

Table 2. Composition of gel SDS-PAGE 8%.

6. Preparation of small RNA duplexes (detailed)

Different guide and passengers **(Figure 29)** bearing some modifications have been used to make different duplexes **(Figure 30)** during my research.

Small RNA duplex A holding a phosphate at the 5' for the guide and the passenger were both unlabeled and annealed together for the target cleavage assay.

Small RNA duplexes B, D and E were radiolabeled with the guide strand (*i.e.*, a $5'$- ^{32}P-radiolabeled guide strand annealed to an unlabeled phosphorylated passenger-strand).

Duplex D and E hold supplemental modifications: Duplex D has a 5' amino linker at the 5' end of the passenger strand and duplex E has a 5' amino linker at the 5' end of the passenger strand and additionally a 2' O-methyl at the position 9 of the passenger.

Small RNA duplex C was radiolabeled with the passenger strand (*i.e.*, a $5'$- ^{32}P-radiolabeled passenger strand annealed to an unlabeled phosphorylated guide-strand).

Preparation of small RNA duplex A phosphorylated:

MQW	29.5 µL
RNasin plus (Promega)	0.5 µL
T4 PNK (TaKaRa)	5 µL
10x PNK buffer (TaKaRa)	5 µL
100 µM single-stranded small RNA	5 µL
10 mM ATP	5 µL
TOTAL	**50 µL**

Table 3. Mixture to prepare small RNA duplex A phosphorylated.

1. The previous reaction mixture **(Table 3)** was incubated for 1h at 37 °C.
2. G-25 MicroSpin column have been prepared as following:
    - Remove the bottom cap
    - Centrifugate column 735g 1min.
    - wash with 500 µL of MQW
    - Centrifugate column 735g 1min.
    - Remove MQW from the column (Repeat 3 x the two last steps)
3. The column was changed and run through the 50 µL initial reaction mixture.

4. Centrifugation 735 x g during 1min.

5. 50 μL of MQW added in the column.

6. Centrifugation 735 x g 1min. (total volume is now 100 μL).

7. The radiolabeled RNA containing 100 μL of eluate was precipitated adding the following products **(Table 4):**

GCG (20mg/mL)	2 μL
NaOAc 3M (1/10x of reaction volume)	10 μL
EtOH 100% (3x volume)	300 μL

Table 4. Ethanol precipitation of the radiolabeled RNA.

8. Centrifugation at 20,000 x g for 30 min. at 4 ˚C.

9. The supernatant was removed and the pellet was kept safe.

10. The pellet was washed with 300 μL of Ethanol 70 % and centrifugated 20,000 x g for 5 min. at 4˚C.

11. The supernatant was removed, the cap stayed open and the pellet dried for ~ 10 min. at RT.

12. The pellet (precipitated RNA) was dissolved in 100 μL of MQW for a final concentration ~ 5 μM of labeled small RNA (concentration was checked with NanoDrop).

13. The duplex was prepared (or it also can be store at - 20˚C).

14. the small RNA duplexes was annealed (200 nM).

Small RNA <u>duplex A</u> phosphorylated on the guide and passenger strand (no radiolabeling):

2x Lysis buffer (without DTT and PIC)	25 μL
1 μM ^{32}P 5' phosphorylated guide strand	10 μL
1 μM ^{32}P 5' phosphorylated passenger strand	15 μL
TOTAL	**50 μL**

Table 5. Annealing of guide and passenger strand (no radiolabeled) to form the duplex.

15. The annealed mixture was incubated **(Table 5)** for 2-3 min. at 95˚C

16. Closed cap was left for ~ 30 min. at RT to anneal.

17. Final product was stored at - 20˚C

Preparation of small RNA duplexes C, B, D and E radiolabeled:

MQW	15.1 μL
RNasin plus (Promega)	0.5 μL
T4 PNK (TaKaRa)	1 μL
10x PNK buffer (TaKaRa)	2 μL
10 μM single-stranded small RNA	1 μL
25 μM [γ-^{32}P]ATP (185 MBq) Perkin Elmer	0.4 μL
TOTAL	**20 μL**

Table 6. Small RNA 32^{P} 5' end radiolabeling.

1. The previous reaction mixture was incubated **(Table 6)** for 1h at 37 ˚C.
2. G-25 MicroSpin column was prepared as following:
    - Remove the bottom cap
    - Centrifugate column 735 x g 1 min.
    - wash with 500 μL of MQW
    - Centrifugate column 735 x g 1 min.
    - Remove MQW from the column. (Repeat 3 x the two last steps)
3. The solution volume was adjusted at 50 μL in the reaction mixture (add 30 μL of MQW).
4. The column was changed and run through the 50 μL reaction mixture.
5. Centrifugation 735 x g 1 min.
6. 50 μL of MQW was added in the column.
7. Centrifugation 735 x g 1min. (total volume is now 100 μL).
8. The radiolabeled RNA contained in 100 μL of eluate was precipitated adding the following products **(Table 4).**
9. Centrifugation at 20,000 x g for 30 min. at 4 ˚C.
10. The supernatant was removed.
11. The pellet was washed with 300 μL of Ethanol 70 % and centrifugated 20,000 x g for 5 min. at 4˚C.
12. The supernatant was removed, with the cap open and the pellet was dried for ~ 10 min. at RT.
13. The pellet (precipitated RNA) was dissolved in 20 μL of MQW for a final concentration ~ 0.5 μM of labeled small RNA.
14. The duplex was prepared (or it also can be store at - 20˚C).

15. Small RNA duplexes annealing (100nM)

Small RNA duplex C radiolabeled with the passenger strand:

2x Lysis buffer (without DTT and PIC)	25 μL
500 nM ^{32}P 5' phosphorylated guide strand	15 μL
500 nM ^{32}P 5'-end radiolabeled passenger strand	10μL
TOTAL	**50 μL**

Table 7. Annealing of guide (radiolabeled) and passenger strand to form the duplex.

Small RNA duplexes B, D and E radiolabeled with the guide strand:

2x Lysis buffer (without DTT and PIC)	25 μL
500 nM ^{32}P 5' phosphorylated passenger strand	15 μL
500 nM ^{32}P 5'-end radiolabeled guide strand	10 μL
TOTAL	**50 μL**

Table 8. Annealing of guide and passenger (radiolabeled) strand to form the duplex.

16. The annealing mixture was incubated **(Table 7 and 8)** for 2-3min. at 95˚C
17. Closed cap was left for ~ 30 min. at RT to anneal.
18. Final product was stored at - 20˚C in RI room.

Name	5' → 3' sequence	passenger / guide	Features and usage
let7_gs_5'A(OH)	**A**GAGGUAGUUGGUUGUAUAGU	Let7 guide	5'A, 5'OH(-P) for ^{32}P labeling
let7_gs_5'U(OH)	**U**GAGGUAGUUGGUUGUAUAGU	Let7 guide	5'U , 5'OH(-P) for ^{32}P labeling
let7_gs_5'G(OH)	**G**GAGGUAGUUGGUUGUAUAGU	Let7 guide	5'G, 5'OH(-P) for ^{32}P labeling
let7_gs_5'BrdA(OH)	**(BrdA)**GAGGUAGUUGGUUGUAUAGU	Let7 guide	5'BrdA, 5'OH(-P) for ^{32}P labeling
let7_gs_5'616(OH)	**(616)**GAGGUAGUUGGUUGUAUAGU	Let7 guide	5'616, 5'OH(-P) for ^{32}P labeling
let7_gs_5'A(P)	**pA**GAGGUAGUUGGUUGUAUAGU	Let7 guide	5'A, 5' end phospholylated
let7_gs_5'U(P)	**pU**GAGGUAGUUGGUUGUAUAGU	Let7 guide	5'U, 5' end phospholylated
let7_gs_5'G(P)	**pG**GAGGUAGUUGGUUGUAUAGU	Let7 guide	5'G, 5' end phospholylated
let7_gs_5'BrdA(P)	**p(BrdA)**GAGGUAGUUGGUUGUAUAGU	Let7 guide	5'BrdA, 5' end phospholylated
let7_gs_5'616(P)	**p(616)**GAGGUAGUUGGUUGUAUAGU	Let7 guide	5'616, 5' end phospholylated
let7_ss_5'p_19i	pUAUACAACCAACUACCUCiCU	Let7 passenger	5' end phospholylated to make complementary base pair with universal base (U→i) at the 5' end of guide strand (i= 5-nitroindole)
let7_ss_5'p_10MM_19i	pUAUACAACC**U**ACUACCUCiCU	Let7 passenger	5' end phospholylated to make complementary base pair with universal base (U→i) at the 5' end of guide strand (i= 5-nitroindole) and a mismatch with the central site (A→U)

Figure 29. Synthetic small RNAs used in my study are summarized in this figure.

The guide and passenger strand of each small RNA duplex is derived from fly *let-7* miRNA. Phosphorylated 5' ends are denoted by the letter p. Nitroindole universal base is noted with the letter i.

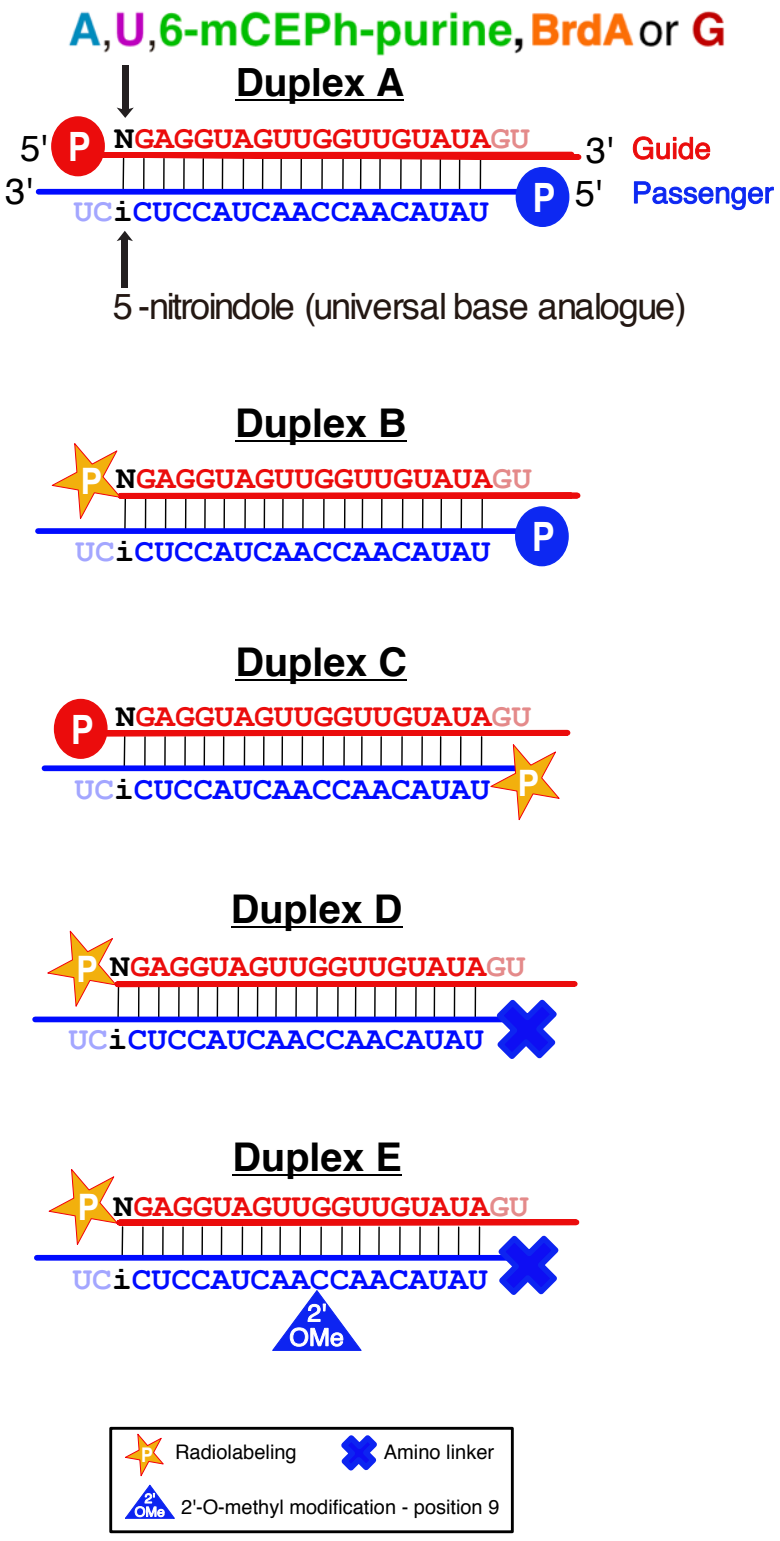

Figure 30. Different duplexes used during my study.

7. Preparation of target mRNA (detailed)

The 182-nt target mRNA for the target cleavage assay with *let-7* siRNAs was in vitro transcribed using T7-Scribe Standard RNA IVT Kit (Cellscript) from PCR products that were amplified with pGL3-basic vector (Promega) as a template.

The following forward primer:

(5′-GCGTAATACGACTCACTATAGTCACATCTCATCTACCTCC-3′)

and reverse primer:

(5′CCCATTTAGGTGACACTATAGATTTACATCGCGTGGATCTACTGGTCTGCCTA AAGAAGGTTGAGGTAGTAGGTTGTATAGTGAAGAGAGGAGTTCATG-3′) (2) were used on this purpose.

The target mRNA was gel purified (UREA gel 8%) and radiolabeled at the 5′- cap by guanylyl transferase and [α-^{32} P] GTP (3,000 Ci/mmole, Perkin Elmer) using the ScriptCap m^{7}G Capping System (CELLSCRIPT)) according to the manufacturer's instructions.

1. The DNA fragment containing the target site complementary to the guide strand was amplified from pGL3 basic vector (Luciferase reporter vector) by PCR **(Table 9)** using the primer previously described and the Taq DNA polymerase KOD plus Neo We decided to choose this enzyme for its high accuracy and fidelity **(Table 10).**

	KOD PLUS Neo	KOD FX Neo
Amplification	+	++
Fidelity	**++**	+

Table 10. Justification of PCR enzyme used.

Mix (x1)

- MQW……..…...…....32 μL
- 10x buffer……..……5 μL
- 2mM dNTP……..……..…5 μL
- 25mM $MgSO_4$……3 μL
- KOD plus……...……..1 μL
- 10μM Fw primer……..…1.5 μL
- 10μM Rv primer……..……1.5 μL
- Template DNA……...……...……1 μL

50 μL Total

< 3-step cycle >		
Pre-denaturation:	94°C, 2 min	
Denaturation:	98°C, 10 sec	
Annealing:	[Tm]°C, 30 sec	25-45 cycles
Extension:	68°C, **30sec/kb**	

Table 9. Protocol used for the PCR

2. the separation of the cDNA fragments obtained was effectuated with an agarose gel (1%) in TAE buffer followed by an electrophoresis (100v, 30-40min).
The EtoH precipitation to help to concentrate the PCR product separated was optional.
After the Excision of the DNA fragments, purification with Nucleo spin clean up kit MACHEREY-NAGEL was managed.
The concentration of cDNA was measured by Nanodrop & stored @ -20˚C or followed by IVT.
3. The transcription reaction was set up at RT with the T7-Scribe Standard RNA IVT Kit (Cellscript) (**Table 11)** by adding the reagents in the order indicated below:

Standard T7-Scribe Standard RNA IVT Reaction	
Component	Amount
RNase-Free Water	x μl
Linearized template DNA with T7 RNAP promoter	1 μg
10X T7-Scribe Transcription Buffer	2 μl
100 mM ATP	1.5 μl
100 mM CTP	1.5 μl
100 mM UTP	1.5 μl
100 mM GTP	1.5 μl
100 mM DTT	2 μl
ScriptGuard RNase Inhibitor	0.5 μl
T7-Scribe Enzyme Solution	2 μl
Total Reaction Volume	20 μl

Table 11. T7-Scribe Standard RNA IVT Kit (Cellscript)

After incubation for 2 hours at 37˚C, to remove the DNA template from the IVT reaction., we applied a DNase I treatment by adding 1 μL of DNase I.
The reaction mixture was incubated 15 min. at 37˚C before perform the RNA purification.

4. To remove residual proteins and unincorporated NTPs from the RNA, the purification of the RNA was made with a UREA gel 8% **(Table 12).**

Urea gel	8M UREA	5 x TBE
Concentrate	Diluant	Buffer
6.4 mL	11.2 mL	2 mL

Table 12. UREA gel 8% composition.

In last it was added:

+ APS……60-80 μL
+ TEMED……..20-30 μL

A volume/volume (v/v) of 2 x sample FA dye was added to the IVT reaction mix and placed at 95 ˚C for 2-3 min. before been loaded in the wells.

The gel was finally run at 500 v, 100 mA for 30 min.

The detection of the RNA in the gel was detected by UV shadowing and cut at the good length.

The band of gel containing the RNA was set in a 2 mL tube with 700 mL of 2x PK buffer rotating O/N.

5. To purify the RNA, isopropanol precipitation was done 24 hours later.

The 2 x PK buffer (containing the RNA) was transferred to a 1.5 mL tube with 700 μL of isopropanol (v/v) and 2 μL of GCG.

We centrifugated at 15,000 g for 30 min. at 4 ˚C , removed the supernatant and kept the pellet.

The pellet was washed with 700 μL of Ethanol 70 % and centrifugation 15,000 g for 5 min. at 4˚C. was proceeded.

The supernatant was removed, and the cap open, we dried the pellet for ~ 10 min. at RT.

The pellet (precipitated RNA) was dissolved in 20 μL of MQW.

The final concentration of the target RNA was checked by NanoDrop before the Cap-radiolabeling. This process (“the capping”) helps to improve the stability of the RNA compared to uncapped RNA and the radiolabeling allowed us to monitor the target cleavage efficiency.

6.The ScriptCapTM m^{7}G capping system was utilized to add a cap to the 5' terminus of our RNA target that has a 5'-triphosphate group obtained from the IVT reaction. According the cellscript protocol, a “cap” or "cap nucleotide" is a guanine (G) nucleoside that is linked via its 5' carbon to a triphosphate group.

This triphosphate group is in turn, linked to the 5' carbon of the most 5' nucleotide of the primary mRNA transcript.

In eukaryote organisms, the N at the position 7 of the G in the cap is methylated.

Such a capped RNA (transcript) can be represented as shown in the **(Figure 31)**

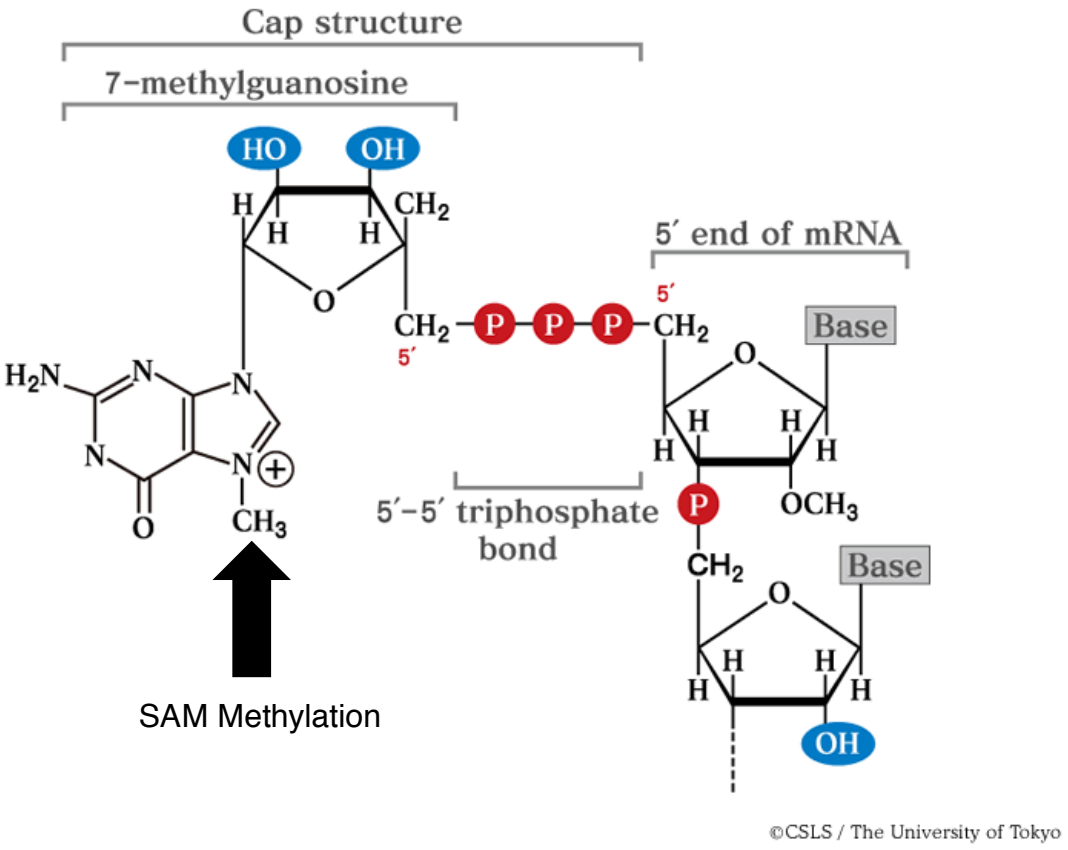

Figure 31. Capped RNA product from a ScriptCap m G Capping (System has a “cap 0” structure).

7. The following reaction mix **(Table 13)** was prepared and incubated at 37°C for 2 hours. A volume/volume (v/v) of 2 x sample FA dye was added to the Cap-radiolabeling reaction mix and placed at 95 ˚C for 2-3 min.

RNase free water	13.5 µL
RNase inhibitor	0.5 µL
10 x script cap buffer	2 µL
SAM 2 mM	1 µL
Target RNA 1 µM	1 µL
Enzyme mix	1 µL
+ GTP 3.3 µM (α^{32}-P)	1 µL
TOTAL	**20 µL**

Table 13. Cap-radiolabeling mixture.

8. The “Cap 0” mRNA target was now ready to be purified by gel purification with a 8% UREA gel before the isopropanol precipitation process.

9. The final product was stocked at - 20°C.

8. Target cleavage assay (detailed)

1. Target mRNA cleavage assays were performed in reactions mixtures preincubated at 25˚C during approximatively 30 min in order to assembly the RISC complex.
The typical reaction mixture **(Table 14)** included:

- 10 µl of of lysate from HEK 293T cells expressing Flag-tagged Ago2 proteins
- 6µL 40× reaction mix
- 2 µL of Ficoll-400 (facilitate the loading of samples onto the gel)
- 2 µL 100 nM 5′-phosphorylated small-RNA duplexes

2. After the addition of 2 µL ~10 nM ^{32}P cap-radiolabeled target mRNA, the time course was launched.

Lysate	10 µL
40 x reaction mix	6 µL
~ 100 nM small RNA duplex cold	2 µL
15% (w/v) Ficoll-400 in 1 x lysis buffer	2 µL
~ 10 nM mRNA target radiolabeled	2 µL
TOTAL	**22 µL**

Table 14. Target cleavage reaction mix

3. At each time point desired, a fraction of 2 µL of the reaction mixture **(Table 14)** was taken and the reactions were stopped by using a shortcut method for RNA sample preparation (developed by Hiro-oki Iwakawa) **(Table 15, 16 and Figure 32)** adding 8 µl of low salt PK solution (10x low salt PK buffer (100 mM HEPES-KOH, pH 7.4, 100 mM EDTA and 1% [w/v] SDS) 1.25x, Proteinase K 12.5%, MQW).
The reaction mixture was after incubated at 55˚C during 10 min.
At the end, an equal volume of 2× formamide dye containing 25 mM EDTA and 0.1% SDS was added and the samples was incubated 5 min at 68˚C and placed at RT.

4. The target substrate (182-nt) and 5′ cleavage product (112-nt) were separated on a 8% denaturing polyacrylamide gel.

5. After electrophoresis, gels were placed on a whatman 3MM paper with a thin cellophane sheet cover and have been dried during ~ 30 min under vacuum in a gel dryer at ~ 80˚C.

6. Gels have been imaged by Typhoon FLA 7000 (GE Healthcare Life Sciences) to be finally quantified using Multi Gauge software (Fujifilm Life Sciences). Figures were obtained using IgorPro (WaveMetrics).

10 % SDS → 1 % (d1/10)	1 mL
0.5 M EDTA → 100 mM (d1/5)	2 mL
1 M hepes-koh → 100 mM (d1/10)	1 mL
MQW	6 mL
TOTAL	**10 mL**

Table 15. Preparation of 10x low salt PK buffer

10 x Low salt PK buffer → 1.25 x	125 μL
Proteinase K	125 μL
MQW	750 μL
TOTAL	**1 mL**

Table 16. Preparation of Low salt PK solution

A shortcut method for RNA sample preparation

Hiro-oki Iwakawa

I developed a shortcut method for RNA sample preparation before loading gel. This method allows us to skip ethanol precipitation in sample preparation.

Materials

- 10 × Low salt PK buffer: 1% SDS, 100 mM EDTA, 100 mM HEPES-KOH (pH7.4)
- Proteinase K (Takara)
- Low salt PK solution: 1.25 × Low salt PK buffer containing 12.5 % Proteinase K
- 2 × formamide dye: 10 mM EDTA pH 8.0, 98% (w/v) deionized formamide, 0.025% (w/v) xylene cyanol, 0.025% bromophenol blue. Store in aliquots at –20 °C.

Methods

1. Mix 2 µl of reaction (lysate or mixture of purified proteins and RNAs) with 8 µl of Low salt PK solution in a 1.5 ml centrifuge tube, and incubate at 55 °C for 10 min.
2. Add 10 ul of 2 × formamide dye into the sample, then incubate at 68 °C for 5 min.
3. Load 5 µl of aliquots into the well of gel.

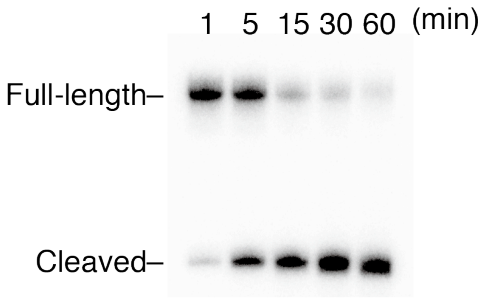

Figure. Target cleavage assay

Figure 32. Shortcut method for RNA sample preparation.

9. In vitro RISC assembly assay and Native gel analysis (detailed)

1. Before start the RISC assembly assay, native gels 1.5–2 mm thick, containing 1.4% (w/v) agarose (Low Range Ultra Agarose, Bio-Rad Laboratories), were cast vertically between glass plates with 0.5-mm-thick bottom spacers (16 cm × 16 cm) for electrophoresis.

2. The Lower and the upper reservoirs of the electrophoresis tank were filled with 0.5 x TBE buffer (44.5 mM Tris, 44.5 mM Borate, 1 mM EDTA) previously cool down at 4˚C.

To remove air bubbles remaining beneath the gel a syringe was used.

To detect intermediate complexes (Pre-RISC and mature RISC) in the Ago2-RISC assembly pathway, reactions incubated at 25 °C consisted of **(Table 17):**

- 10 µl lysate
- 6 µl 40× reaction mix
- 2 µl 15% (w/v) Ficoll-400 in lysis buffer x1 (facilitate the loading of samples onto the native gel)
- 2 µl of ~ 50 nM small RNA duplexes with the guide strand
- 2 µl 50 nM 2′-*O*-methyl antisense oligonucleotide (ASO)

Lysate	10 µL
40× reaction mix	6 µL
15% (w/v) Ficoll-400 in lysis buffer x1	2 µL
~ 50 nM small RNA duplexes with the guide strand	2 µL
50 nM 2′-*O*-methyl antisense oligonucleotide (ASO)	2 µL
TOTAL	**22 µL**

Table 17. RISC assembly reaction.

3. 2'-O-methyl ASO containing a 5-nitroindole was used as the target: 5'mUmCmUmUmCmAmCmUmAmUmAmCmAmAmCmCmUmAmCmUmAmCmCmUmC/5-nitroindole/mAmCmCmUmU-3'.

4. This antisense oligonucleotide was complementary to the guide-strand sequence of duplex A, B, D and duplex E, except for one central mismatch.

Preparation of the 40× reaction mix and lysis buffer (30 mM HEPES-KOH, pH 7.4, 100 mM potassium acetate and 2 mM magnesium acetate) has been described in detail in materials and methods annex.

For an alternative native gel analysis, with the Duplex C the passenger strand was radiolabeled instead of the guide strand. (In this configuration, the 2'-O-methyl ASO containing a 5-nitroindole was complementary to the passenger-strand sequence).

5. After incubation, 1.4 μL of sample for each time point desired was loaded per agarose-gel well.

6. The RISC complexes were resolved by the vertical, native 1.4% agarose gel electrophoresis at 355 V for 1.5 h in a 4°C cold room with ice-cold 0.5× Tris-borate-EDTA buffer kept cold with several ice-sticks in the vertical buffer chamber.

7. Once electrophoresis done, agarose gel was flipped over a Hybond N+ membrane to prevent any smear when the gel will dry. The Hybond N+ membrane holding the gel was deposited on a Whatman 3MM paper and a thin cellophane plastic sheet was added to cover the gel.

8. Gel was dried for~ 30 min. with a gel dryer at 80°C under a vacuum.

9. After been dried complexes in the gel were detected by PhosphorImager (FLA-7000 image analyzer, Fujifilm) and quantified using Multi Gauge software (Fujifilm).

10. For all experiments, gels shown in a single figure originated from experiments that were conducted at the same time and that were exposed to the same phosphorimaging plate.

Data and figures were prepared using IgorPro (WaveMetrics).

10. Micrococcal nuclease treatment

A RISC assembly assay was done without inclusion of the 2'-O-methyl ASO containing a 5-nitroindole. To exclude any possible endogenous RNA to link the radiolabeled guide, HEK293T lysate was treated with a Micrococcal nuclease.

Typically for 100 µl of lysate treatment:

- 4 µL of micrococcal nuclease diluted x 125 in naïve lysate (from 2.000.000 gel U/mL, NEB for a final concentration 16.000 gel U/mL) was added. (Note the naïve lysate was diluted 5x in lysis buffer).
- 1 µL 100 mM $Ca(OAc)_2$ was added for a final concentration at 1 nM and incubated at 25°c for 20 min.
- Finally, 2 µL 200 mM EGTA for a final concentration 4 nM was added to stop the reaction and use this lysate to launch the RISC assembly assay (without target).

11. Materials and methods annex

5x Lysis buffer

1 M HEPES-KOH pH 7.4 (final [C]= 30 mM)	150 mL
1 M KOAc (final [C]= 100 mM)	500 mL
1 M $Mg(OAc)_2$ (final [C]= 2 mM)	10 mL
MQW	340 mL
TOTAL	**1 L**

1x Lysis buffer

1 M HEPES-KOH pH 7.4 (final [C]= 30 mM)	1.5 mL
1 M KOAc (final [C]= 100 mM)	5 mL
1 M $Mg(OAc)_2$ (final [C]= 2 mM)	100 µL
MQW	43.4 mL
TOTAL	**50 mL**

Optional:
+ 1 M DTT add 250 µl for 50 mL
+ PIC (25x) (Roche) add 1 large tablet for 50 mL

40x reaction mix

MQW	71 µL
500 mM creatine monophosphate *	20 µL
1 M DTT	2 µL
40 U/µL RNasin plus	1 µL
100 mM ATP	4 µL
1 M KOAc	16 µL
500 mM $Mg(OAc)_2$	2.24 µL
creatine phosphokinase **	6 µL
TOTAL	**122.24 µL**

* 16.4 mg of powder diluted in 100 µL of MQW
** 2 µL of 10 U/µL stock diluted in 8 µL lysis buffer 1 x

2x formamide loading buffer

(w/v) deionized formamide	98 %
EDTA pH 8.0	10 mM
(w/v) xylene cyanol	0.025 %
(w/v) bromophenol blue	0.025 %

2x proteinase K buffer

Tris-Cl pH 7.5	200 mM
EDTA pH 8.0	25 mM
Sodium chloride	300 mM
(w/v) SDS	2 %

VI. References

Adams, D., Gonzalez-Duarte, A., O'Riordan, W.D., Yang, C.-C., Ueda, M., Kristen, A.V., Tournev, I., Schmidt, H.H., Coelho, T., Berk, J.L., Lin, K.-P., Vita, G., Attarian, S., Planté-Bordeneuve, V., Mezei, M.M., Campistol, J.M., Buades, J., Brannagan, T.H., Kim, B.J., Oh, J., Parman, Y., Sekijima, Y., Hawkins, P.N., Solomon, S.D., Polydefkis, M., Dyck, P.J., Gandhi, P.J., Goyal, S., Chen, J., Strahs, A.L., Nochur, S.V., Sweetser, M.T., Garg, P.P., Vaishnaw, A.K., Gollob, J.A., Suhr, O.B., 2018. Patisiran, an RNAi Therapeutic, for Hereditary Transthyretin Amyloidosis. N. Engl. J. Med. 379, 11–21. https://doi.org/10.1056/NEJMoa1716153

Agrawal, N., Dasaradhi, P.V.N., Mohmmed, A., Malhotra, P., Bhatnagar, R.K., Mukherjee, S.K., 2003. RNA interference: biology, mechanism, and applications. Microbiol. Mol. Biol. Rev. 67, 657–685. https://doi.org/10.1128/mmbr.67.4.657-685.2003

Altuvia, Y., Landgraf, P., Lithwick, G., Elefant, N., Pfeffer, S., Aravin, A., Brownstein, M.J., Tuschl, T., Margalit, H., 2005. Clustering and conservation patterns of human microRNAs. Nucleic Acids Res. 33, 2697–2706. https://doi.org/10.1093/nar/gki567

Amarzguioui, M., Holen, T., Babaie, E., Prydz, H., 2003. Tolerance for mutations and chemical modifications in a siRNA. Nucleic Acids Res. 31, 589–595. https://doi.org/10.1093/nar/gkg147

Aravin, A.A., Lagos-Quintana, M., Yalcin, A., Zavolan, M., Marks, D., Snyder, B., Gaasterland, T., Meyer, J., Tuschl, T., 2003. The small RNA profile during Drosophila melanogaster development. Dev. Cell 5, 337–350.

Aravin, A.A., Naumova, N.M., Tulin, A.V., Vagin, V.V., Rozovsky, Y.M., Gvozdev, V.A., 2001. Double-stranded RNA-mediated silencing of genomic tandem repeats and transposable elements in the D. melanogaster germline. Curr. Biol. 11, 1017–1027.

Arkov, A.L., Wang, J.-Y.S., Ramos, A., Lehmann, R., 2006. The role of Tudor domains in germline development and polar granule architecture. Development 133, 4053–4062. https://doi.org/10.1242/dev.02572

Bartel, D.P., 2009. MicroRNAs: target recognition and regulatory functions. Cell 136, 215–233. https://doi.org/10.1016/j.cell.2009.01.002

Behm-Ansmant, I., Rehwinkel, J., Doerks, T., Stark, A., Bork, P., Izaurralde, E., 2006. mRNA degradation by miRNAs and GW182 requires both CCR4:NOT deadenylase and DCP1:DCP2 decapping complexes. Genes Dev. 20, 1885–1898. https://doi.org/10.1101/gad.1424106

Behlke M.A.Progress towards in vivo Use of siRNAs Mol. Ther. 2006, 13 4,644-670 https://doi.org/10.1016/j.ymthe.2006.01.001

Bitko, V., Musiyenko, A., Shulyayeva, O., Barik, S., 2005. Inhibition of respiratory viruses by nasally administered siRNA. Nat. Med. 11, 50–55. https://doi.org/10.1038/nm1164

Bumcrot, D., Manoharan, M., Koteliansky, V., Sah, D.W.Y., 2006. RNAi therapeutics: a potential new class of pharmaceutical drugs. Nat. Chem. Biol. 2, 711–719. https://doi.org/10.1038/nchembio839

Bushati, N., Cohen, S.M., 2007. microRNA functions. Annu. Rev. Cell Dev. Biol. 23, 175–205.

Castel, S.E., Martienssen, R.A., 2013. RNA interference in the nucleus: roles for small RNAs in transcription, epigenetics and beyond. Nat. Rev. Genet. 14, 100–112. https://doi.org/10.1038/nrg3355

Chen, C.-Y.A., Zheng, D., Xia, Z., Shyu, A.-B., 2009. Ago-TNRC6 triggers microRNA-mediated decay by promoting two deadenylation steps. Nat. Struct. Mol. Biol. 16, 1160–1166. https://doi.org/10.1038/nsmb.1709

Chen, P.Y., Weinmann, L., Gaidatzis, D., Pei, Y., Zavolan, M., Tuschl, T., Meister, G., 2008. Strand-specific 5'-O-methylation of siRNA duplexes controls guide strand selection and targeting specificity. RNA 14, 263–274. https://doi.org/10.1261/rna.789808

Chiu, Y.-L., Rana, T.M., 2002. RNAi in human cells: basic structural and functional features of small interfering RNA. Mol. Cell 10, 549–561.

Choung, S., Kim, Y.J., Kim, S., Park, H.-O., Choi, Y.-C., 2006. Chemical modification of siRNAs to improve serum stability without loss of efficacy. Biochem. Biophys. Res. Commun. 342, 919–927. https://doi.org/10.1016/j.bbrc.2006.02.049

Cogoni, C., Irelan, J.T., Schumacher, M., Schmidhauser, T.J., Selker, E.U., Macino, G., 1996. Transgene silencing of the al-1 gene in vegetative cells of Neurospora is mediated by a cytoplasmic effector and does not depend on DNA-DNA interactions or DNA methylation. EMBO J. 15, 3153–3163.

Cummins, L.L., Owens, S.R., Risen, L.M., Lesnik, E.A., Freier, S.M., McGee, D., Guinosso, C.J., Cook, P.D., 1995. Characterization of fully 2'-modified oligoribonucleotide hetero- and homoduplex hybridization and nuclease sensitivity. Nucleic Acids Res. 23, 2019–2024. https://doi.org/10.1093/nar/23.11.2019

Czauderna, F., Fechtner, M., Dames, S., Aygün, H., Klippel, A., Pronk, G.J., Giese, K., Kaufmann, J., 2003. Structural variations and stabilising modifications of synthetic siRNAs in mammalian cells. Nucleic Acids Res. 31, 2705–2716. https://doi.org/10.1093/nar/gkg393

de Fougerolles, A., Vornlocher, H.-P., Maraganore, J., Lieberman, J., 2007. Interfering with disease: a progress report on siRNA-based therapeutics. Nat Rev Drug Discov 6, 443–453. https://doi.org/10.1038/nrd2310

De, N., Young, L., Lau, P.-W., Meisner, N.-C., Morrissey, D.V., MacRae, I.J., 2013. Highly complementary target RNAs promote release of guide RNAs from human Argonaute2. Mol. Cell 50, 344–355. https://doi.org/10.1016/j.molcel.2013.04.001

Denli, A.M., Tops, B.B.J., Plasterk, R.H.A., Ketting, R.F., Hannon, G.J., 2004. Processing of primary microRNAs by the Microprocessor complex. Nature 432, 231–235. https://doi.org/10.1038/nature03049

Duxbury, M.S., Matros, E., Ito, H., Zinner, M.J., Ashley, S.W., Whang, E.E., 2004. Systemic siRNA-mediated gene silencing: a new approach to targeted therapy of cancer. Ann. Surg. 240, 667–674; discussion 675-676. https://doi.org/10.1097/01.sla.0000140755.97224.9a

Egli, M., Manoharan, M., 2019. Re-Engineering RNA Molecules into Therapeutic Agents. Acc. Chem. Res. 52, 1036–1047. https://doi.org/10.1021/acs.accounts.8b00650

Elbashir, S.M., Harborth, J., Lendeckel, W., Yalcin, A., Weber, K., Tuschl, T., 2001. Duplexes of 21-nucleotide RNAs mediate RNA interference in cultured mammalian cells. Nature 411, 494–498. https://doi.org/10.1038/35078107

Elkayam, E., Kuhn, C.-D., Tocilj, A., Haase, A.D., Greene, E.M., Hannon, G.J., Joshua-Tor, L., 2012. The Structure of Human Argonaute-2 in Complex with miR-20a. Cell 150, 100–110. https://doi.org/10.1016/j.cell.2012.05.017

Elkayam, E., Parmar, R., Brown, C.R., Willoughby, J.L., Theile, C.S., Manoharan, M., Joshua-Tor, L., 2017. siRNA carrying an (E)-vinylphosphonate moiety at the 5′ end of the guide strand augments gene silencing by enhanced binding to human Argonaute-2. Nucleic Acids Res. 45, 3528–3536. https://doi.org/10.1093/nar/gkw1171

Eystathioy, T., Jakymiw, A., Chan, E.K.L., Séraphin, B., Cougot, N., Fritzler, M.J., 2003. The GW182 protein colocalizes with mRNA degradation associated proteins hDcp1 and hLSm4 in cytoplasmic GW bodies. RNA 9, 1171–1173. https://doi.org/10.1261/rna.5810203

Findley, S.D., Tamanaha, M., Clegg, N.J., Ruohola-Baker, H., 2003. Maelstrom, a Drosophila spindle-class gene, encodes a protein that colocalizes with Vasa and RDE1/AGO1 homolog, Aubergine, in nuage. Development 130, 859–871. https://doi.org/10.1242/dev.00310

Fire, A., Xu, S., Montgomery, M.K., Kostas, S.A., Driver, S.E., Mello, C.C., 1998. Potent and specific genetic interference by double-stranded RNA in Caenorhabditis elegans. Nature 391, 806–811. https://doi.org/10.1038/35888

Frank, F., Sonenberg, N., Nagar, B., 2010. Structural basis for 5'-nucleotide base-specific recognition of guide RNA by human AGO2. Nature 465, 818–822. https://doi.org/10.1038/nature09039

Friedrich, I., Shir, A., Klein, S., Levitzki, A., 2004. RNA molecules as anti-cancer agents. Semin. Cancer Biol. 14, 223–230. https://doi.org/10.1016/j.semcancer.2004.04.001

Ghildiyal, M., Zamore, P.D., 2009. Small silencing RNAs: an expanding universe. Nat. Rev. Genet. 10, 94–108. https://doi.org/10.1038/nrg2504

Giladi, H., Ketzinel-Gilad, M., Rivkin, L., Felig, Y., Nussbaum, O., Galun, E., 2003. Small interfering RNA inhibits hepatitis B virus replication in mice. Mol. Ther. 8, 769–776. https://doi.org/10.1016/s1525-0016(03)00244-2

Golzio, M., Mazzolini, L., Moller, P., Rols, M.P., Teissié, J., 2005. Inhibition of gene expression in mice muscle by in vivo electrically mediated siRNA delivery. Gene Ther. 12, 246–251. https://doi.org/10.1038/sj.gt.3302405

Gregory, R.I., Yan, K.-P., Amuthan, G., Chendrimada, T., Doratotaj, B., Cooch, N., Shiekhattar, R., 2004. The Microprocessor complex mediates the genesis of microRNAs. Nature 432, 235–240. https://doi.org/10.1038/nature03120

Gu, W., Shirayama, M., Conte, D., Vasale, J., Batista, P.J., Claycomb, J.M., Moresco, J.J., Youngman, E.M., Keys, J., Stoltz, M.J., Chen, C.-C.G., Chaves, D.A., Duan, S., Kasschau, K.D., Fahlgren, N., Yates, J.R., Mitani, S., Carrington, J.C., Mello, C.C., 2009. Distinct argonaute-mediated 22G-RNA pathways direct genome surveillance in the C. elegans germline. Mol. Cell 36, 231–244. https://doi.org/10.1016/j.molcel.2009.09.020

Guo, S., Kemphues, K.J., 1995. par-1, a gene required for establishing polarity in C. elegans embryos, encodes a putative Ser/Thr kinase that is asymmetrically distributed. Cell 81, 611–620. https://doi.org/10.1016/0092-8674(95)90082-9

Guo, S., Huang, F., Guo, P., 2006. Construction of folate-conjugated pRNA of bacteriophage phi29 DNA packaging motor for delivery of chimeric siRNA to nasopharyngeal carcinoma cells. Gene Ther. 13, 814–820. https://doi.org/10.1038/sj.gt.3302716

Guo, P., Coban, O., Snead, N.M., Trebley, J., Hoeprich, S., Guo, S., Shu, Y., 2010. Engineering RNA for targeted siRNA delivery and medical application. Adv. Drug Deliv. Rev. 62, 650–666. https://doi.org/10.1016/j.addr.2010.03.008

Hamilton, A.J., Baulcombe, D.C., 1999. A species of small antisense RNA in posttranscriptional gene silencing in plants. Science 286, 950–952. https://doi.org/10.1126/science.286.5441.950

Hammond, S.M., Bernstein, E., Beach, D., Hannon, G.J., 2000. An RNA-directed nuclease mediates post-transcriptional gene silencing in Drosophila cells. Nature 404, 293–296. https://doi.org/10.1038/35005107

Hall, T.M.T., 2005. Structure and function of argonaute proteins. Structure 13, 1403–1408. https://doi.org/10.1016/j.str.2005.08.005

Han, J., Lee, Y., Yeom, K.-H., Kim, Y.-K., Jin, H., Kim, V.N., 2004. The Drosha-DGCR8 complex in primary microRNA processing. Genes Dev 18, 3016–3027. https://doi.org/10.1101/gad.1262504

Harborth, J., Elbashir, S.M., Bechert, K., Tuschl, T., Weber, K., 2001. Identification of essential genes in cultured mammalian cells using small interfering RNAs. J. Cell. Sci. 114, 4557–4565.

Haraszti, R.A., Roux, L., Coles, A.H., Turanov, A.A., Alterman, J.F., Echeverria, D., Godinho, B.M.D.C., Aronin, N., Khvorova, A., 2017. 5′-Vinylphosphonate improves tissue accumulation and efficacy of conjugated siRNAs in vivo. Nucleic Acids Res. 45, 7581–7592. https://doi.org/10.1093/nar/gkx507

Horwich, M.D., Li, C., Matranga, C., Vagin, V., Farley, G., Wang, P., Zamore, P.D., 2007. The Drosophila RNA methyltransferase, DmHen1, modifies germline piRNAs and single-stranded siRNAs in RISC. Curr. Biol. 17, 1265–1272. https://doi.org/10.1016/j.cub.2007.06.030

Iki, T., Yoshikawa, M., Nishikiori, M., Jaudal, M.C., Matsumoto-Yokoyama, E., Mitsuhara, I., Meshi, T., Ishikawa, M., 2010. In vitro assembly of plant RNA-induced silencing complexes facilitated by molecular chaperone HSP90. Mol. Cell 39, 282–291. https://doi.org/10.1016/j.molcel.2010.05.014

Ipsaro, J.J., Haase, A.D., Knott, S.R., Joshua-Tor, L., Hannon, G.J., 2012. The structural biochemistry of Zucchini implicates it as a nuclease in piRNA biogenesis. Nature 491, 279–283. https://doi.org/10.1038/nature11502

Iwasaki, S., Kobayashi, M., Yoda, M., Sakaguchi, Y., Katsuma, S., Suzuki, T., Tomari, Y., 2010. Hsc70/Hsp90 chaperone machinery mediates ATP-dependent RISC loading of small RNA duplexes. Mol. Cell 39, 292–299. https://doi.org/10.1016/j.molcel.2010.05.015

Iwasaki, S., Sasaki, H.M., Sakaguchi, Y., Suzuki, T., Tadakuma, H., Tomari, Y., 2015. Defining fundamental steps in the assembly of the Drosophila RNAi enzyme complex. Nature 521, 533–536. https://doi.org/10.1038/nature14254

Izumi, N., Shoji, K., Sakaguchi, Y., Honda, S., Kirino, Y., Suzuki, T., Katsuma, S., Tomari, Y., 2016. Identification and Functional Analysis of the Pre-piRNA 3' Trimmer in Silkworms. Cell 164, 962–973. https://doi.org/10.1016/j.cell.2016.01.008

Jahns, H., Roos, M., Imig, J., Baumann, F., Wang, Y., Gilmour, R., Hall, J., 2015. Stereochemical bias introduced during RNA synthesis modulates the activity of phosphorothioate siRNAs. Nat Commun 6, 6317. https://doi.org/10.1038/ncomms7317

Jinek, M., Doudna, J.A., 2009. A three-dimensional view of the molecular machinery of RNA interference. Nature 457, 405–412. https://doi.org/10.1038/nature07755

Johnston, M., Geoffroy, M.-C., Sobala, A., Hay, R., Hutvagner, G., 2010. HSP90 protein stabilizes unloaded argonaute complexes and microscopic P-bodies in human cells. Mol. Biol. Cell 21, 1462–1469. https://doi.org/10.1091/mbc.e09-10-0885

Kawamata, T., Tomari, Y., 2011. Native gel analysis for RISC assembly. Methods Mol. Biol. 725, 91–105. https://doi.org/10.1007/978-1-61779-046-1_7

Kawamata, T., Yoda, M., Tomari, Y., 2011. Multilayer checkpoints for microRNA authenticity during RISC assembly. EMBO Rep. 12, 944–949. https://doi.org/10.1038/embor.2011.128

Kawaoka, S., Izumi, N., Katsuma, S., Tomari, Y., 2011. 3' end formation of PIWI-interacting RNAs in vitro. Mol. Cell 43, 1015–1022. https://doi.org/10.1016/j.molcel.2011.07.029

Kennerdell, J.R., Carthew, R.W., 1998. Use of dsRNA-mediated genetic interference to demonstrate that frizzled and frizzled 2 act in the wingless pathway. Cell 95, 1017–1026. https://doi.org/10.1016/s0092-8674(00)81725-0

Khvorova, A., Watts, J.K., 2017. The chemical evolution of oligonucleotide therapies of clinical utility. Nat. Biotechnol. 35, 238–248. https://doi.org/10.1038/nbt.3765

Kitabwalla, M., Ruprecht, R.M., 2002. RNA interference--a new weapon against HIV and beyond. N. Engl. J. Med. 347, 1364–1367. https://doi.org/10.1056/NEJMcibr022294

Khvorova, A., Watts, J.K., 2017. The chemical evolution of oligonucleotide therapies of clinical utility. Nat Biotechnol 35, 238–248. https://doi.org/10.1038/nbt.3765

Kim D.H., Rossi J.J. 2007 Strategies for silencing human disease using RNA interference Nat. Rev. Genet. 2007, 8, 173-184

Kuhn, C.-D., Joshua-Tor, L., 2013. Eukaryotic Argonautes come into focus. Trends Biochem. Sci. 38, 263–271. https://doi.org/10.1016/j.tibs.2013.02.008

Kuramochi-Miyagawa, S., Kimura, T., Yomogida, K., Kuroiwa, A., Tadokoro, Y., Fujita, Y., Sato, M., Matsuda, Y., Nakano, T., 2001. Two mouse piwi-related genes: miwi and mili. Mech. Dev. 108, 121–133.

Kuttenkeuler, D., Boutros, M., 2004. Genome-wide RNAi as a route to gene function in Drosophila. Brief Funct Genomic Proteomic 3, 168–176. https://doi.org/10.1093/bfgp/3.2.168

Kwak, P.B., Tomari, Y., 2012. The N domain of Argonaute drives duplex unwinding during RISC assembly. Nat. Struct. Mol. Biol. 19, 145–151. https://doi.org/10.1038/nsmb.2232

Lagos-Quintana, M., Rauhut, R., Lendeckel, W., Tuschl, T., 2001. Identification of novel genes coding for small expressed RNAs. Science 294, 853–858. https://doi.org/10.1126/science.1064921

Layzer, J.M., McCaffrey, A.P., Tanner, A.K., Huang, Z., Kay, M.A., Sullenger, B.A., 2004. In vivo activity of nuclease-resistant siRNAs. RNA 10, 766–771. https://doi.org/10.1261/rna.5239604

Lazzaretti, D., Tournier, I., Izaurralde, E., 2009. The C-terminal domains of human TNRC6A, TNRC6B, and TNRC6C silence bound transcripts independently of Argonaute proteins. RNA 15, 1059–1066. https://doi.org/10.1261/rna.1606309

Lee, R.C., Feinbaum, R.L., Ambros, V., 1993. The C. elegans heterochronic gene lin-4 encodes small RNAs with antisense complementarity to lin-14. Cell 75, 843–854. https://doi.org/10.1016/0092-8674(93)90529-y

Lee, Y., Jeon, K., Lee, J.-T., Kim, S., Kim, V.N., 2002. MicroRNA maturation: stepwise processing and subcellular localization. EMBO J. 21, 4663–4670. https://doi.org/10.1093/emboj/cdf476

Leung, A.K.L., Sharp, P.A., 2013. Quantifying Argonaute proteins in and out of GW/P-bodies: implications in microRNA activities. Adv. Exp. Med. Biol. 768, 165–182. https://doi.org/10.1007/978-1-4614-5107-5_10

Leung, R.K.M., Whittaker, P.A., 2005. RNA interference: from gene silencing to gene-specific therapeutics. Pharmacol. Ther. 107, 222–239. https://doi.org/10.1016/j.pharmthera.2005.03.004

Leuschner, P.J.F., Ameres, S.L., Kueng, S., Martinez, J., 2006. Cleavage of the siRNA passenger strand during RISC assembly in human cells. EMBO Rep 7, 314–320. https://doi.org/10.1038/sj.embor.7400637

Li, S., Lian, S.L., Moser, J.J., Fritzler, M.L., Fritzler, M.J., Satoh, M., Chan, E.K.L., 2008. Identification of GW182 and its novel isoform TNGW1 as translational repressors in Ago2-mediated silencing. J. Cell. Sci. 121, 4134–4144. https://doi.org/10.1242/jcs.036905

Lima, W.F., Prakash, T.P., Murray, H.M., Kinberger, G.A., Li, W., Chappell, A.E., Li, C.S., Murray, S.F., Gaus, H., Seth, P.P., Swayze, E.E., Crooke, S.T., 2012. Single-stranded siRNAs activate RNAi in animals. Cell 150, 883–894. https://doi.org/10.1016/j.cell.2012.08.014

Lin, S., Gregory, R.I., 2015. MicroRNA biogenesis pathways in cancer. Nat. Rev. Cancer 15, 321–333. https://doi.org/10.1038/nrc3932

Little, S.J., Holte, S., Routy, J.-P., Daar, E.S., Markowitz, M., Collier, A.C., Koup, R.A., Mellors, J.W., Connick, E., Conway, B., Kilby, M., Wang, L., Whitcomb, J.M., Hellmann, N.S., Richman, D.D., 2002. Antiretroviral-drug resistance among patients recently infected with HIV. N. Engl. J. Med. 347, 385–394. https://doi.org/10.1056/NEJMoa013552

Liu, J., Valencia-Sanchez, M.A., Hannon, G.J., Parker, R., 2005. MicroRNA-dependent localization of targeted mRNAs to mammalian P-bodies. Nat. Cell Biol. 7, 719–723. https://doi.org/10.1038/ncb1274

Loakes, D., Brown, D.M., 1994. 5-Nitroindole as an universal base analogue. Nucleic Acids Res. 22, 4039–4043. https://doi.org/10.1093/nar/22.20.4039

Lorenz, C., Hadwiger, P., John, M., Vornlocher, H.-P., Unverzagt, C., 2004. Steroid and lipid conjugates of siRNAs to enhance cellular uptake and gene silencing in liver cells. Bioorg. Med. Chem. Lett. 14, 4975–4977. https://doi.org/10.1016/j.bmcl.2004.07.018

Lund, E., Güttinger, S., Calado, A., Dahlberg, J.E., Kutay, U., 2004. Nuclear export of microRNA precursors. Science 303, 95–98. https://doi.org/10.1126/science.1090599

Luteijn, M.J., Ketting, R.F., 2013. PIWI-interacting RNAs: from generation to transgenerational epigenetics. Nat. Rev. Genet. 14, 523–534. https://doi.org/10.1038/nrg3495

Luteijn, M.J., van Bergeijk, P., Kaaij, L.J.T., Almeida, M.V., Roovers, E.F., Berezikov, E., Ketting, R.F., 2012. Extremely stable Piwi-induced gene silencing in Caenorhabditis elegans. EMBO J. 31, 3422–3430. https://doi.org/10.1038/emboj.2012.213

Manoharan, M., 2004. RNA interference and chemically modified small interfering RNAs. Curr Opin Chem Biol 8, 570–579. https://doi.org/10.1016/j.cbpa.2004.10.007

Martinez, J., Patkaniowska, A., Urlaub, H., Lührmann, R., Tuschl, T., 2002. Single-stranded antisense siRNAs guide target RNA cleavage in RNAi. Cell 110, 563–574. https://doi.org/10.1016/s0092-8674(02)00908-x

Meister, G., 2013. Argonaute proteins: functional insights and emerging roles. Nat. Rev. Genet. 14, 447–459. https://doi.org/10.1038/nrg3462

Meister, G., Landthaler, M., Patkaniowska, A., Dorsett, Y., Teng, G., Tuschl, T., 2004. Human Argonaute2 mediates RNA cleavage targeted by miRNAs and siRNAs. Mol. Cell 15, 185–197. https://doi.org/10.1016/j.molcel.2004.07.007

Miyoshi, K., Tsukumo, H., Nagami, T., Siomi, H., Siomi, M.C., 2005. Slicer function of Drosophila Argonautes and its involvement in RISC formation. Genes Dev 19, 2837–2848. https://doi.org/10.1101/gad.1370605

Mohn, F., Handler, D., Brennecke, J., 2015. Noncoding RNA. piRNA-guided slicing specifies transcripts for Zucchini-dependent, phased piRNA biogenesis. Science 348, 812–817. https://doi.org/10.1126/science.aaa1039

Monia, B.P., Johnston, J.F., Sasmor, H., Cummins, L.L., 1996. Nuclease resistance and antisense activity of modified oligonucleotides targeted to Ha-ras. J. Biol. Chem. 271, 14533–14540. https://doi.org/10.1074/jbc.271.24.14533

Monteys, A.M., Spengler, R.M., Wan, J., Tecedor, L., Lennox, K.A., Xing, Y., Davidson, B.L., 2010. Structure and activity of putative intronic miRNA promoters. RNA 16, 495–505. https://doi.org/10.1261/rna.1731910

Nair, J.K., Attarwala, H., Sehgal, A., Wang, Q., Aluri, K., Zhang, X., Gao, M., Liu, J., Indrakanti, R., Schofield, S., Kretschmer, P., Brown, C.R., Gupta, S., Willoughby, J.L.S., Boshar, J.A., Jadhav, V., Charisse, K., Zimmermann, T., Fitzgerald, K., Manoharan, M., Rajeev, K.G., Akinc, A., Hutabarat, R., Maier, M.A., 2017. Impact of enhanced metabolic stability on pharmacokinetics and pharmacodynamics of GalNAc-siRNA conjugates. Nucleic Acids Res. 45, 10969–10977. https://doi.org/10.1093/nar/gkx818

Nakanishi, K., Weinberg, D.E., Bartel, D.P., Patel, D.J., 2012. Structure of yeast Argonaute with guide RNA. Nature 486, 368–374. https://doi.org/10.1038/nature11211

Napoli, C., Lemieux, C., Jorgensen, R., 1990. Introduction of a Chimeric Chalcone Synthase Gene into Petunia Results in Reversible Co-Suppression of Homologous Genes in trans. Plant Cell 2, 279–289. https://doi.org/10.1105/tpc.2.4.279

Naqvi, A.R., Islam, M.N., Choudhury, N.R., Haq, Q.M.R., 2009. The fascinating world of RNA interference. Int. J. Biol. Sci. 5, 97–117. https://doi.org/10.7150/ijbs.5.97

Naruse, K., Matsuura-Suzuki, E., Watanabe, M., Iwasaki, S., Tomari, Y., 2018. In vitro reconstitution of chaperone-mediated human RISC assembly. RNA 24, 6–11. https://doi.org/10.1261/rna.063891.117

Ngô, H., Tschudi, C., Gull, K., Ullu, E., 1998. Double-stranded RNA induces mRNA degradation in Trypanosoma brucei. Proc. Natl. Acad. Sci. U.S.A. 95, 14687–14692. https://doi.org/10.1073/pnas.95.25.14687s

Nishida, K.M., Okada, T.N., Kawamura, T., Mituyama, T., Kawamura, Y., Inagaki, S., Huang, H., Chen, D., Kodama, T., Siomi, H., Siomi, M.C., 2009. Functional involvement of Tudor and dPRMT5 in the piRNA processing pathway in Drosophila germlines. EMBO J. 28, 3820–3831. https://doi.org/10.1038/emboj.2009.365

Nishimasu, H., Ishizu, H., Saito, K., Fukuhara, S., Kamatani, M.K., Bonnefond, L., Matsumoto, N., Nishizawa, T., Nakanaga, K., Aoki, J., Ishitani, R., Siomi, H., Siomi, M.C., Nureki, O., 2012. Structure and function of Zucchini endoribonuclease in piRNA biogenesis. Nature 491, 284–287. https://doi.org/10.1038/nature11509

Novina, C.D., Sharp, P.A., 2004. The RNAi revolution. Nature 430, 161–164. https://doi.org/10.1038/430161a

Nykänen, A., Haley, B., Zamore, P.D., 2001. ATP requirements and small interfering RNA structure in the RNA interference pathway. Cell 107, 309–321. https://doi.org/10.1016/s0092-8674(01)00547-5

Oelgeschläger, M., Larraín, J., Geissert, D., De Robertis, E.M., 2000. The evolutionarily conserved BMP-binding protein Twisted gastrulation promotes BMP signalling. Nature 405, 757–763. https://doi.org/10.1038/35015500

Okada, C., Yamashita, E., Lee, S.J., Shibata, S., Katahira, J., Nakagawa, A., Yoneda, Y., Tsukihara, T., 2009. A high-resolution structure of the pre-microRNA nuclear export machinery. Science 326, 1275–1279. https://doi.org/10.1126/science.1178705

Pandey, A.K., Agarwal, P., Kaur, K., Datta, M., 2009. MicroRNAs in diabetes: tiny players in big disease. Cell. Physiol. Biochem. 23, 221–232. https://doi.org/10.1159/000218169

Park, J.H., Shin, S.-Y., Shin, C., 2017. Non-canonical targets destabilize microRNAs in human Argonautes. Nucleic Acids Res 45, 1569–1583. https://doi.org/10.1093/nar/gkx029

Parrish, J.Z., Xue, D., 2003. Functional genomic analysis of apoptotic DNA degradation in C. elegans. Mol. Cell 11, 987–996. https://doi.org/10.1016/s1097-2765(03)00095-9

Pasquinelli, A.E., Reinhart, B.J., Slack, F., Martindale, M.Q., Kuroda, M.I., Maller, B., Hayward, D.C., Ball, E.E., Degnan, B., Müller, P., Spring, J., Srinivasan, A., Fishman, M., Finnerty, J., Corbo, J., Levine, M., Leahy, P., Davidson, E., Ruvkun, G., 2000. Conservation of the sequence and temporal expression of let-7 heterochronic regulatory RNA. Nature 408, 86–89. https://doi.org/10.1038/35040556

Peacock, H., Kannan, A., Beal, P.A., Burrows, C.J., 2011. Chemical Modification of siRNA Bases to Probe and Enhance RNA Interference. J Org Chem 76, 7295–7300. https://doi.org/10.1021/jo2012225

Prakash, T.P., Kinberger, G.A., Murray, H.M., Chappell, A., Riney, S., Graham, M.J., Lima, W.F., Swayze, E.E., Seth, P.P., 2016. Synergistic effect of phosphorothioate, 5′-vinylphosphonate and GalNAc modifications for enhancing activity of synthetic siRNA. Bioorganic & Medicinal Chemistry Letters 26, 2817–2820. https://doi.org/10.1016/j.bmcl.2016.04.063

Prakash, T.P., Lima, W.F., Murray, H.M., Li, W., Kinberger, G.A., Chappell, A.E., Gaus, H., Seth, P.P., Bhat, B., Crooke, S.T., Swayze, E.E., 2015. Identification of metabolically stable 5'-phosphate analogs that support single-stranded siRNA activity. Nucleic Acids Res. 43, 2993–3011. https://doi.org/10.1093/nar/gkv162

Radhakrishnan, S.K., Layden, T.J., Gartel, A.L., 2004. RNA interference as a new strategy against viral hepatitis. Virology 323, 173–181. https://doi.org/10.1016/j.virol.2004.02.021

Rajasethupathy, P., Antonov, I., Sheridan, R., Frey, S., Sander, C., Tuschl, T., Kandel, E.R., 2012. A role for neuronal piRNAs in the epigenetic control of memory-related synaptic plasticity. Cell 149, 693–707. https://doi.org/10.1016/j.cell.2012.02.057

Reinhart, B.J., Slack, F.J., Basson, M., Pasquinelli, A.E., Bettinger, J.C., Rougvie, A.E., Horvitz, H.R., Ruvkun, G., 2000. The 21-nucleotide let-7 RNA regulates developmental timing in Caenorhabditis elegans. Nature 403, 901–906. https://doi.org/10.1038/35002607

Robbins, M., Judge, A., Liang, L., McClintock, K., Yaworski, E., MacLachlan, I., 2007. 2'-O-methyl-modified RNAs act as TLR7 antagonists. Mol. Ther. 15, 1663–1669. https://doi.org/10.1038/sj.mt.6300240

Rondinone, C.M., 2006. Minireview: ribonucleic acid interference for the identification of new targets for the treatment of metabolic diseases. Endocrinology 147, 2650–2656. https://doi.org/10.1210/en.2006-0147

Rouget, C., Papin, C., Boureux, A., Meunier, A.-C., Franco, B., Robine, N., Lai, E.C., Pelisson, A., Simonelig, M., 2010. Maternal mRNA deadenylation and decay by the piRNA pathway in the early Drosophila embryo. Nature 467, 1128–1132. https://doi.org/10.1038/nature09465

Ruiz, F., Vayssié, L., Klotz, C., Sperling, L., Madeddu, L., 1998. Homology-dependent gene silencing in Paramecium. Mol. Biol. Cell 9, 931–943. https://doi.org/10.1091/mbc.9.4.931

Saini, H.K., Griffiths-Jones, S., Enright, A.J., 2007. Genomic analysis of human microRNA transcripts. Proc. Natl. Acad. Sci. U.S.A. 104, 17719–17724. https://doi.org/10.1073/pnas.0703890104

Schirle, N.T., MacRae, I.J., 2012. The Crystal Structure of Human Argonaute2. Science 336, 1037–1040. https://doi.org/10.1126/science.1221551

Schirle, N.T., Sheu-Gruttadauria, J., Chandradoss, S.D., Joo, C., MacRae, I.J., 2015. Water-mediated recognition of t1-adenosine anchors Argonaute2 to microRNA targets. Elife 4. https://doi.org/10.7554/eLife.07646

Schwarz, D.S., Hutvágner, G., Du, T., Xu, Z., Aronin, N., Zamore, P.D., 2003. Asymmetry in the assembly of the RNAi enzyme complex. Cell 115, 199–208. https://doi.org/10.1016/s0092-8674(03)00759-1

Serman, A., Le Roy, F., Aigueperse, C., Kress, M., Dautry, F., Weil, D., 2007. GW body disassembly triggered by siRNAs independently of their silencing activity. Nucleic Acids Res. 35, 4715–4727. https://doi.org/10.1093/nar/gkm491

Setten, R.L., Rossi, J.J., Han, S.-P., 2019. The current state and future directions of RNAi-based therapeutics. Nat Rev Drug Discov 18, 421–446. https://doi.org/10.1038/s41573-019-0017-4

Shankar, P., Manjunath, N., Lieberman, J., 2005. The prospect of silencing disease using RNA interference. JAMA 293, 1367–1373. https://doi.org/10.1001/jama.293.11.1367

Sheth, U., Parker, R., 2003. Decapping and decay of messenger RNA occur in cytoplasmic processing bodies. Science 300, 805–808. https://doi.org/10.1126/science.1082320

Siomi, M.C., Mannen, T., Siomi, H., 2010. How does the royal family of Tudor rule the PIWI-interacting RNA pathway? Genes Dev. 24, 636–646. https://doi.org/10.1101/gad.1899210

Siomi, M.C., Sato, K., Pezic, D., Aravin, A.A., 2011. PIWI-interacting small RNAs: the vanguard of genome defence. Nat. Rev. Mol. Cell Biol. 12, 246–258. https://doi.org/10.1038/nrm3089

Stessl, M., Marchetti-Deschmann, M., Winkler, J., Lachmann, B., Allmaier, G., Noe, C.R., 2009. A proteomic study reveals unspecific apoptosis induction and reduction of glycolytic enzymes by the phosphorothioate antisense

oligonucleotide oblimersen in human melanoma cells. J Proteomics 72, 1019–1030. https://doi.org/10.1016/j.jprot.2009.06.001

Svitkin, Y.V., Sonenberg, N., 2004. An efficient system for cap- and poly(A)-dependent translation in vitro. Methods Mol. Biol. 257, 155–170. https://doi.org/10.1385/1-59259-750-5:155

Svoboda, P., Stein, P., Hayashi, H., Schultz, R.M., 2000. Selective reduction of dormant maternal mRNAs in mouse oocytes by RNA interference. Development 127, 4147–4156.

Tabara, H., Grishok, A., Mello, C.C., 1998. RNAi in C. elegans: soaking in the genome sequence. Science 282, 430–431. https://doi.org/10.1126/science.282.5388.430

Tam, O.H., Aravin, A.A., Stein, P., Girard, A., Murchison, E.P., Cheloufi, S., Hodges, E., Anger, M., Sachidanandam, R., Schultz, R.M., Hannon, G.J., 2008. Pseudogene-derived small interfering RNAs regulate gene expression in mouse oocytes. Nature 453, 534–538. https://doi.org/10.1038/nature06904

Till, S., Lejeune, E., Thermann, R., Bortfeld, M., Hothorn, M., Enderle, D., Heinrich, C., Hentze, M.W., Ladurner, A.G., 2007. A conserved motif in Argonaute-interacting proteins mediates functional interactions through the Argonaute PIWI domain. Nat. Struct. Mol. Biol. 14, 897–903. https://doi.org/10.1038/nsmb1302

Timmons, L., Court, D.L., Fire, A., 2001. Ingestion of bacterially expressed dsRNAs can produce specific and potent genetic interference in Caenorhabditis elegans. Gene 263, 103–112. https://doi.org/10.1016/s0378-1119(00)00579-5

Timmons, L., Fire, A., 1998. Specific interference by ingested dsRNA. Nature 395, 854. https://doi.org/10.1038/27579

Tomari, Y., Matranga, C., Haley, B., Martinez, N., Zamore, P.D., 2004. A protein sensor for siRNA asymmetry. Science 306, 1377–1380. https://doi.org/10.1126/science.1102755

Tuzmen, S., Tuzmen, P., Arora, S., Mousses, S., Azorsa, D., 2011. RNAi-Based Functional Pharmacogenomics. Disease Gene Identification 271–290. https://doi.org/10.1007/978-1-61737-954-3_18

Ui-Tei, K., Naito, Y., Zenno, S., Nishi, K., Yamato, K., Takahashi, F., Juni, A., Saigo, K., 2008. Functional dissection of siRNA sequence by systematic DNA substitution: modified siRNA with a DNA seed arm is a powerful tool for mammalian gene silencing with significantly reduced off-target effect. Nucleic Acids Res. 36, 2136–2151. https://doi.org/10.1093/nar/gkn042

Vagin, V.V., Sigova, A., Li, C., Seitz, H., Gvozdev, V., Zamore, P.D., 2006. A distinct small RNA pathway silences selfish genetic elements in the germline. Science 313, 320–324. https://doi.org/10.1126/science.1129333

Vasileva, A., Tiedau, D., Firooznia, A., Müller-Reichert, T., Jessberger, R., 2009. Tdrd6 is required for spermiogenesis, chromatoid body architecture, and regulation of miRNA expression. Curr. Biol. 19, 630–639. https://doi.org/10.1016/j.cub.2009.02.047

Vaucheret, H., Fagard, M., 2001. Transcriptional gene silencing in plants: targets, inducers and regulators. Trends Genet. 17, 29–35.

Wall, N.R., Shi, Y., 2003. Small RNA: can RNA interference be exploited for therapy? Lancet 362, 1401–1403. https://doi.org/10.1016/S0140-6736(03)14637-5

Watanabe, T., Takeda, A., Tsukiyama, T., Mise, K., Okuno, T., Sasaki, H., Minami, N., Imai, H., 2006. Identification and characterization of two novel classes of small RNAs in the mouse germline: retrotransposon-derived siRNAs in oocytes and germline small RNAs in testes. Genes Dev. 20, 1732–1743. https://doi.org/10.1101/gad.1425706

Wianny, F., Zernicka-Goetz, M., 2000. Specific interference with gene function by double-stranded RNA in early mouse development. Nat. Cell Biol. 2, 70–75. https://doi.org/10.1038/35000016

Wightman, B., Ha, I., Ruvkun, G., 1993. Posttranscriptional regulation of the heterochronic gene lin-14 by lin-4 mediates temporal pattern formation in C. elegans. Cell 75, 855–862. https://doi.org/10.1016/0092-8674(93)90530-4

Wilson, R.C., Tambe, A., Kidwell, M.A., Noland, C.L., Schneider, C.P., Doudna, J.A., 2015. Dicer-TRBP complex formation ensures accurate mammalian microRNA biogenesis. Mol. Cell 57, 397–407. https://doi.org/10.1016/j.molcel.2014.11.030

Wu, L., Fan, J., Belasco, J.G., 2006. MicroRNAs direct rapid deadenylation of mRNA. Proc. Natl. Acad. Sci. U.S.A. 103, 4034–4039. https://doi.org/10.1073/pnas.0510928103

Yekta, S., Shih, I.-H., Bartel, D.P., 2004. MicroRNA-directed cleavage of HOXB8 mRNA. Science 304, 594–596. https://doi.org/10.1126/science.1097434

Yi, R., Qin, Y., Macara, I.G., Cullen, B.R., 2003. Exportin-5 mediates the nuclear export of pre-microRNAs and short hairpin RNAs. Genes Dev. 17, 3011–3016. https://doi.org/10.1101/gad.1158803

Yigit, E., Batista, P.J., Bei, Y., Pang, K.M., Chen, C.-C.G., Tolia, N.H., Joshua-Tor, L., Mitani, S., Simard, M.J., Mello, C.C., 2006. Analysis of the C. elegans

Argonaute family reveals that distinct Argonautes act sequentially during RNAi. Cell 127, 747–757. https://doi.org/10.1016/j.cell.2006.09.033

Yoda, M., Kawamata, T., Paroo, Z., Ye, X., Iwasaki, S., Liu, Q., Tomari, Y., 2010. ATP-dependent human RISC assembly pathways. Nat. Struct. Mol. Biol. 17, 17–23. https://doi.org/10.1038/nsmb.1733

Zambrowicz, B.P., Turner, C.A., Sands, A.T., 2003. Predicting drug efficacy: knockouts model pipeline drugs of the pharmaceutical industry. Curr Opin Pharmacol 3, 563–570.

Zamore, P.D., Tuschl, T., Sharp, P.A., Bartel, D.P., 2000. RNAi: double-stranded RNA directs the ATP-dependent cleavage of mRNA at 21 to 23 nucleotide intervals. Cell 101, 25–33. https://doi.org/10.1016/S0092-8674(00)80620-0

VII. Acknowledgments

I would like to express my sincere gratitude to my advisor Prof. Yukihide Tomari for his continuous support to my Ph.D study and related research, for his patience, motivation and immense knowledge. His guidance helped me throughout my research and writing of this thesis. I could not have imagined having a better mentor for my Ph.D.

Besides my advisor, I would like to thank my thesis committee members (in alphabetic order): Prof. Shuya Fukai, Prof. Nono Tomita, Prof. Kumiko Ui-tei and Prof. Yuichiro Watanabe. It was my honor to have them involved in monitoring my thesis and I am truly grateful for their insightful comments and encouragement.

I am thankful to all my professors I was lucky to meet from high school who transmitted me the fundamental knowledge to succeed. A special mention to Prof. Agnès Bernet for her humanity and the direction she showed me.

My sincere thanks also goes to Prof. Samuel Sidi, and Prof. Toshiki Watanabe, who provided me the opportunity to join their team as an intern, and gave access to their laboratory and research facilities. Without their precious support to help me grow up as a scientist, it would not have been possible to conduct this research in my thesis.

I thank my fellow labmates for the stimulating discussions we have had in the last three years.

I would also like to thank my friends. I will not go into details here as I am sure they are aware of the importance they played in this time of my life.

Thank you my “Tokyo team” during my PhD time Dips, Fumiko, Loic, Misha, Kaori, Marek, Thiago, Mikael, Nicolo, Rumi, Maho, Shino, Jun, Giseok, Juan, Keiko, Bastien, Agnes, Marika, Ayano, Mew, Ayako, Alexis, Chieko, Chihiro, Eddie, Megumi and Tomoki.

My heart also goes out to those not here anymore, Melissa, Sofiane, Jérémy, I hope you guys are well and having fun where you are.

Last but not the least, I would like to thank my family for supporting me spiritually with their love throughout my thesis and in my life in general. A special dedication is written in French for them in the next chapter.

VIII. Remerciements
(Dedications)

The following dedications will be written in French

Thank you for your understanding.

A mes parents Philippe & Agnès, pour leur amour sans limite.

Sonnet à Marie

Je vous envoie un bouquet que ma main
Vient de trier de ces fleurs épanies ;
Qui ne les eût à ce vêpre cueillies,
Chutes à terre elles fussent demain.

Cela vous soit un exemple certain
Que vos beautés, bien qu'elles soient fleuries,
En peu de temps cherront toutes flétries,
Et, comme fleurs, périront tout soudain.

Le temps s'en va, le temps s'en va, ma dame ;
Las ! le temps, non, mais nous nous en allons,
Et tôt serons étendus sous la lame ;

Et des amours desquelles nous parlons,
Quand serons morts, n'en sera plus nouvelle.
Pour c'aimez-moi cependant qu'êtes belle.

Pierre de Ronsard (Continuation des Amours, 1555)

Je vous aime.

A Louis-Joseph et sa maman,

Mon fils, tu es ma vie, pour l'éternité et bien au-delà.

A jamais dans mon cœur.

A Akiko, ma lumière.

Avec de l'amour, tout est possible.

A ma famille,

Mes frères (Alexandre et Romain) et soeurs (Solène et Cyrielle)
(et leurs conjoints)
Ma nièce (Margaux) et mes neveux (Lucas et elliot)
Mes grands-parents ici ou la-bàs
Bidouille petit chien des lumières et Yuzu.

Unit pour toujours.